

FINAL REPORT

Novel Anaerobic Wastewater Treatment System for Energy Generation at Forward Operating Bases

SERDP Project ER-2218

AUGUST 2016

Kathryn A. Guy
Martin A. Page
**U.S. Army Engineer Research and Development
Center (ERDC)**

Lance Schideman
Illinois Sustainable Technology Center

Gerardine Botte
Russ College of Engineering

Distribution Statement A

This document has been cleared for public release



Page Intentionally Left Blank

This report was prepared under contract to the Department of Defense Strategic Environmental Research and Development Program (SERDP). The publication of this report does not indicate endorsement by the Department of Defense, nor should the contents be construed as reflecting the official policy or position of the Department of Defense. Reference herein to any specific commercial product, process, or service by trade name, trademark, manufacturer, or otherwise, does not necessarily constitute or imply its endorsement, recommendation, or favoring by the Department of Defense.

Page Intentionally Left Blank

REPORT DOCUMENTATION PAGE				Form Approved OMB No. 0704-0188	
Public reporting burden for this collection of information is estimated to average 1 hour per response, including the time for reviewing instructions, searching existing data sources, gathering and maintaining the data needed, and completing and reviewing this collection of information. Send comments regarding this burden estimate or any other aspect of this collection of information, including suggestions for reducing this burden to Department of Defense, Washington Headquarters Services, Directorate for Information Operations and Reports (0704-0188), 1215 Jefferson Davis Highway, Suite 1204, Arlington, VA 22202-4302. Respondents should be aware that notwithstanding any other provision of law, no person shall be subject to any penalty for failing to comply with a collection of information if it does not display a currently valid OMB control number. PLEASE DO NOT RETURN YOUR FORM TO THE ABOVE ADDRESS.					
1. REPORT DATE (DD-MM-YYYY) August 2016		2. REPORT TYPE Final		3. DATES COVERED (From - To)	
4. TITLE AND SUBTITLE Novel Anaerobic Wastewater Treatment System for Energy Generation at Forward Operating Bases: Final Report on Environmental Restoration Project ER-2218				5a. CONTRACT NUMBER	
				5b. GRANT NUMBER	
				5c. PROGRAM ELEMENT NUMBER SERDP Environmental Restoration	
6. AUTHOR(S) Kathryn A. Guy, Martin A. Page, Lance Schideman, and Gerardine Botte				5d. PROJECT NUMBER Project ER-2218	
				5e. TASK NUMBER	
				5f. WORK UNIT NUMBER	
7. PERFORMING ORGANIZATION NAME(S) AND ADDRESS(ES) U.S. Army Engineer Research and Development Center Construction Engineering Research Laboratory P.O. Box 9005 Champaign, IL 61826-9005				8. PERFORMING ORGANIZATION REPORT NUMBER ERDC/CERL TR-16-13	
9. SPONSORING / MONITORING AGENCY NAME(S) AND ADDRESS(ES) Strategic Environmental Research and Development Program (SERDP) 4800 Mark Center Drive, Suite 17D08 Alexandria, VA 22350-3605				10. SPONSOR/MONITOR'S ACRONYM(S) SERDP	
				11. SPONSOR/MONITOR'S REPORT NUMBER(S) ER-2218	
12. DISTRIBUTION / AVAILABILITY STATEMENT Approved for public release; distribution is unlimited.					
13. SUPPLEMENTARY NOTES					
14. ABSTRACT Forward Operating Bases (FOBs) currently lack sustainable wastewater treatment options, creating operational inefficiency, personnel vulnerability, and environmental degradation. The objective of this research was to develop a sustainable wastewater treatment system for FOBs that converts wastewater contaminants, including organics and ammonia, into harvestable products for energy production. The system aims to combine sustainable materials with recent technological advances to treat wastewater with minimal material input and reduced disposal issues, while producing a net return on energy. The wastewater treatment system designed under this project will benefit the Department of Defense by reducing the costs, logistical burden, and risks associated with wastewater management at FOBs. Further development of the technology into a full-scale unit is expected to yield an efficient system for onsite treatment that is simple to operate and produces fuels for electrical and thermal energy generation. This positive-net-energy approach will support self-sufficient-FOB design goals. The integrated system would also reduce the logistical burden and risks associated with transporting waste and importing fuel, chemicals, and water. The proposed system will reduce the FOB environmental footprint and impact on indigenous populations, demonstrating innovative and effective environmental stewardship.					
15. SUBJECT TERMS Water quality; Water-Purification; Sustainability; Sewage; Refuse as fuel; Energy conservation; Military bases; Forward operating bases (FOBs)					
16. SECURITY CLASSIFICATION OF:			17. LIMITATION OF ABSTRACT	18. NUMBER OF PAGES	19a. NAME OF RESPONSIBLE PERSON
a. REPORT Unclassified	b. ABSTRACT Unclassified	c. THIS PAGE Unclassified	SAR	107	19b. TELEPHONE NUMBER (include area code)

Page Intentionally Left Blank

Abstract

Forward Operating Bases (FOBs) currently lack sustainable wastewater treatment options, creating operational inefficiency, personnel vulnerability, and environmental degradation. The objective of this research was to develop a sustainable wastewater treatment system for FOBs that converts wastewater contaminants, including organics and ammonia, into harvestable products for energy production. The system aims to combine sustainable materials with recent technological advances to treat wastewater with minimal material input and reduced disposal issues, while producing a net return on energy.

The wastewater treatment system designed under this project will benefit the Department of Defense by reducing the costs, logistical burden, and risks associated with wastewater management at FOBs. Further development of the technology into a full-scale unit is expected to yield an efficient system for onsite treatment that is simple to operate and produces fuels for electrical and thermal energy generation. This positive-net-energy approach will support self-sufficient-FOB design goals. The integrated system would also reduce the logistical burden and risks associated with transporting waste and importing fuel, chemicals, and water. The proposed system will reduce the FOB environmental footprint and impact on indigenous populations, demonstrating innovative and effective environmental stewardship.

DISCLAIMER: The contents of this report are not to be used for advertising, publication, or promotional purposes. Citation of trade names does not constitute an official endorsement or approval of the use of such commercial products. All product names and trademarks cited are the property of their respective owners. The findings of this report are not to be construed as an official Department of the Army position unless so designated by other authorized documents.

DESTROY THIS REPORT WHEN NO LONGER NEEDED. DO NOT RETURN IT TO THE ORIGINATOR.

Contents

Abstract.....	ii
Figures and Tables.....	v
Preface	ix
Executive Summary	x
1 Introduction	1
1.1 Background.....	1
1.2 Objectives.....	1
1.3 Technical approach	2
1.3.1 AnMBR for removal of organics	3
1.3.2 Clinoptilolite for ammonia sequestration	4
1.3.3 Ammonia electrolysis with the GreenBox™.....	4
1.4 Potential benefits.....	5
2 Materials and Methods	7
2.1 AnMBR for removal of organics	7
2.1.1 Methods to measure baseline capabilities of AnMBR technology for FOB wastewater treatment	7
2.1.2 Testing high throughput AnMBR capabilities for treating representative FOB wastewater	8
2.1.3 Testing AnMBR capabilities for treating highly concentrated fob wastewater/sludge	11
2.1.4 Methods to optimize AnMBR performance	18
2.1.5 Hybrid AnMBR reactor design for optimization testing.....	23
2.1.6 Clinoptilolite for ammonia sequestration	24
2.1.6.1 Ammonia solution composition and flow rates.....	25
2.1.7 Clinoptilolite selection and preparation.....	25
2.1.8 Column setup	26
2.1.9 Regeneration procedures.....	29
2.1.10 Ammonia analysis methods	29
2.2 Ammonia electrolysis	30
2.2.1 Bench-scale demonstration	30
2.2.2 Ammonia electrolysis modeling	32
3 Results and Discussion	34
3.1 Results.....	34
3.2 Benefits	37
3.3 Testing high throughput AnMBR capabilities for treating representative FOB wastewater	37
3.4 Testing AnMBR capabilities for treating highly concentrated FOB wastewater/sludge	38
3.4.1 Operation at mesophilic temperature (35°C).....	38

3.4.2	Operation at ambient temperature (20 °C)	46
3.4.3	AnMBR energy analysis	48
3.4.4	Optimizing AnMBR performance.....	52
3.5	Organic sequestration experiments	58
3.5.1	AnMBR optimization via design modification.....	63
3.5.2	Ammonia sequestration on clinoptilolite	64
3.5.3	Ammonia electrolysis.....	73
3.5.4	Ammonia electrolysis model	79
4	Conclusions and Implications for Future Research/Implementation.....	85
	Literature Cited	87
	Appendix A: Publications Produced by this Study	91
	Articles in peer-reviewed journals.....	91
	Conference abstracts.....	91
	Appendix B: Supplemental Information for Table 1.....	92
	Influent wastewater characteristics	92
	Renewable fuel yields.....	92
	Energy usage	94
	Energy cost savings	94
	Water demand reduction	95
	Sludge reduction	95
	System size	95
	Acronyms	96
	Report Documentation Page	

Figures and Tables

Figures

Figure 1. The anaerobic wastewater treatment process strategically combines anaerobic membrane bioreactor (AnMBR) technology with clinoptilolite ion exchange and GreenBox™ ammonia electrolysis. The system generates both methane and hydrogen fuels.	3
Figure 2. High rate AnMBR process chamber for biodegradation of soluble organics and separation of particulates.	10
Figure 3. Tracer testing to confirm water flow through the membrane element. Solid humic acid sodium salt tracer was added near potential leak sites prior to turning on the effluent pump. Turning on the effluent pump pulled the water away from the module fittings and through (into) the membrane element.	11
Figure 4. Highly concentrated wastewater feedstock.	12
Figure 5. Continuous AnMBR design schematic.	13
Figure 6. Continuous AnMBR system physical setup.	13
Figure 7. Modified sediment filters prior to application in the AnMBR system.	15
Figure 8. Custom-built Membrana membrane, before (A and B) and after (C and D) housing modifications.	15
Figure 9. Acid phase sequencing batch experimental setup.	21
Figure 10. Methane phase semi batch experimental setup, a total of three reactors were set up for PS + solid, Bioc and ADS methane phase reactors.	21
Figure 11. Dried PS solid for the control, Bioc blend for the Bioc acid phase sequencing batch reactor and ADS for the ADS acid phase sequencing batch reactor.	22
Figure 12. Hybrid AnMBR reactor design for optimization testing.	24
Figure 13. Multi-column clinoptilolite column design allowing for simultaneous loading and regeneration cycles.	27
Figure 14. Control code for microcontrollers on clinoptilolite columns.	28
Figure 15. Virtual image of the microcontroller and column setup.	28
Figure 16. Calibration samples using salicylate colorimetric methods to measure ammonia concentrations.	30
Figure 17. 30 W ammonia electrolyzer from E3 Clean Technologies.	31
Figure 18. Conceptual design for integrated ACE wastewater treatment system.	37
Figure 19. Percent COD removal in the AnMBR system.	41
Figure 20. Methane production per gram of VS added (12-day moving average) and theoretical maximum in the AnMBR system.	42
Figure 21. Soluble COD concentrations in the influent and pre-digestion phase of the AnMBR system.	43
Figure 22. Methane production levels in the AnMBR system upon switching from mesophilic to ambient temperature operating conditions in the methane phase.	47
Figure 23. Ambient temperature batch test methane production.	48

Figure 24. Estimated net energy recovery (energy out) per liter of wastewater treated via four different process scenarios for influent VS concentrations ranging from 0.4 to 20 g/L.	50
Figure 25. Soluble COD concentrations in methane phase of the continuous AnMBR system over time.	51
Figure 26. Sulfide concentrations in AnMBR system over time during operation with and without bioaugmentation.	53
Figure 27. Methane production in the continuous AnMBR system over time during operation with and without bioaugmentation.	54
Figure 28. Chemical oxygen demand (COD) removal in the AnMBR system over time during operation with and without bioaugmentation.	55
Figure 29. Equilibrium liquid phase COD concentrations for candidate adsorbents and ion-exchange resins showing after 16 days of contact time in filtered AnMBR effluent (initial liquid phase COD = 3882 mg/L).	56
Figure 30. Equilibrium liquid-phase concentrations of volatile fatty acids after 27 days contact time with various dosages (10, 100 and 250 g/L) of GAC, Tanex resin, and A510 resin in filtered AnMBR effluent.	57
Figure 31. Biogas production per gram of COD _{added} from batch test digestion of filtered AnMBR effluent with various adsorbent (GAC, Tanex, and A510), dosages (10, 100 and 250 g/L).	58
Figure 32. The addition of Tanex to a high-throughput AnMBR bioreactor may aid in sequestering organic contaminants during reactor startup to promote high organic levels in the reactor which can promote anaerobic culture maturation.	59
Figure 33. Soluble COD concentration in the methane phase of the continuous AnMBR system before and after shock-loading with and without the addition of Purolite® Tanex under ambient temperature operation.	60
Figure 34. One of three mesh bags that were deployed into the continuous AnMBR system containing approximately 370 g of Purolite® Tanex each.	60
Figure 35. Methane production in the continuous AnMBR system before and after shock-loading with and without the addition of Purolite® Tanex under ambient temperature operation.	62
Figure 36. Relationships between COD conversion in an AnMBR for two different reactors. The blue diamonds represent data collected in the current study for treating FOB-representative waste water (influent COD 1300) and using adsorbent augmentation in the high throughput AnMBR at ERDC. The red squares represent data collected in pilot-scale studies on a commercial system treating less concentrated wastewater (influent COD 300-550 mg/L). Based on these data, the projected HRT required for treating FOB-representative wastewater is 24 hours.	64
Figure 37. AmmoChip loading runs at 60 mL/min. Initial concentration = 85 mg/L-N.	65
Figure 38. Repeat loading cycles on regenerated clinoptilolite.	66
Figure 39. Regeneration of saturated clinoptilolite at pH 5.7, 9.4, and 11.7.	67
Figure 40. Clinoptilolite regeneration using a stop-flow method.	68
Figure 41. Effect of competing ions on ammonia sequestration (3.75 mM Ca ⁺² or 1.02 mM K ⁺).	69

Figure 42. Ammonia breakthrough at 1.87 mM, 3.74 mM, and 0 mM Ca^{2+} levels. The 0 mM run followed regeneration of the column after the calcium runs demonstrating restored capacity	70
Figure 43. Ammonia loading experiment data for real waste water.....	71
Figure 44. Ammonia breakthrough observed in three serially operated load columns.....	72
Figure 45. Repeat loading of the primary column in multi-column operation.	72
Figure 46. Effect of varying NaOH concentrations on ammonia electrolysis.....	73
Figure 47. Effect of varying ammonia concentrations on ammonia electrolysis	74
Figure 48. Ammonia electrolysis runs at 20 g/L NH_4Cl . $A_0 = 22$ A.....	75
Figure 49. Ammonia levels measured in anode and cathode solutions during an electrolysis experiment. Total ammonia is the sum of the measured concentrations.	76
Figure 50. Comparison of current readings to ammonia concentrations of the anode, cathode, and total solution.	77
Figure 51. Impact of flow rate on ammonia electrolysis performance.....	78
Figure 52. Calculated and measured current density versus cell voltage at low concentrations of NH_4Cl and KOH : $1 \times 10^{-5} \text{ mol cm}^{-3}$ and $1 \times 10^{-4} \text{ mol cm}^{-3}$ respectively. The decrease in conversion at higher cell voltages can be attributed to depletion of reactant and/or electrode poisoning (Estejab et al. 2015).	81
Figure 53. Calculated and measured current density versus cell voltage at high concentrations of NH_4Cl and KOH : $7 \times 10^{-5} \text{ mol cm}^{-3}$ and $1.5 \times 10^{-4} \text{ mol cm}^{-3}$ respectively. The decrease in current density at higher cell voltages can be attributed to electrode poisoning (Estejab et al. 2015).	82
Figure 54. Predicted current density as a function of NH_4Cl concentration for different cell voltages and 0.1M KOH concentration. Right axis is the ratio of hydroxide ion to ammonia concentration at the anode. For voltages below 0.80 V (dashed lines) increasing reactant concentration to more than 0.0295M NH_4Cl causes $[\text{OH}^-]/[\text{NH}_3]$ to be less than 3 and current density decreases. For voltages above 0.80 V (solid lines) catalyst poisoning is the reason for the decrease of the current density (Estejab et al. 2015).	83
Figure 55. ASPEN Plus schematic for the simulation of the ammonia GreenBox and its adjacent unit operations. The inlet stream to the GreenBox will be the outlet from the ion-exchange membrane and will contain ammonium ions, hydroxide ions, ammonia and water in equilibrium. The outlet streams from the FLASH represent an instantaneous gas-liquid phase separation.....	84

Tables

Table 1. Estimated energy savings, energy production, water savings, and sludge reduction for the proposed technology.	6
Table 2. Adjusted FOB wastewater influent characteristics accounting for future graywater reuse.....	8
Table 3. Synthetic wastewater formulation to meet adjusted wastewater influent characteristics.	9

Table 4. Characteristics of each batch of primary sludge substrate collected and used over the course of this study.....	12
Table 5. AnMBR system control and data logging.....	17
Table 6. Design parameters for the AnMBR system.	17
Table 7. Description of operating periods (after start-up) in the AnMBR system over the course of this study.	18
Table 8. Bench scale influent and inoculum characteristics.	22
Table 9. Description of candidate adsorbent/ion-exchange resin materials.	23
Table 10. Sources of clinoptilolite identified.	25
Table 11. Summary of operating conditions of the ammonia GreenBox used in the semi-empirical model development.	32
Table 12. Performance summary data for the baseline AnMBR system operating at an HRT of 8 hours. Over 40 effluent samples were analyzed in these studies, representing several months of operating time.	38
Table 13. Average sulfide concentrations in the AnMBR system during operation with and without bioaugmentation.	44
Table 14. Energy balance calculation values and resulting estimated kJ of net energy recovery (energy out) per liter of wastewater treated under four different operating scenarios: mesophilic operation (37 °C) with or without bioaugmentation, and ambient temperature (20 °C) operation with or with bioaugmentation.....	49
Table 15. Average soluble COD and VFA concentrations in acid phase during operation with and without bioaugmentation.....	53
Table 16. Reduction in organic matter content of wastewater, as measured by COD analysis, due to exposure to varying dose of ion-exchange resin.	59
Table 17. Experimental values of hydrogen and nitrogen production.....	78
Table 18. Optimum parameters for Equations 6 and 7 generated from experimental measurements for the conditions tested in Table 9 (Estejab et al. 2015).....	80

Preface

This study was conducted for the Strategic Environmental Research and Development Program (SERDP) under Project ER-2218, “Novel Anaerobic Wastewater Treatment System for Energy Generation at Forward Operating Bases.” The technical monitor for the SERDP Program Office was Dr. Andrea Leeson, Deputy Director and Environmental Restoration Program Manager.

The work was performed by the Materials and Structures Branch of the Facilities Division (CEERD-CFM), U.S. Army Engineer Research and Development Center, Construction Engineering Research Laboratory (ERDC-CERL). At the time of publication, Vicki L. Van Blaricum was Chief, CEERD-CFM; Donald K. Hicks was Chief, CEERD-CF; and Kurt Kinnevan, CEERD-CZT, was the Technical Director for Adaptive and Resilient Installations. The Deputy Director of ERDC-CERL was Dr. Kirankumar Topudurti and the Director was Dr. Ilker Adiguzel.

The authors wish to thank the following student research assistants at Ohio University (OU), Athens, OH, the University of Illinois at Urbana-Champaign (UIUC), and ERDC-CERL, who made numerous substantive contributions to project execution: Damilola Daramola and Ali Estejab (OU); Ana Martin-Ryals Matthew Ong, and Peng Li (UIUC); Brooke A. Divan (ERDC-CERL research assistant at the time of the study, now CEERD-CFM), Clinton Cender, Brittany Webb, Chelsea Skinner, and Kathryn East (ERDC-CERL).

The Commander of ERDC was COL Bryan S. Green and the Director was Dr. Jeffery P. Holland.

Executive Summary

The wastewater treatment system designed in this project will benefit the Department of Defense by reducing the costs, logistical burden, and risks associated with wastewater management at forward operating bases. The novel approach pursued in this research utilizes three sustainable technologies in concert: anaerobic membrane bioreactors (AnMBRs), clinoptilolite ion exchange (IX), and GreenBox™ ammonia electrolysis.

Conventional AnMBR operation at an elevated temperature of 35 °C reduced chemical oxygen demand (COD) by 98% when treating highly concentrated waste streams at a hydraulic retention time (HRT) of 21 days. Operation of an AnMBR for treating FOB wastewater (1360 mg/L COD) at low temperature (20 °C) resulted in COD reduction levels of 65–80%. Gas production was less efficient under these conditions, but conversion of organic nitrogen to ammonia was still achieved. The final design recommendation for integration of AnMBR technology into the system was HRT 24 hours; ambient temperature; bioseeding of initial reactor and utilization of granulated activated carbon (GAC) and Tanex™ resin to decrease startup times and decrease sensitivity to variable operating conditions.

Bench-scale examination of clinoptilolite-mediated removal of ammonium by ion exchange indicated that this is an effective and robust approach for control and concentration of ammonium. Column regeneration optimized using a 10% NaCl/0.5% NaOH mixture, making it consistent with downstream brine processing plans. The final design recommendation for integration of clinoptilolite ion exchange is multi-column arrangement; a stop-flow regeneration process to maximize ammonia concentration in the regenerant brine; and load times adjusted for local calcium maximums.

Ammonia electrolysis studies using the Greenbox were performed to assess feasibility of this technology as an alternative to conventional biological nitrification/denitrification processes. Current output is optimized with increasing ammonia concentration. Improved performance was obtained by lowering the flow rate. Reducing NaOH concentrations from 5 M (recommended) to 0.5 M lowered chemical requirements and increased safety. The final design recommendation for integration is flow rate of 150 mL/min; 0.5 M NaOH background solution; multiple passes of ammonia solution to align with clinoptilolite regeneration cycles; and return of treated brine for subsequent clinoptilolite regeneration.

1 Introduction

1.1 Background

Forward Operating Bases (FOBs) currently lack sustainable wastewater treatment options, resulting in operational inefficiency, personnel vulnerability, and environmental degradation. The development of sustainable wastewater treatment solutions has been identified as an important area of research for FOBs (Noblis 2010). The treatment of wastewater on-site with minimal energy and chemical inputs will reduce the logistical burdens and costs associated with the transportation of materials to and from FOBs. The availability of treated water for reuse will further decrease this burden as water and fuel combine to account for a large majority of supply shipments in Afghanistan and Iraq (Noblis 2010). Sustainable wastewater systems that fit within the constraints of FOB operations and that can be incorporated into larger net-zero energy design schemes provide an opportunity to reduce costs while improving security and environmental stewardship.

Conventional wastewater treatment relies heavily on activated sludge processes for secondary treatment, in which removal of organics and other oxygen-demanding constituents is a primary goal. The aeration required to support this process represents a major energy cost – typically more than half of the total energy used for wastewater treatment (Wallis-Lage and Levesque 2009). In pursuit of more energy-efficient approaches to wastewater treatment, researchers have proposed that anaerobic reactor technology be applied to a greater extent as an alternative to aerobic activated sludge processes. However, anaerobic bioreactor schemes are incapable of removing ammonia (USEPA 2008), thereby requiring a subsequent aerobic process to convert ammonia to nitrate. Ammonia is a critical contaminant in wastewater, as it represents a considerable portion of biological oxygen demand (BOD) and is toxic to aquatic organisms at low levels.

1.2 Objectives

The project objective is to develop a sustainable wastewater treatment system for FOBs that converts wastewater contaminants, including organics

and ammonia, into harvestable products for energy production and integrates into self-sufficient FOB design schemes. The system aims to combine sustainable materials with recent technological advances to treat wastewater with minimal material input and reduced disposal issues, while producing a net return on energy. Design goals for treated water include meeting the following metrics: BOD < 30 mg/L (COD < 90 mg/L), TSS < 30 mg/L, and EC < 2 cfu/mL.

The research is novel in that it synergistically integrated three embryonic technologies to achieve not only feasibility within the limitations of a FOB operating environment but also the generation of valuable fuels for renewable energy production. The three enabling technologies were AnMBRs, clinoptilolite ion exchange (IX) for ammonia sequestration, and ammonia electrolysis.

The specific questions to be answered by this research were:

1. How can AnMBRs be optimally integrated with ammonia sequestration and ammonia electrolysis processes to achieve water quality goals, minimize sludge production, minimize energy consumption, and produce usable fuels?
2. How can the proposed system be optimized to meet the design constraints imposed by the FOB environment, including scalability, energy efficiency, and operational simplicity, minimization of chemical inputs and outputs, and integration with self-sufficient FOB design schemes?

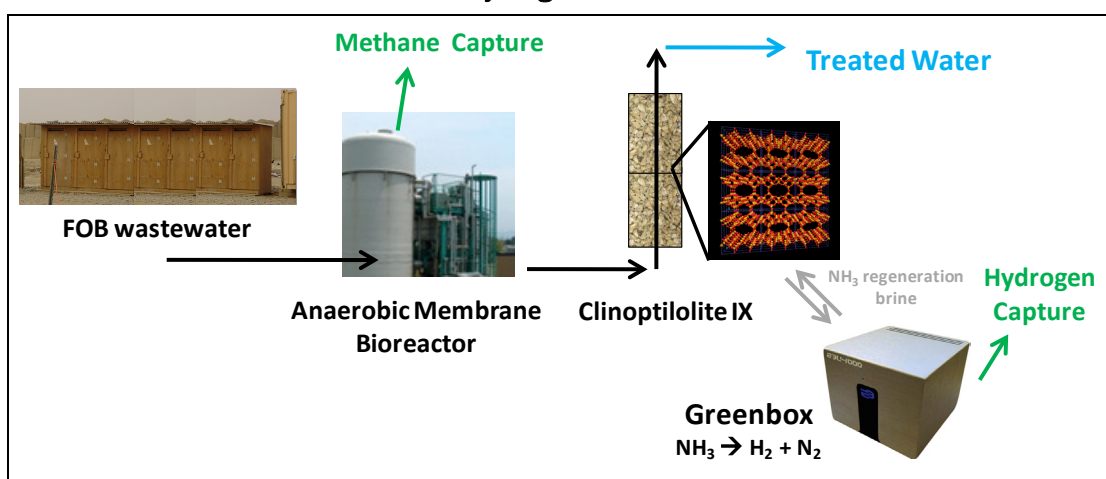
1.3 Technical approach

The novel approach pursued in this research utilizes three sustainable technologies in concert: anaerobic membrane bioreactors (AnMBRs), clinoptilolite ion exchange (IX), and GreenBox™ ammonia electrolysis. The synergistic combination of these technologies results in an anaerobic treatment system that is capable of removing ammonia, a critical pollutant in municipal waste streams that is conventionally degraded using energy-intensive aeration processes. The component technologies were initially at an embryonic stage of development. Therefore, research efforts focused initially on the optimization of each in the context of the FOB operating environment, followed by system integration and pilot scale evaluation.

The complete wastewater treatment system generates two forms of useful fuel—methane and hydrogen—that can be easily converted into electrical

and thermal energy. The system was designed to require minimal chemical inputs, reduce sludge production, be simple to operate, and be scalable. This approach makes anaerobic treatment of wastewater not only practical but also a potential new source of energy for FOBs. A general schematic of the system is provided in Figure 1, with descriptions of each component following.

Figure 1. The anaerobic wastewater treatment process strategically combines anaerobic membrane bioreactor (AnMBR) technology with clinoptilolite ion exchange and GreenBox™ ammonia electrolysis. The system generates both methane and hydrogen fuels.



1.3.1 AnMBR for removal of organics

AnMBR technology is applied to degrade organics in wastewater and generate methane, which can be harvested for electrical and thermal energy using microturbine cogeneration. Although anaerobic treatment schemes have been studied for decades, AnMBRs are still considered embryonic technologies (Berube et al. 2006; USEPA 2008). AnMBRs were shown to reduce chemical oxygen demand (COD) by 90% in synthetic wastewater with influent COD values of 460 mg/L, at hydraulic retention times (HRTs) greater than 3 hour, and the AMBRs produced in excess of 0.25 m³ methane per kg COD removed from municipal wastewater, at a methane gas concentration of 70% (Hu and Stuckey 2006). This equates to approximately 40% of the COD removed being converted to methane. Purification of the methane for use with microturbines can be achieved with minimal losses through ammonia stripping by clinoptilolite ion exchange and hydrogen sulfide removal either by GAC adsorption or degradation by phototrophic anaerobes (i.e., *Cholorobium limicola*). With careful attention to

reactor design, they can be made highly efficient in terms of physical footprint and operational stability. Key enabling technologies for AnMBRs include hydrophilic, foulant-resistant membranes and strategies for reducing scale formation on the membrane surface (Hu and Stuckey 2006; Choo et al. 2000). AnMBR technology is expected to be robust in the presence of compounds typically found in wastewater streams. However, the addition of certain organic chemicals (i.e., chloroform), elevated ammonia concentrations, or high levels of personal care products could affect microbial viability and efficiency (Mignone 2005; Fountoulakis et al. 2004).

1.3.2 Clinoptilolite for ammonia sequestration

Clinoptilolite ion exchange is utilized to sequester ammonia from the AnMBR process stream. Clinoptilolite is a naturally occurring zeolite that acts as a molecular sieve with high selectivity and capacity for ammonia (~2 meq/g). The use of clinoptilolite for the removal of ammonia from municipal wastewater has been considered for decades, but the disposal of the concentrated ammonia brine has been a barrier to widespread use. However, clinoptilolite is still being investigated at leading research institutions, with degradation and reuse of the ammonia brine remaining a key focus of ongoing research (Hegger 2010). In the integrated treatment system, the brine is considered as a valuable resource for generating hydrogen.

1.3.3 Ammonia electrolysis with the GreenBox™

The ammonia brine waste stream created during regeneration of spent clinoptilolite media is delivered to the GreenBox™ ammonia electrolysis system. GreenBox* is a newly developed system that converts ammonia to useful hydrogen fuel using a small current and metal electrodes to drive the thermodynamically favorable electrolytic conversion of ammonia to hydrogen and nitrogen gas (Bonnin et al. 2008, Vitse et al. 2005). Under ideal operating conditions, for every 1.58 kWh of electrical input, the system can generate 1 kg hydrogen or over 16.2 kWh of electrical energy when harnessed with fuel cell technology. The GreenBox system is ideal for treating concentrated ammonia streams because there is no ammonia concentration limitation, which is a major impediment for conventional biological ammonia conversion schemes that are generally limited by oxygen

* GreenBox is a trademark of E3 Clean Technologies, Inc., Athens, OH 45701.

transfer rate. In fact, the efficiency of hydrogen production with the GreenBox system increases at higher ammonia concentrations. Additionally, the caustic brine coming from a clinoptilolite regeneration process is optimal for ammonia conversion in terms of pH and salinity. Thus, it is the perfect complement to other component technologies, completing the wastewater treatment system.

1.4 Potential benefits

The successful integration of AnMBR, clinoptilolite ion-exchange, and GreenBox ammonia electrolysis may provide the following benefits for the DoD:

- Support self-sufficient FOB design schemes by reducing the costs of wastewater management at FOBs and by providing an efficient system for onsite treatment that is net-energy-positive.
- Meet practical constraints of operational simplicity and system size.
- Reduce risk to personnel by decreasing transport of chemicals, water, and waste.
- Generate energy in formats that can be used onsite (methane and hydrogen) and are compatible with silent base camp capabilities (hydrogen fuel cells).
- Provide water effluent that is suitable for toilet flushing or Reverse Osmosis Water Purification Unit (ROWPU) treatment and subsequent reuse for showering and laundry.
- Preserve the environment at FOBs, reducing the environmental impact on indigenous communities while demonstrating innovative environmental stewardship.

Based on theoretical estimates of the efficiency of the proposed system and recent FOB studies performed for SERDP (Noblis 2010), significant benefits are expected in terms of energy, logistics, and water supply (Table 1). See Appendix B supporting documents for estimation methods used for Table 1. These estimates were generated based on the assumption of treating moderate strength wastewater and were performed in comparison to *aerobic* membrane bioreactor systems, a commercially-available wastewater treatment option. The estimates indicate that the proposed system would result in a substantial decrease in the logistical burden associated with wastewater treatment, water use, and energy consumption at FOBs. The system will be capable of producing more energy than it consumes, which will support self-sufficient FOB design goals. The energy and

logistics savings can result in rapid return on investment (ROI) for the Department of Defense (DoD). Calculated payback for operation in a FOB environment is less than one year for the clinoptilolite and Greenbox™ components.

Table 1. Estimated energy savings, energy production, water savings, and sludge reduction for the proposed technology.

FOB Characteristics			Conventional Technology*		Proposed Technology				
Base Size (persons)	Water Use (kgpd)	Waste-water Treated (kgpd)	Net Energy Balance (kwh/d)	Sludge Production (kgpd)	System Size (m³)	Net Energy Balance (kwh/d)	Water Demand Reduction (kgpd)	Reduced Sludge (kg/d)	Energy Cost Savings (\$/yr)
50	1.75	1.75	-13	9	3 (Quadcon)	+0.2	0.4	2	14.5K
500	17.5	17.5	-133	90	10 (Milvan)	+2	4.5	19	145K
1,500	52.5	52.5	-400	270	30 (Milvan)	+5	13.4	56	435K
10,000	350	350	-2667	1800	210 (7 Milvans)	+34.7	87.5	377	2.9M

* Conventional technology assumed to be *aerobic* membrane bioreactors.

The system footprint and modularity will be compatible with FOB transport constraints, with the smallest module fitting in a Quadcon, and the largest module fitting into a Milvan/International Standardization Organization (ISO) container.

Additional logistical benefits will result from using an anaerobic approach. Anaerobic systems generate less sludge than aerobic systems, and the anaerobic stabilization of the sludge will make it suitable for onsite disposal, if space is available. If space is not available onsite, fewer trucks will be required for sludge hauling. Water demand reductions would also be achieved, as the system will be designed to produce effluent water of suitable quality for non-potable reuse applications, such as toilet flushing, and equipment washing. Additional water savings (not shown in Table 1) could be achieved by integrating the proposed system with a ROWPU unit to produce water of higher quality. ROWPU units employ polymeric membrane systems to treat onsite water to a potable level. While ROWPU-treated reuse water might not be accepted for drinking, it will be suitable for showers, laundry, and other nearly potable applications.

2 Materials and Methods

The work entailed optimization of the component technologies followed by component integration and pilot scale system evaluation. AnMBR, clinoptilolite IX, and the GreenBox were each optimized for removal of organics, ammonia sequestration, and ammonia electrolysis for hydrogen production, respectively. After each component technology was optimized at the bench scale, the ability to function as an integrated system was evaluated.

2.1 AnMBR for removal of organics

AnMBR technology was evaluated and optimized for the biodegradation of organics in wastewater and associated generation of methane. Based on new concepts generated specifically in support of this proposal, a novel AnMBR reactor design was investigated. Baseline evaluations were performed at bench scale followed by a series of performance optimization through additive components and design modification.

The design goals for the AnMBR system were as follows*:

BOD < 30 mg/L (COD < 90 mg/L)
TSS < 30 mg/L
EC < 2 cfu/mL

when treating wastewater that is representative of FOB waste streams. Achieving these levels of treatment would allow for direct discharge of the wastewater into the local environment or to additional treatment systems for water reuse.

2.1.1 Methods to measure baseline capabilities of AnMBR technology for FOB wastewater treatment

Bench scale AnMBR systems were evaluated using synthetic wastewater with composition and design loadings that are representative of influent wastewater streams at FOBs. Sealed anaerobic reactor systems with foulant-resistant, hollow-fiber ultrafiltration (UF) membranes were set up at both ERDC-CERL and UIUC to assess performance against different types

* Biochemical oxygen demand (BOD), Total suspended solids (TSS), E. Coli (EC).

of wastewater streams that would be found at FOBs. The ERDC-CERL research team focused on treating representative FOB wastewater, and the UIUC team focused primarily on treating sludge associated with FOB wastewater processes that could be applicable to low-water waste streams (i.e., pit latrines) at outposts and smaller bases, and also for managing residual sludge associated with clarifiers and membrane bioreactors at bases supporting more than 100 persons.

2.1.2 Testing high throughput AnMBR capabilities for treating representative FOB wastewater

2.1.2.1 FOB wastewater quality for high throughput scenarios

In preparation for testing, an analysis of wastewater management at future FOBs was performed and the associated implications for influent wastewater quality were estimated. For future FOBs, it was estimated that each soldier requires 40 gpd of clean water, consistent with Force Provider planning factors, and 75% of which is discharged as gray water and can be reused at a recovery ratio of 80% (USAPHC 2010). This scenario is consistent with the ASAALT TecD4a goal of reducing FOB water demand by 75%. In this reuse scheme, the revised clean water demand is 16 gpd (10 gpd potable, 6 gpd for makeup of non-recovered gray water). Thus, the wastewater treatment system will also see 16 gpd. However, the waste stream will be more concentrated than conventional treatment streams, assuming the graywater reuse system rejects salts and does not provide TSS/BOD reductions (Table 2).

Table 2. Adjusted FOB wastewater influent characteristics accounting for future graywater reuse.

Parameter	Avg Treated Source water mg/L	Percent of WW influent:		Combined WW mg/L
		63%	38%	
		Blackwater mg/L	Gray water brine mg/L	
TDS	300	700	2500	1375
TKN	x	85	25	62.5
TSS	x	1500	750	1218.75
BOD5	x	400	400	400

Based on these calculations, a synthetic wastewater formulation was prepared with the following formulation (Table 3).

Table 3. Synthetic wastewater formulation to meet adjusted wastewater influent characteristics.

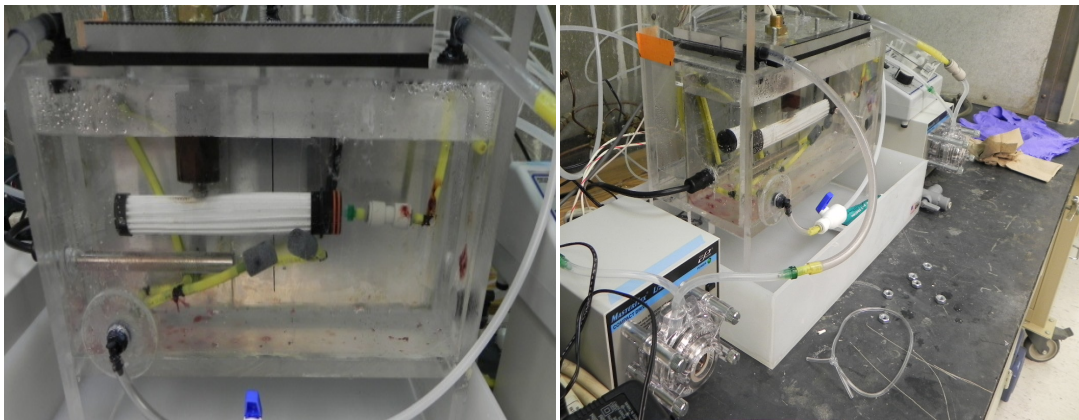
Component	ppm
Milk powder	464
Beef extract powder	390
Yeast extract powder	183.75
SDS	9
Sodium Phosphate	18
Test dust	31.25
Urea	201
NH ₄ Cl	47.75

The resulting influent COD value for this formulation was 1380 ± 260 ppm, based on over 12 randomly timed samples during experimental studies. COD values were typically 2.5–3X higher than BOD values. All influent TSS values were greater than 1000 ppm.

2.1.2.2 High-throughput AnMBR technology testing

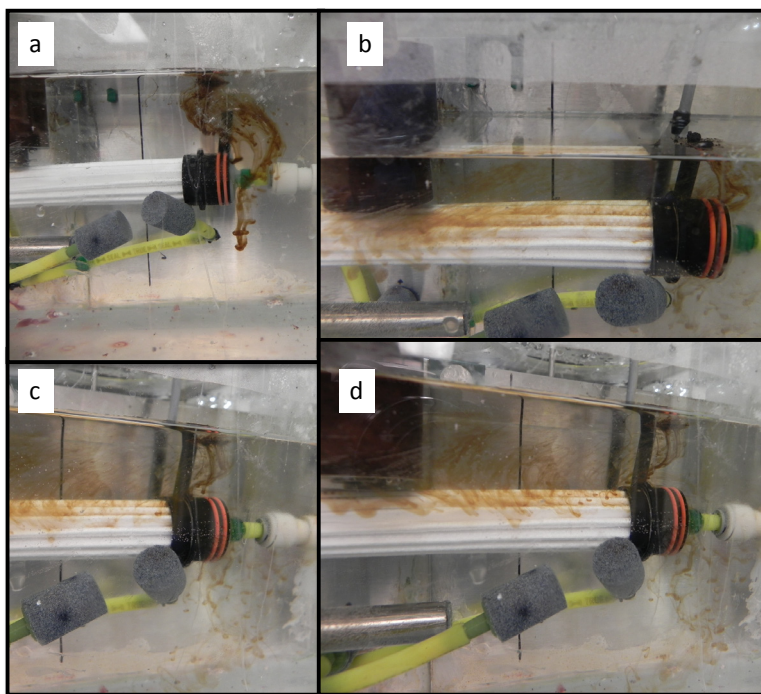
A bench-scale version of the FOB-containerized AnMBR system was custom designed and assembled at ERDC. The reactor was reconfigured to account for design improvements made during the first two quarters of the project. The high-throughput organic concentration chamber will be used to sequester dissolved organics using adsorbent media and also to preliminary biodegradation. It has a hydraulic retention time (HRT) of 3 hours, controlled via the effluent flow pump that pulls water through the membrane. As the membrane fouls, the effluent flow pump can be adjusted to maintain the target HRT. Sustained flow of influent into the reactor is controlled through a float switch that activates the influent flow pump when the reactor volume decreases by 8%. The system is shown in Figure 2.

Figure 2. High rate AnMBR process chamber for biodegradation of soluble organics and separation of particulates.



Tracer testing was performed on all reactors to confirm that the effluent water was being pulled through the membrane and not through any leaks in the reactor piping. For tracing, solid humic acid was added at the top of the water tank, which dissolves slowly and forms a dark brown color. When the humic acid was first added near potential leak locations, water was being pumped into the tank only, causing a clockwise rotation (Figure 3a). Next, the effluent pump was turned on, resulting in flow of water toward the membrane filter surface (Figure 3b). When the influent pump was turned off, the flow was directed entirely toward the membrane (Figure 3c). After a short time under these flow conditions it was clear that the flow was only exiting the reactor through the membrane (Figure 3d).

Figure 3. Tracer testing to confirm water flow through the membrane element. Solid humic acid sodium salt tracer was added near potential leak sites prior to turning on the effluent pump. Turning on the effluent pump pulled the water away from the module fittings and through (into) the membrane element.



2.1.3 Testing AnMBR capabilities for treating highly concentrated fob wastewater/sludge

The primary sludge (PS) substrate used over the course of this study was collected from the Urbana wastewater treatment facility in 4 batches. For each batch, 150-200 L of PS was collected in 5 gallon plastic buckets and stored at 4 °C until use. Table 4 describes the characteristics of each batch of PS. In the case of Batches 4 and 5, the total and volatile solids content (TS and VS) were slightly higher than previous batches, therefore both of these batches of PS were diluted prior to feeding (Figure 4). The TS and VS concentrations for Batches 4 and 5 after dilution are shown in parenthesis in the table below. Total and soluble COD data shown for Batches 4 and 5 in the table below are after dilution.

Table 4. Characteristics of each batch of primary sludge substrate collected and used over the course of this study.

	Batch 1	Batch 2	Batch 3	Batch 4*	Batch 5*
Date Collected	10/22/12	5/10/13	11/13/12	5/12/14	12/4/14
Days of Use	87-302	303-485	486-666	667-947	948-present
pH	5.34	5.55	5.35	5.43	5.58
C:H:N:O ⁺ (by mass)	44:6:3:30	39:5:3:28	43:6:5:23	43:6:3:31	42:6:4:29
Theoretical CH ₄ (ml/g VS)	469.4 ±23.2	402.7 ±8.8	469.3 ±15.9	436.0 ±15.6	436.8 ±16.4
Total Solids (g/L)	25.2 ±4.4	24.8 ±5.6	24.4 ±4.7	38.8 ±1.7 (24.2 ±3.3)	39.6 ±4.1 (24.0 ±3.2)
Volatile Solids (g/L)	18.6 ±5.2	19.1 ±5.2	18.6 ±4.3	32.5 ±4.3 (19.5 ±3.4)	22.3 ±1.0 (18.1 ±0.4)
Total COD (mg/L)	43375 ±5495	29186 ±8900	30590 ±9100	36891 ±11684	39499 ±5944
Soluble COD (mg/L)	5360 ±1121	5242 ±960	5374 ±1798	6464 ±1300	7244 ±880

*Batches 4 and 5 were diluted prior to feeding in order to better match previous influent VS concentrations. TS and VS values after dilution are shown in parenthesis. Total and soluble COD data shown for Batch 4 and 5 are after dilution.

*The percentage of oxygen was determined by subtracting the percentage of the other three elements and the ash content from 100.

Figure 4. Highly concentrated wastewater feedstock.



The continuous pilot AnMBR system was set up as a two-phase anaerobic digestion system with physically separate acid phase and methane phase tanks since it provides improved control and optimization of both processes (Hernandez and Edyvean 2011). The pre-digestion, or acid phase (AP), reactor was seeded with a 1:4 mixture of PS and primary effluent, respectively, from the Urbana-Champaign Sanitary District Northeast Treatment Facility's primary settling tank. The methane phase (MP) reactor was seeded with anaerobic sludge from the primary anaerobic digester at the Urbana-Champaign Sanitary District Northeast Wastewater Treatment

Plant. Figure 5 shows the two-phase pilot AnMBR system design schematic, while Figure 6 provides a picture of the physical reactor setup at UIUC.

Figure 5. Continuous AnMBR design schematic.

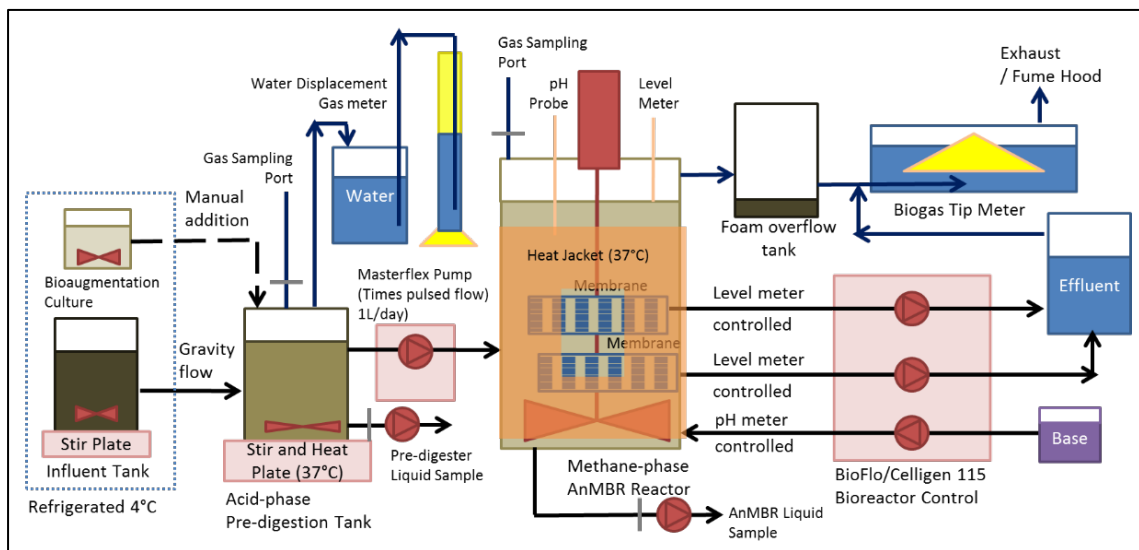
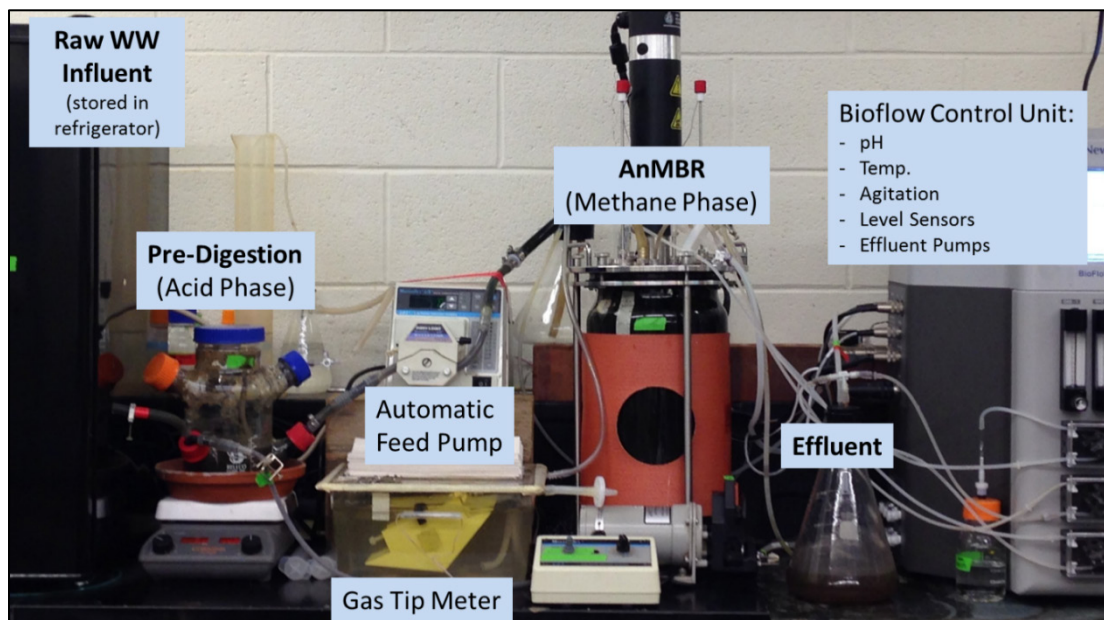


Figure 6. Continuous AnMBR system physical setup.



Automatic feeding was carried out via a computer Python script used to command a Labjack U3 DAC which controlled a Masterflex LS 07523-40 pump that intermittently pumped liquid from the 2.5 L gastight AP reactor (Belco) to the gastight MP reactor that provided the targeted daily flow rate. When this pump transferred liquids between the AP and MP reactors,

it also drew new influent wastewater into the AP reactor from a stirred and refrigerated influent storage tank (4°C). Heating for the AP reactor was provided by a heated magnetic stir plate, and the reactor was completely mixed using a magnetic stir bar attached to an impeller inside the reactor. The MP reactor consisted of a 14 L New Brunswick BioFlo 115 bioreactor. A BioFlo control unit provided mixing, and control of temperature, pH control and water level. Default settings for mixing and pH were 120 RPM and 7.4, respectively. The Bioflo unit controlled the pumping of effluent out through submerged microfiltration membranes in the MP reactor that monitored and maintained the desired reactor liquid level. MP biogas was continuously measured using a Wet Tip Gas Meter. A gas outlet from the effluent tank was connected to a tip meter to account for any gas that may be pulled through the membranes.

For the majority of operation, two 10 µm pore size, 0.11 m² cylindrical Omnifilter RS14-DS sediment filter cartridges served as the submerged membrane filtration component of the AnMBR system. A flux of <5 L m⁻² h⁻¹ was targeted to minimize fouling (Skouteris et al., 2012). Each filter cartridge was able to initially achieve 0.373 L m⁻² h⁻¹ at a flowrate of 1L/day. However, replacement of the filter cartridges was required every 3-5 months to maintain the required flowrate. To accommodate placement of the filter cartridges in the MP reactor, each cartridge was cut in half as shown in Figure 7.

Early in the project, a custom-built 0.2 µm pore size, 0.15 m² polyethersulfone hollow-fiber membrane was ordered from Membrana GmbH, and it was intended to be used as the membrane filtration component in the AnMBR system. This membrane selection was based on literature reports of advantageous membrane characteristics for an AnMBR system including: hydrophilic and negatively charged hollow-fibers made from organic polymers with a 0.1 – 0.45 µm pore size (Bérubé et al. 2006; Hai et al. 2005; Kang et al. 2002; Singhanian et al. 2012). However, the Membrana membrane installed between Days 131 and 190 was unable to achieve the required effluent flow rate due to the housing design, which plugged with sludge during use in the pilot AnMBR reactor. The original Membrana membrane module is shown in Figure 8A and Figure 8B. The Membrana membrane housing was modified on Day 138 to have larger holes in an attempt to decrease plugging of the membrane housing and improve liquid flow through the membrane. Figure 8C and Figure 8D show the casing modifications made to the membrane housing. However, this modification

was only partially effective and despite the significantly greater surface area of the Membrana membrane, the sediment filters were able to achieve greater reactor flow rates and membrane surface fluxes. Another likely contributing factor to lower flux with the Membrana membrane was the tight bundling of the hollow fibers, which probably made the innermost fibers inaccessible after significant biofouling.

Figure 7. Modified sediment filters prior to application in the AnMBR system.

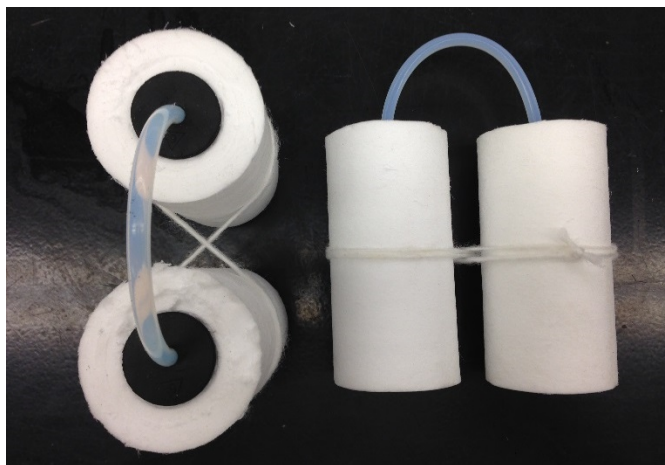
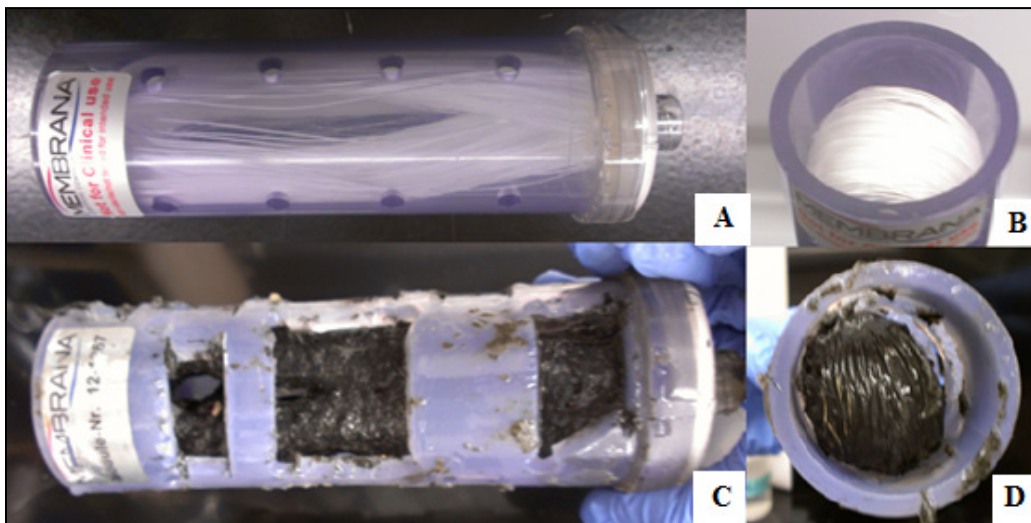


Figure 8. Custom-built Membrana membrane, before (A and B) and after (C and D) housing modifications.



Due to the Membrana membrane's insufficient flux, the system was switched back to using the sediment filter cartridges. At this time, an extra filter cartridge was added to decrease the loading on a single membrane. On Day 198, the two sediment filters were modified by halving their length

and connecting the two ends with a flexible tube, which allowed for a decrease in AnMBR reactor liquid volume, and thereby lowering the AnMBR reactor HRT. The membrane selection in this case was significantly affected by the lack of commercially available membranes for laboratory scale membrane bioreactors. For larger scale practical applications there is a wide variety of commercially viable membrane systems that have proven to be effective for membrane bioreactors in wastewater treatment applications. For instance, Kubota, Siemens-US Filter, and GE-Zenon all make membrane bioreactor systems that have been successfully used in full-scale wastewater treatment plants.

The AnMBR for treating highly concentrated waste streams was designed with the following major features (see Table 5 and Table 6):

- Wastewater sequentially flows from a feed tank to a pre-digestion tank, the main AnMBR reactor, and an effluent tank.
- Raw wastewater flows from the feed tank into the pre-digestion tank by gravity as material is pumped from the pre-digestion tank into the AnMBR at a rate of roughly 1L/day, corresponding to a 12 day HRT. In order to use higher velocities and tube sizes suitable for passing wastewater solids, the main AnMBR reactor is actually fed for 3 minutes every 4 hours at 58 ml/min from the pre-digestion tank, which corresponds to a flow rate of 1.044L/day. As wastewater is pumped into the AnMBR, the same amount of water is passed through the membrane in this reactor and flows into the effluent tank.
- The feed tank is stored in a refrigerator set at 4 °C in order to minimize biological activity prior to entering the pre-digestion tank. The pre-digestion tank and the main AnMBR are operated at a mesophilic temperature of 37 °C for optimum microbial performance.
- Bioculture addition was done either manually or by programmed pumping depending upon the dosage rate. Solid-liquid separation will be achieved using a Membrana-Charlotte submerged ultrafiltration (UF) membrane module with a surface area of 0.03–0.05 m² and a design flux of 1–5 LMH. Temporarily, a 10 µm filter is being used while the ultrafiltration membrane module is being constructed, as noted earlier.
- The pre-digestion reactor is a 2L Bellco bioreactor flask and is operated at a HRT of 2 days. A New Brunswick Bioflo/Celligen 115 Bioreactor is used as the main AnMBR reactor. The 14 L working volume—including the space occupied by the mechanical agitator—is adequate for holding

the membrane, the agitator, and a liquid volume of over 12 L. There are extra volume and ports which provide the potential to integrate adsorbents, such as IEX resin, both internally and externally.

- Automated flow control is provided in and out of the AnMBR reactor as well as for periodic backwashing of the membrane. A wet tip gas meter, with a resolution of 35ml, is used to measure constant AnMBR biogas production. Biogas quantity data is recorded at set time intervals (e.g., current setting is every 5 minutes). Other automation features that come with the Bioflo include wet/dry level sensors, dissolved oxygen, pH, temperature and mixing controls.

Table 5. AnMBR system control and data logging.

Control Unit	System component	Function
Bioflo Controller	pH meter	Control base/acid addition
	Wet level meter	Feedback to operate effluent pump
Computer/ Data Acquisition Device	Masterflex pumps (programmable)	Control pumping and timing of feeding and backwashing
	Flowmeter	Log effluent flow rate data
	Biogas tip meter	Log biogas production data
	Pressure sensor	Monitor and log transmembrane pressure data

Table 6. Design parameters for the AnMBR system.

Parameters	Pre-digestion tank	AnMBR reactor
Flow rate (L/day)	1	1
HRT (days)	2	12
Temperature (°C)	37±1	37±1
pH control	5-6	7.0-7.8
Bioaugmentation	Based on cell count #/g VS	---
Membrane	---	Submerged, hollow-fiber, 0.2 µm pore size, hydrophilic
Organic loading rate (OLR) (g VS/L-day)	TBD	TBD
Flux (LMH)	1-5	1-5

Over the course of this study, the pilot AnMBR system was operated for more than 1000 days. During this time, a working liquid volume of 1-1.5 L and an average HRT of 1 day was maintained in the AP reactor, while a working liquid volume of 10-12 L and an average HRT of 12 days was maintained in the MP reactor. The system experienced a start-up period of

126 days, during which time some fluctuations and adjustments in organic loading rate (OLR) were made. The OLR after start-up was maintained near 1.4 g COD/L·day.

After start-up, the system performance was evaluated over four different operating periods: (1) Bioaugmentation 1, (2) No Bioaugmentation, (3) Bioaugmentation 2, and (4) Ambient (Temperature) with Bioaugmentation. The first three periods of operation were carried out under mesophilic temperatures (37 °C), and investigated the effects of daily bioaugmentation in the acid phase on overall system performance. The bioculture used for Bioaugmentation 1 consisted of recycled anaerobic sludge from the methane phase and a proprietary bioculture blend to the acid phase of the system. During the Bioaugmentation 2 period, the bioculture was changed to only include the proprietary bioculture blend and did not include the recycled anaerobic sludge used during the previous Bioaugmentation 1 period. Finally, during the last period of operation, bioaugmentation to the acid phase continued as during Bioaugmentation 2, while the temperature in the methane phase was reduced to ambient conditions (20 °C). Table 7 summarizes the operating parameters in both phases of the AnMBR system during the four periods of operation.

Table 7. Description of operating periods (after start-up) in the AnMBR system over the course of this study.

	Bioaugmentation 1 (Day 126-226)		No Bioaugmentation (Day 227-374)		Bioaugmentation 2 (Day 375-653)		Ambient Temp. (Day 654-present)	
	AP	MP	AP	MP	AP	MP	AP	MP
OLR (gCOD/ L d ⁻¹)	1.73 ±0.9	—	1.43 ±0.3	—	1.39 ±0.5	—	1.30 ±0.5	—
pH	4.7 ±0.2	7.5 ±0.1	5.4 ±0.7	7.5 ±0.1	5.3 ±0.5	7.6±0.1	5.4 ±0.7	7.4 ±0.6
Temperature (°C)	37 ±3	37 ±1	37 ±3	37 ±1	37 ±3	37±1	37 ±3	20 ±2
Bioaugmentation	3.9% of VS 50:50 sludge + proprietary	—	—		3.9% of VS proprietary	—	3.9% of VS proprietary	—

2.1.4 Methods to optimize AnMBR performance

Following the measurement of baseline capabilities of the AnMBR, experimental work focused on optimizing the rapid establishment of a mature anaerobic microbial ecosystem to include hydrolytic, acidogenic, acetogenic, and methanogenic microorganisms. Bioreactor maturation enhancement strategies were evaluated to minimize time between reactor startup and peak performance. These included reactor seeding with cus-

tom biocultures, water quality adjustment, anion-exchange resin augmentation, and temperature control. To bolster AnMBR robustness and performance, the use of anion-exchange resin as a support for microbial growth and as a buffer for distributing peak organic loads was investigated.

Bioaugmentation. In general, a typical anaerobic digestion process consists of four main steps: hydrolysis, acidogenesis, acetogenesis and finally methanogenesis, which produces the desired bio-methane end product (Metcalf and Eddy 2004; Nwuche and Ugoji 2008, 2010). Previous research has identified hydrolysis as a common rate-limiting step in anaerobic digestion and proposed different pretreatment methods to enhance hydrolysis rates (Parawira et al. 2004; Nair et al. 2005). Most of the pretreatment methods used in previous studies can be categorized as either physical pretreatment (e.g., thermal, ultrasonic or mechanical mixing etc.) or chemical pretreatment (e.g., alkaline, thermochemical etc.) (Park et al. 2005). Biological augmentation of the bacterial community that performs hydrolysis is another approach to improving this rate limiting step, but this has not received much attention in previous research.

Besides hydrolysis, acetogenesis has also been identified as a potentially rate-limiting step by several studies, which noted that acetogens are slow growers, sensitive to physical and chemical conditions (e.g., pH, temperature, etc.), and their metabolism is less thermodynamically favorable than some of its competitors (Mahmood et al. 2006, Amani et al. 2011). For instance, sulfate reducing bacteria are a major competitor with acetogens that consume the same fatty acid substrates and produce an undesirable by-product, hydrogen sulfide. This side reaction reduces methane production because it reduces the amount of fatty acids that are converted by acetogens into acetate, which is one of the two primary substrates for methanogens. Even worse, hydrogen sulfide causes corrosion problems during combustion of biomethane and can have toxic effects on many microorganisms (Chen et al. 2008). One study has shown that enriching acetogenic species under mesophilic and thermophilic anaerobic digestion can increase metabolic activity of acetogens in anaerobic processes (Ryan et al. 2010). This can help in two ways: first by shifting the microbial community to increase the kinetics of a potentially rate-limiting step, and second by decreasing the relative proportion of organic substrates converted to undesirable by products.

A specific bioaugmentation strategy was investigated for targeting improvements in the rate-limiting steps of hydrolysis and acetogenesis during anaerobic digestion. Bioaugmentation was applied daily to the acid phase reactor, and two different bioculture mixtures were investigated. Beneficial effects of bioaugmentation on substrate hydrolysis and acetogenesis, as indicated by increased acid phase soluble COD and acetic acid concentrations, were investigated along with the subsequent benefits to methane production. The following sections provide detailed discussion regarding bioculture selection and AnMBR system performance with and without bioaugmentation.

A schematic of the bench-scale reactor operation is shown in Figure 9 and Figure 10. The bench-scale batch digestion system used AP sequencing batch reactors with an operational volume of 150 ml and 3 days HRT. Methane phase reactors were operated as semi-batch reactors with a bi-daily addition of 10 ml substrate from the acid phase sequencing batch reactors for the first 20 days. On Day 0, 30 ml anaerobic digestion sludge (ADS) was added as initial inoculum into the methane phase reactor. Each day, bioculture was added to the AP reactors in the amount equivalent to 5% of the substrates from AP reactor volatile solid (VS) content. Biogas, SCOD, HAc, HPr, HBu, total VFAs, pH, TS, and VS were analyzed and compared among the following different treatments: (a) PS + solid control, (b) Bioc, (c) ADS and (d) Bioc + ADS. Additionally, at least three measures of total/soluble carbohydrates, total/soluble protein and lipids were performed at steady state in order to evaluate the degree of hydrolysis between bioaugmentation and non-bioaugmentation. The dried PS solid used as additional solids, and the proprietary bioculture blend and concentrated ADS used as bioaugmented biocultures are shown in Figure 11. The characteristics of the substrate and two biocultures (Bioc and ADS) are listed in Table 8.

Figure 9. Acid phase sequencing batch experimental setup.

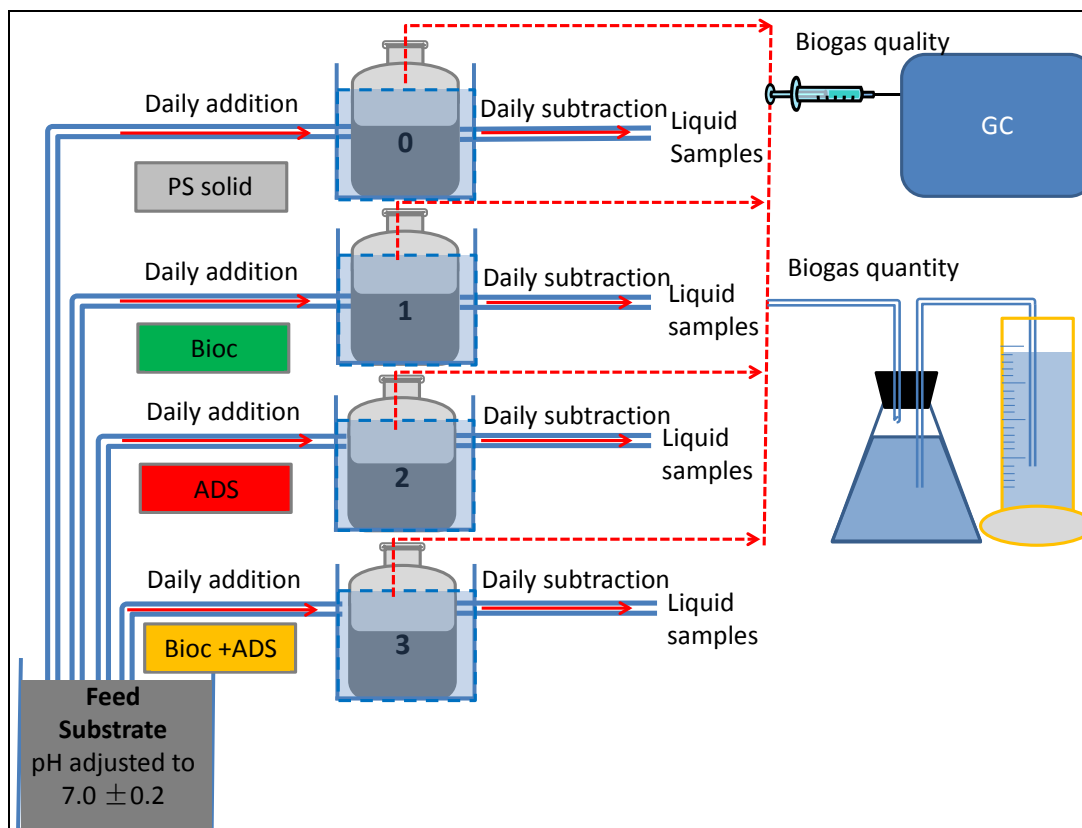


Figure 10. Methane phase semi batch experimental setup, a total of three reactors were set up for PS + solid, Bioc and ADS methane phase reactors.

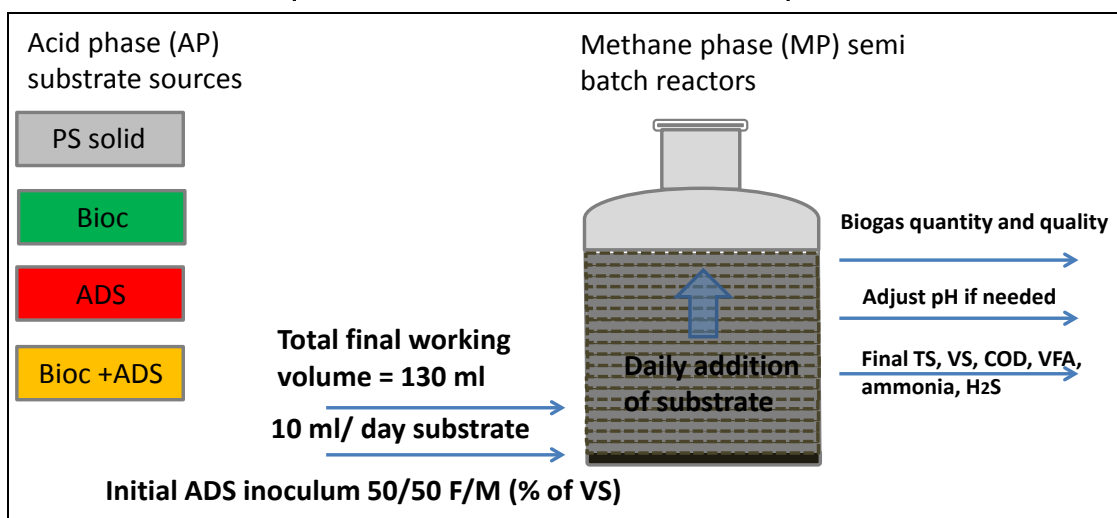


Figure 11. Dried PS solid for the control, Bioc blend for the Bioc acid phase sequencing batch reactor and ADS for the ADS acid phase sequencing batch reactor.



Table 8. Bench scale influent and inoculum characteristics.

	PS	ADS	Bioc
TS (g/l or %)	40.3 ± 0.3	10.5 ± 0.2	84.4 % ± 1.5 %
VS (g/l or %)	33.3 ± 0.1	7.5 ± 0.2	81.7 % ± 1.1 %
TSS (g/l or %)	29.9 ± 1.8	9 ± 0.3	72.7 % ± 1.1 %
VSS (g/l or %)	23.7 ± 1.7	7.1 ± 0.3	70.5 % ± 0.6 %
SCOD (mg/l)	5017 ± 293	---	---
Total VFA (mg/l)	2946 ± 106	ND	ND
C (% of total VS)	45.5 ± 0.9	---	---
H (% of total VS)	6.3 ± 0.1	---	---
N (% of total VS)	3.5 ± 0.1	---	---
O* (% of total VS)	44.7 ± 0.9	---	---
pH	5.87 ± 0.06	7.20 ± 0.03	
NH ₃ -N (g/l)	0.58 ± 0.06	---	---
Carbohydrates (g Glu-eq/l)	12.0 ± 0.2	---	---
Proteins (g BSA-eq/l)	8.1 ± 0.3	---	---
Lipids (g/l)	10.6 ± 0.6	---	---

Note: values represent mean ± standard deviation; PS, primary sludge; Bioc, proprietary bioculture bioaugmentation treatment; ADS, anaerobic digestion sludge bioaugmentation treatment. '---' not available; 'ND' not detected at detection limit of 100 ppm; Glu-eq is glucose equivalent, BSA-eq is bovine serum albumin equivalent.

2.1.4.1 Adsorbents for AnMBR enhancement

To further improve organics removal and methane production in the AnMBR system, the addition of adsorbents was investigated. The adsorbents can serve as a temporary physico-chemical sink for soluble organics, reducing the amount that escapes from the system and extending the time available for conversion into methane. As a result, methane production

and effluent quality can be improved. In addition, previous literature has shown that the addition of adsorbents can be beneficial in mitigating shock-loading events and improving membrane flux by providing additional scouring of the membrane surface (Akram and Stuckey 2013, Yoo et al. 2012).

Several candidate adsorbents and ion-exchange materials were investigated for their potential to adsorb soluble organics, in particular VFAs, and to improve methane production. The best of these materials was then deployed in the pilot-scale continuous AnMBR system to investigate and quantify the benefits provided by the adsorbent in terms of reactor performance and stabilization during shock-loading events. Five adsorbent materials for implementation into the continuous AnMBR system were evaluated in terms of their ability to adsorb sCOD, specifically volatile fatty acids (VFAs), and their benefit to methane production. Table 9 provides a description of the various candidate adsorbent materials that were investigated. These materials were chosen for their ability to adsorb negatively charged organic compounds (i.e., VFAs and other sCOD). Two different commercially available strong- and weak-base anion-exchange resins were tested and compared to granular activated carbon (GAC).

Table 9. Description of candidate adsorbent/ion-exchange resin materials.

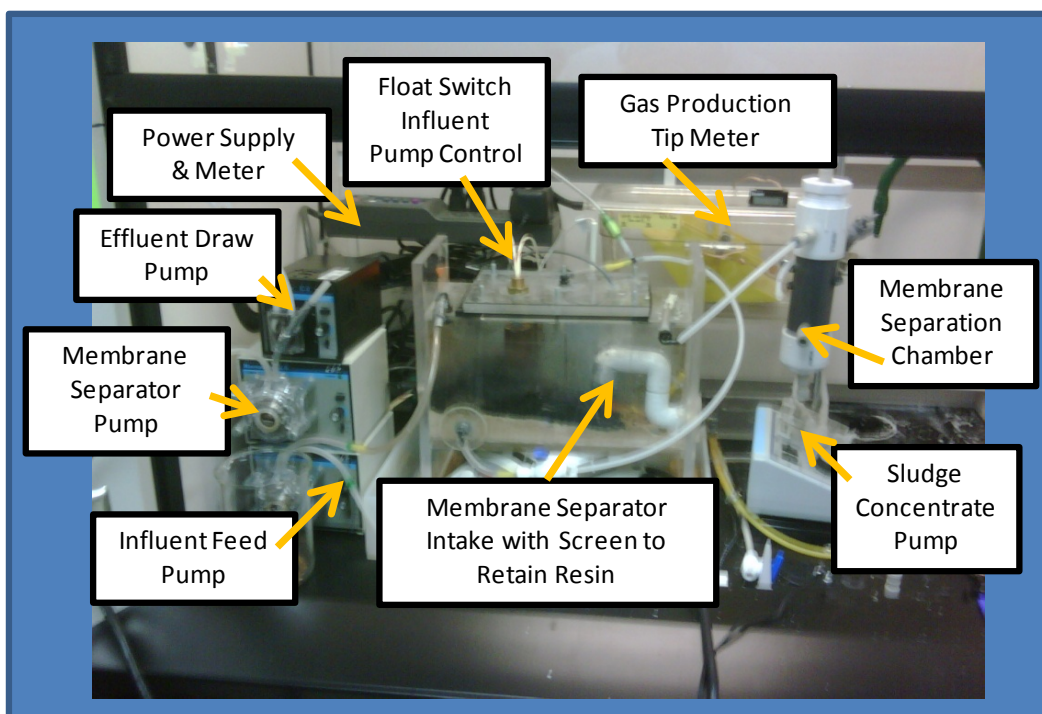
Resin/Adsorbent	Type	Matrix	Ionic Form	Functional Group	Size (mm)
Granular Activated Carbon	adsorbent	activated carbon	na	na	1.2-1.6
Purolite® Tanex™	mixed strong base anion-exchange resins	Styrene & Acrylic w/ Divinylbenzene	Cl ⁻	Quarternary Amine	0.3-1.2
Purolite® A510	strong base anion-exchange resin	Macroporous Polystyrene w/ Divinylbenzene	Cl ⁻	Type II Quarternary Ammonium	0.3-1.2
Purolite® A845	weak base anion-exchange resin	Gel Polyacrylic w/ Divinylbenzene	OH ⁻	Tertiary Amine	0.3-1.2
Purolite® A830	weak base anion-exchange resin	Macroporous Polystyrene w/ Divinylbenzene	OH ⁻	Complex Amine	0.3-1.2

2.1.5 Hybrid AnMBR reactor design for optimization testing

A modified bench-scale AnMBR system was built for optimization testing (Figure 12). The primary modification was the separation of the membrane

module from the bioreactor, which facilitated membrane isolation capability for cleaning cycles and fouling evaluations. For retention of adsorbents in the processing chamber, a screened vertical intake port within the bioreactor will facilitate retention of resin and GAC particles, while allowing bioflocs and small particulates to be delivered to the membrane separator for sludge concentration. Biogas generation was measured using a tip meter.

Figure 12. Hybrid AnMBR reactor design for optimization testing.



Experiments were performed in this system to study augmentation of the bioreactor with Tanex™ ion-exchange resin, granular activated carbon, and commercial biocultures. Bioculture dosing was either at startup (for the high throughput AnMBR studies) or continuous (for the highly concentrated wastewater AnMBR treatment studies).

2.1.6 Clinoptilolite for ammonia sequestration

Selective removal of ammonia via ion exchange onto clinoptilolite was investigated. Key parameters determined during this process were ammonia

* Tanex is a trademark of Purolite, Bala Cynwyd, PA 19004.

composition and flow rates, clinoptilolite selection and preparation, column setup, regeneration procedures, and ammonia analysis methods.

2.1.6.1 Ammonia solution composition and flow rates

To assess the capability of clinoptilolite for ammonia sequestration, its ion-exchange capacity and selectivity were evaluated using representative AnMBR effluent. It is expected that gray water reuse will become more prevalent at FOBs in the near future resulting in more concentrated effluent brines in the wastewater stream. Accordingly, a value of 80 mg/L-N was chosen for the ammonia concentration, which is on the high end of measured wastewater values in traditional treatment systems. The ammonia was introduced as aqueous ammonium chloride (NH_4Cl). Real water runs were made using water from the AnMBR or from the Urbana-Champaign Sanitary District Northeast Treatment Facility following primary treatment.

Working backwards from an expected full-scale design with a 1 m x 1 m clinoptilolite column footprint, a design flow rate of 3.96 L/hr was calculated. To provide the same flux through the clinoptilolite column in the bench-scale and final designs, a flow rate of 60 mL/min was calculated for the column diameter. At times, the flow rate was modified slightly due to pump limitations or experimental design.

2.1.7 Clinoptilolite selection and preparation

Sources of clinoptilolite for study focused on those that were commercially available. However, some samples from bulk suppliers were also obtained. Table 10 below lists the sources of clinoptilolite identified.

Table 10. Sources of clinoptilolite identified.

Manufacturer	COTS/Bulk	Product name	Particle Size
API	COTS	AmmoChips	~8 mm
Ida-Ore	COTS	Pet Fresh Enviroguard Shoe Powder Carpet Deodorizer	Powders
KMI	Bulk	-	Various
Northern Filter Media	COTS	Zeobest	~1 mm
St. Cloud	Bulk	-	Various

Initially, AmmoChips were chosen due to their larger size and easy availability through multiple vendors. While their size was beneficial for not creating large amounts of back pressure, ammonia diffusion into the particles was an issue (see Results and Discussion). Zeobest resulted in more optimal performance with acceptable back pressure.

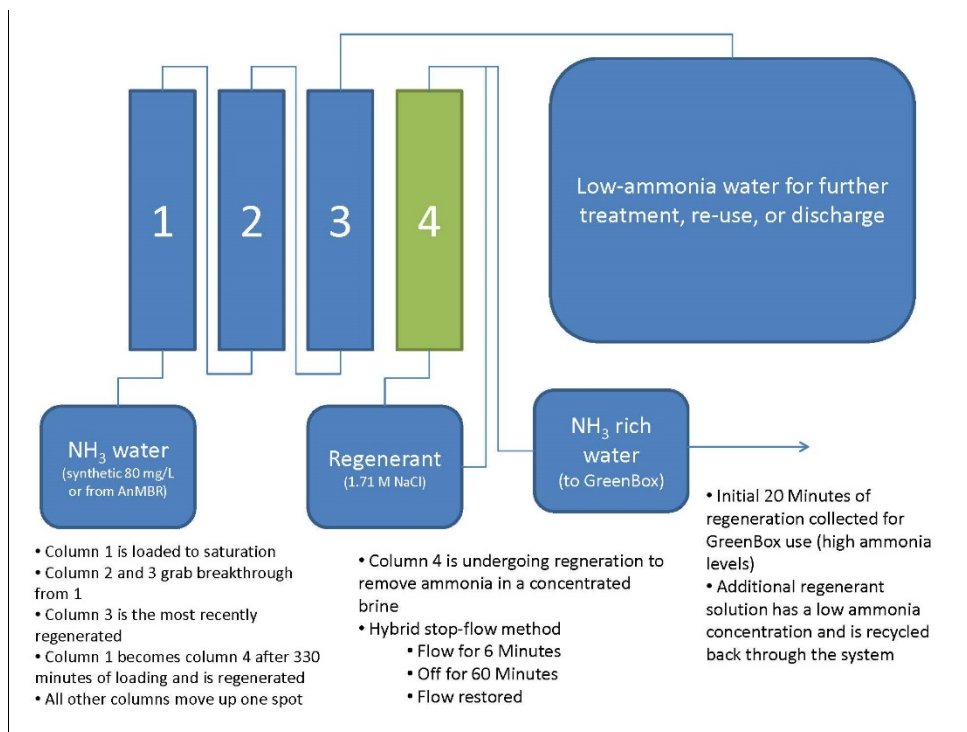
Prior to the first use, all clinoptilolite was well rinsed to remove surface dust and other small particulates. The media was then treated with a 10% NaCl solution to ensure all active sites were in the sodium form. In flow setups, the NaCl was introduced at a rate of 20-50 mL/min. Additional particulates were removed during this treatment.

2.1.8 Column setup

The clinoptilolite columns were operated in an up flow manner. Ammonia or regenerant solution was introduced at the bottom of the column via flexible tubing. A small piece of filter material prevented the clinoptilolite from flowing downward into the tubing. 75g of the Zeobest material provided a balance between significant ammonia uptake and a reasonable loading cycle. Solution exits through the top of the column and enters a flow meter before being redirected back into the system or sent to waste.

Initial evaluation and optimization studies utilized a single column or a set of columns where each functioned individually. As the design progressed towards integration, a multi-column series design was implemented (Figure 13). The series operation of three columns allowed the first column to become fully loaded while the additional columns collected any ammonia breakthrough. A fourth column in this design undergoes regeneration while the others are being loaded.

Figure 13. Multi-column clinoptilolite column design allowing for simultaneous loading and regeneration cycles.



Along with the new configuration, some rudimentary automation was integrated into the system. The series of four columns are controlled by solenoid valves through a programmed microcontroller. The flow path of the columns was mapped out allowing for a program to be compiled in the Arduino microcontroller software. A set of low current relays were employed and paired the solenoid valves in order to maximize the microcontroller's available control nodes. Figure 14 shows the current version of the control code for the system. Each sub-program 0 through 4 activates the system according to the time delay listed at the beginning of the loop. There are twelve available control nodes on the microcontroller, each of which are identified as "digitalwrite(-)". The "LOW/HIGH" states represent the open or closed nature of the valves associated with each node during a particular sub-program. Figure 15 shows a virtual image of the microcontroller and the column setup.

Figure 14. Control code for microcontrollers on clinoptilolite columns.

```

int powerState = 0;

void setup(){
  SubA();
}

void loop(){
  powerState = digitalRead(13);
  //pin13 is power input

  if (powerState==LOW){
    Sub0();
  }

  else{ //button pressed, activate sequences
    Sub1();
    delay(600000);
    Sub0();
    delay(250);
    Sub2();
    delay(600000);
    Sub0();
    delay(250);
    Sub3();
    delay(600000);
    Sub0();
    delay(250);
    Sub4();
    delay(600000);
    Sub0();
    delay(250);
  }
}

void SubA(){
  pinMode(1,OUTPUT);
  pinMode(2,OUTPUT);
  pinMode(3,OUTPUT);
  pinMode(4,OUTPUT);
  pinMode(5,OUTPUT);
  pinMode(6,OUTPUT);
  pinMode(7,OUTPUT);
  pinMode(8,OUTPUT);
  pinMode(9,OUTPUT);
  pinMode(10,OUTPUT);
  pinMode(11,OUTPUT);
  pinMode(12,OUTPUT);
  pinMode(13,INPUT);
}

void Sub0(){
  digitalWrite(1,LOW); //closed
  digitalWrite(2,LOW); //closed
  digitalWrite(3,LOW); //closed
  digitalWrite(4,LOW); //closed
  digitalWrite(5,LOW); //closed
  digitalWrite(6,LOW); //closed
  digitalWrite(7,LOW); //closed
  digitalWrite(8,LOW); //closed
  digitalWrite(9,LOW); //closed
  digitalWrite(10,LOW); //closed
  digitalWrite(11,LOW); //closed
  digitalWrite(12,LOW); //closed
}

void Sub1(){
  digitalWrite(1,HIGH); //open
  digitalWrite(2,HIGH); //open
  digitalWrite(3,HIGH); //open
  digitalWrite(4,LOW); //closed
  digitalWrite(5,LOW); //closed
  digitalWrite(6,LOW); //closed
  digitalWrite(7,LOW); //closed
  digitalWrite(8,LOW); //closed
  digitalWrite(9,LOW); //closed
  digitalWrite(10,LOW); //closed
  digitalWrite(11,LOW); //closed
  digitalWrite(12,HIGH); //open
}

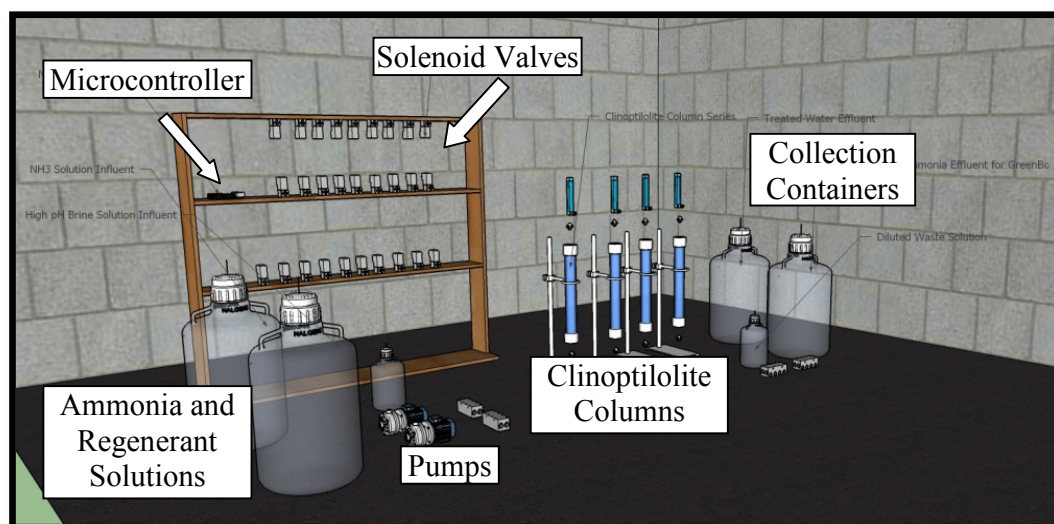
void Sub2(){
  digitalWrite(1,LOW); //closed
  digitalWrite(2,LOW); //closed
  digitalWrite(3,HIGH); //open
  digitalWrite(4,HIGH); //open
  digitalWrite(5,HIGH); //open
  digitalWrite(6,LOW); //closed
  digitalWrite(7,LOW); //closed
  digitalWrite(8,LOW); //closed
  digitalWrite(9,HIGH); //open
  digitalWrite(10,LOW); //closed
  digitalWrite(11,LOW); //closed
  digitalWrite(12,LOW); //closed
}

void Sub3(){
  digitalWrite(1,LOW); //closed
  digitalWrite(2,LOW); //closed
  digitalWrite(3,LOW); //closed
  digitalWrite(4,LOW); //closed
  digitalWrite(5,HIGH); //open
  digitalWrite(6,HIGH); //open
  digitalWrite(7,LOW); //closed
  digitalWrite(8,HIGH); //open
  digitalWrite(9,LOW); //closed
  digitalWrite(10,HIGH); //open
  digitalWrite(11,LOW); //closed
  digitalWrite(12,LOW); //closed
}

void Sub4(){
  digitalWrite(1,LOW); //closed
  digitalWrite(2,LOW); //closed
  digitalWrite(3,LOW); //closed
  digitalWrite(4,LOW); //closed
  digitalWrite(5,LOW); //closed
  digitalWrite(6,LOW); //closed
  digitalWrite(7,HIGH); //open
  digitalWrite(8,HIGH); //open
  digitalWrite(9,LOW); //closed
  digitalWrite(10,LOW); //closed
  digitalWrite(11,HIGH); //open
  digitalWrite(12,LOW); //closed
}

```

Figure 15. Virtual image of the microcontroller and column setup.



2.1.9 Regeneration procedures

Regeneration of the clinoptilolite was performed to release the captured ammonia and to clean the media for subsequent loading. A 10% NaCl solution was chosen as the primary regenerant solution. The abundance of Na⁺ ions in the solution favored replacement of the NH₄⁺ ions attached to the active sites on the clinoptilolite and released them into the brine. If required, pH of the regenerant solution was increased through the addition of sodium hydroxide (NaOH).

Since a continuous flow of NaCl through the clinoptilolite resulted in slow removal of the ammonia and a dilute final ammonia concentration, a stop-flow method for regeneration was developed. The regenerant pump was started briefly to fill the column with 120 mL of NaCl brine (6 min at 20 mL/min). The pump was then shut off which allowed the brine to react with the ammonia-loaded media for one hour. When the pump was restarted, a more concentrated ammonia effluent was achieved.

2.1.10 Ammonia analysis methods

Ammonia concentration was measured using the salicylate colorimetric method. Initially, analysis was performed using pillow reagent packs from Hach. However, to reduce costs and simplify analysis, kits for measuring ammonia levels in aquariums were preferred. Both methods involve the reaction of ammonia to form 5-aminosalicylate and subsequent oxidation to form a green colored compound (Figure 16). The darker the color that results, the higher the concentration of ammonia present in the sample. The processed samples were then analyzed using a UV-VIS spectrometer to measure absorbance at 700 nm. The absorption value observed is compared to a calibration curve to determine sample concentration. The calibration was linear in the 0.2 to 1.3 mg/L-N region. Samples that were too concentrated to analyze directly were diluted to fall within the acceptable range.

Figure 16. Calibration samples using salicylate colorimetric methods to measure ammonia concentrations.

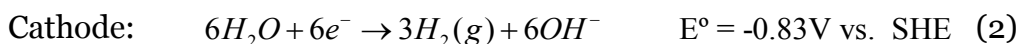
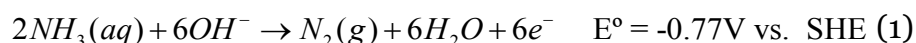


2.2 Ammonia electrolysis

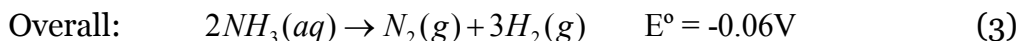
2.2.1 Bench-scale demonstration

The ammonia GreenBox electrolyzer is based on technology developed at Ohio University (Botte 2010, Botte 2012). During electrolysis, ammonia is converted to nitrogen at the anode and water is reduced to hydrogen at the cathode, based on the following reactions:

Anode:

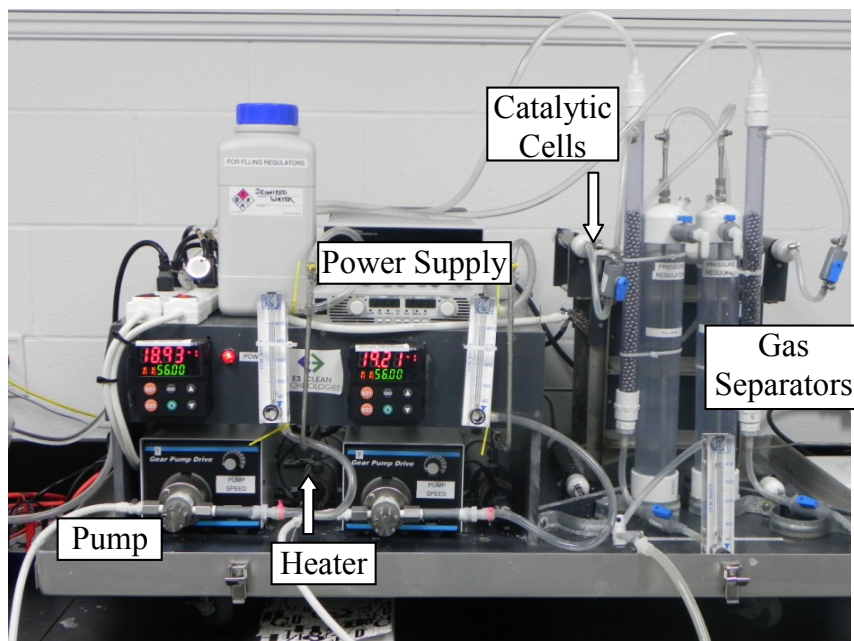


Therefore, the combined reactions result in ammonia conversion to nitrogen and hydrogen:



The ammonia electrolyzer used at ERDC-CERL was a 30W unit purchased from E3 Clean Technologies. Figure 17 identifies the key components of the ammonia electrolyzer.

Figure 17. 30 W ammonia electrolyzer from E3 Clean Technologies.



Flow through the electrolyzer begins at the anode and cathode reservoirs. Both reservoirs contain a sodium hydroxide solution. Ammonia in the form of ammonium chloride is added to the anode reservoir. Individual pumps control the rate of solution uptake and resistive heaters bring both solutions to the desired operational temperature. Flow continues into the catalyst cells where there is a water permeable membrane separating the anode and cathode sections. Voltage applied across this membrane and the metallic catalysts convert ammonia into nitrogen and hydrogen gases. Back pressure on exit valves controls the flow of water across the membrane ensuring equal flow rates through the degassers. The degassing units are tubes containing stainless steel spheres. The spheres provide nucleation sites to draw the hydrogen and nitrogen products out of solution. Gases exit out the top of the tube and to tip meters for volume measurements. Typically, the anode and cathode solutions are recycled back into the reservoirs for continuous treatment.

Ammonia electrolysis was monitored by analyzing the cathode and anode solutions for ammonia levels using the testing methods described previously. The current generated was also recorded and under ideal conditions could be used to measure ammonia concentrations directly. Constant monitoring of the system was required as manual adjustments were needed as the electrolysis progressed, especially with regards to equalizing the return flow from the catalytic cells.

2.2.2 Ammonia electrolysis modeling

Ammonia electrolysis was simulated using a semi-empirical model that combined experimental measurements and theoretical expressions describing the reactor conditions (thermodynamics, kinetics and flow rates) for optimum conversion and yield. The electrolyzer model was then deployed within ASPEN Plus, a software package used by chemical engineers for reaction simulation, to be combined with the other unit operations (AnMBRs and ion exchange columns).

The ammonia GreenBox is a parallel-plate electrolyzer using platinum deposited on expanded nickel using previously described methods (Botte 2010; Boggs and Botte 2010). Experiments were performed under the conditions in Table 11 to generate values for validating the mathematical formulae in the model, where NH_4Cl and KOH acts as the ammonia and hydroxide ions source in reactions (1) and (2).

Table 11. Summary of operating conditions of the ammonia GreenBox used in the semi-empirical model development.

Property	Value
Flow rate ($\text{cm}^3 \text{ min}^{-1}$)	1 - 2
Electrode Area (cm^2)	219
Low Concentration (mol cm^{-3})	$[\text{KOH}] = 1 \times 10^{-4}$ $[\text{NH}_4\text{Cl}] = 1 \times 10^{-5}$
High Concentration (mol cm^{-3})	$[\text{KOH}] = 1.5 \times 10^{-4}$ $[\text{NH}_4\text{Cl}] = 7 \times 10^{-5}$
Voltage (V) vs. Hg/HgO	-0.1 -0.2 -0.3 -0.4
Electrode separation (cm)	0.9

The performance of the electrolyzer is described by the current density generated at a certain voltage and flowrate. This current density is as a result of the flow of ions based on fluid flow and gradients in potential and concentration (Newman and Thomas-Alyea, 2004).

$$N_i = -z_i u_i F c_i \nabla \phi - D_i \nabla c_i + v c_i \quad (4)$$

$$i = F \sum_i z_i N_i \quad (5)$$

Where,

N = the flux ($\text{mol cm}^{-2} \text{sec}^{-1}$)

z = charge

u = mobility ($\text{cm}^2 \text{mol}^{-1} \text{J}^{-1} \text{s}^{-1}$)

F = Faraday's constant (C mol^{-1})

c = concentration (mol cm^{-3})

ϕ = potential (V)

D_i = diffusivity ($\text{cm}^2 \text{s}^{-1}$)

v = velocity (cm s^{-1})

i = current density (A cm^{-2})

subscript i = each ionic species present

These equations (Equation 4 and Equation 5) are due to conditions occurring in the bulk of the solution and can be simplified based on assumptions detailed by White et al. (1983) and Mader et al. (1986), summarized in Estejab et al. (2015). In addition, the boundary conditions at the anode are based on ammonia microkinetics developed by Diaz and Botte (2015), while the boundary conditions at the cathode are based on the hydrogen evolution reaction. Overall, these equations were solved simultaneously using a combination of a FORTRAN subroutine (Newman and Thomas-Alyea 2004, Botte 2005) and parameter estimation.

The working semi-empirical model was inserted into ASPEN Plus using a modified version of the User-Defined Model Two provided in ASPEN Plus. This incorporation of the semi-empirical model provided a user friendly interface for easy manipulation of variables required for electrochemical reactor design: cell voltage, cell geometry, and inlet conditions. More importantly, the use of ASPEN Plus provides the physical transport properties for all the ionic and non-ionic species present in this system using a combination of the Redlich-Kwong equation of state and the Electrolyte-NRTL activity coefficient model (Aspen Technology, Inc 2012).

3 Results and Discussion

3.1 Results

The three ACE (Anaerobic, Clinoptilolite, Electrolysis) components were studied and optimized individually at bench scale in Years 1 and 2 of the project, respectively. Enhancement of the performance and energy efficiency of AnMBR technology was attempted through inclusion of adsorbents and biocultures, and temperature effects were noted. Conventional AnMBR operation at an elevated temperature of 35 °C with a low volumetric loading rate (1 L/day) and high organic loading rate of 2.5-3.5 g/L COD/day resulted in 98% reduction in COD when treating highly concentrated waste streams at a HRT of 21 days. Methane conversion rates near the theoretical maximum were also established under these operating conditions. The inclusion of custom anaerobic biocultures was shown to benefit some processes in anaerobic degradation pathway, but the overall impact on steady state operations was limited. However, these cultures may be beneficial to accelerating reactor equilibration and/or upset recovery.

Common adsorbents such as GAC and Tanex ion-exchange resin were shown to be capable of adsorbing wastewater contaminants effectively. As such, including these materials within a bioreactor may provide a useful buffering capability as well as an additional means of retaining organisms within an AnMBR in the non-solution phase, which may have benefits during startup or if the reactor operation is upset. However, the capacity for adsorbents to enhance treatment for sustained periods is limited due to the high organic concentration in FOB wastewater. In-situ bioregeneration during low loading times is feasible and may increase the robustness of these systems in intermittent loading conditions. Operation of an AnMBR for the treatment of FOB wastewater (1360 mg/L COD) at low temperature (20 °C) and an HRT of 8 hours resulted in COD removal levels of 65-80%. Gas production was less efficient under these conditions (40-50% of theoretical maximum), but conversion of organic nitrogen to ammonia was still achieved. To improve performance, the following enhancement methods were assessed: inclusion of adsorbents, use of a downstream polishing bio-filter, increased HRT, and increased temperature. The inclusion of fresh adsorbents appeared to help startup rates but the beneficial effect was not sustained.

The use of a downstream biologically activated carbon (BAC) filter initially improved performance but the biofilter similarly became overwhelmed by the high effluent organic of the AnMBR, with the loading rate exceeding the bioregeneration rate. Increasing the HRT to 24 hours is projected to provide adequate performance for the project metrics of decreasing the BOD to less than 30 mg/L (COD < ~90 mg/L). Increasing the reactor temperature is also projected to provide acceptable performance, but a detailed energy analysis that modeled heat loss to the surrounding environment indicated that operation at ambient temperature and higher HRT would be a better option with respect to fuel consumption, despite the additional tank volume requirements (or capacity rating decrease). Based on these bench scale results, the final design recommendation for integration of AnMBR technology into the Anaerobic-Clinoptilolite-Electrolysis (ACE) platform is: HRT 24 hours, ambient temperature, bioseeding of initial reactor and utilization of GAC and Tanex to decrease startup times and decrease sensitivity to variable operating conditions, and back-flushing of the UF membrane for at least 15 seconds of every 30 minutes of operation.

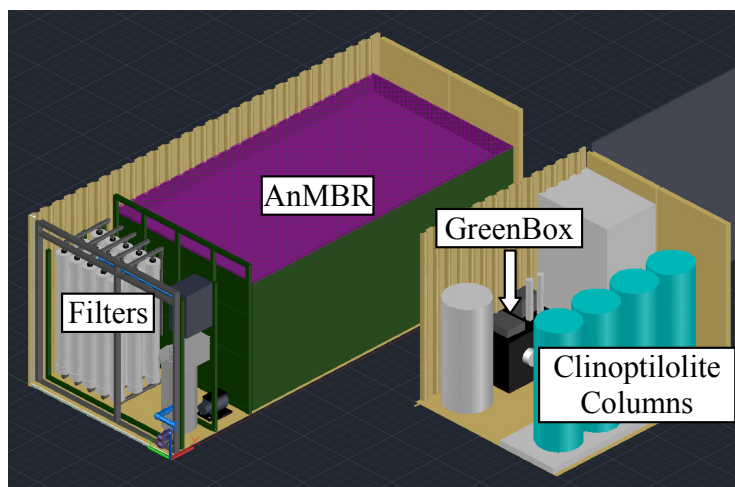
Bench scale characterization and optimization studies of clinoptilolite-mediated removal of ammonium by ion exchange indicated that this is an effective and robust approach for control and concentration of ammonium. Baseline experiments performed in clean solutions spiked with ammonium chloride were used to determine an effective clinoptilolite particle size that promotes rapid ammonium uptake and regeneration without inducing too much resistance to flow (pressure drop or head loss) through the filter bed. The breakthrough of ammonium at various flow rates, pH values, and cycle numbers was characterized. An ammonium removal capacity of 25 mg/g of clinoptilolite was observed in clean solutions. Column regeneration was successful under many different regeneration conditions, but using a 10% NaCl/ 0.5% NaOH mixture was found to be optimal and consistent with downstream brine processing plans. The ammonia concentration factor was 400X using a stop-flow regeneration method. Challenge testing in solutions containing calcium (1.87 or 3.75 mM) or potassium (1.02 mM) indicated that calcium provides the greatest level of competitive inhibition of ammonia uptake. In the presence of calcium, the ammonia capacity decreased to 12 mg/g of clinoptilolite. Experiments performed with actual wastewater effluent resulted in an ammonia capacity level similar to calcium dosed solutions. Based on these bench scale results, the final design recommendation for integration of clinoptilolite ion exchange

technology into the ACE platform is: Multi-column arrangement with three columns loaded in series and one being regenerated, a stop-flow regeneration process to maximize ammonia concentration in the regenerant brine, and load times adjusted for local calcium maximums in treated water.

Bench scale characterization and optimization studies of ammonia electrolysis by the Greenbox were performed to assess feasibility of this technology as an alternative to conventional biological nitrification/denitrification processes. Current output is optimized with increasing ammonia concentration until a point of catalyst saturation is reached. Improved performance was obtained by lowering the flow rate from 600 mL/min to 150 mL/min. Regeneration methods developed for the clinoptilolite columns are able to produce brine compatible with the operating range of the GreenBox. Recycling of the ammonia solution through the electrolysis cells is required to reduce ammonia concentrations to acceptable levels, but can be accomplished to align with new batches of brine produced following clinoptilolite regeneration. Performance of the GreenBox was not significantly affected by reducing NaOH concentrations from 5 M to 0.5 M. The 10X reduction in NaOH concentrations will reduce the chemical requirement for clinoptilolite regeneration/ammonia electrolysis and the safety risks associated with concentrated caustics. Based on these bench scale results, the final design recommendation for integration of AnMBR technology into the ACE platform is: flow rate of 150 mL/min, 0.5 M NaOH background solution, multiple passes of ammonia solution to align with clinoptilolite regeneration cycles, and return of treated brine for subsequent clinoptilolite regeneration.

Integration studies were performed using the bench scale systems operating in series under realistic operating conditions. A clinoptilolite column was plumbed directly downstream of a continuously operating 21 gpd AnMBR system. The spent regeneration brine was then manually transferred to the Greenbox. Successful generation of methane and hydrogen fuels was achieved. Based on integrated system results and individual technology optimization, the full-scale integrated design concept shown in Figure 18 is recommended. The larger module would contain the AnMBR and filters. An additional smaller module would house the four column clinoptilolite design and the ammonia electrolysis unit. Depending on the base size, the modules will be in separate shipping containers.

Figure 18. Conceptual design for integrated ACE wastewater treatment system.



3.2 Benefits

The wastewater treatment system designed under this project will benefit the DoD by reducing the costs, logistical burden, and risks associated with wastewater management at FOBs. Further development of the technology into a full scale unit is expected to yield an efficient system for onsite treatment that is simple to operate and produces fuels for electrical and thermal energy generation. This positive net-energy approach will support self-sufficient FOB design goals. The integrated system would also reduce the logistical burden and risks associated with transporting waste and importing fuel, chemicals, and water. The proposed system will reduce the FOB environmental footprint and impact on indigenous populations, demonstrating innovative environmental stewardship. The research results also benefit the broader scientific community by creating and building understanding of new, sustainable technologies that can be applied to other environmental problems (Botte 2015, see conference listing).

3.3 Testing high throughput AnMBR capabilities for treating representative FOB wastewater

A bench scale system was tested at ERDC for direct treatment of FOB-representative wastewater with influent COD of 1200-1400 mg/L and TSS >1000 mg/L. The baseline HRT for these studies was 8 hours, since that was shown to be effective in municipal AnMBR technology studies. While it was recognized that municipal wastewater COD and TSS levels are generally about 4–5X lower than FOB wastewater, the 8 hour HRT was utilized as baseline to determine the effect. Several tests were conducted with

this high-throughput AnMBR at ambient temperature to provide a baseline against which to optimize performance (Table 12). Three multi-week tests were performed in which methane generation was observed within 1 week of reactor startup. However, conversion of organics was generally limited at the 8 hour HRT. Due to the use of an ultrafiltration membrane, TSS values in the effluent were quite low. Also, the polyethersulfone (PES) ultrafiltration membranes used in this study retained water permeability, albeit at about 10% of the initial clean water flux.

Table 12. Performance summary data for the baseline AnMBR system operating at an HRT of 8 hours. Over 40 effluent samples were analyzed in these studies, representing several months of operating time.

Parameter	Value at Equilibrium Operation
Influent COD (mg/L)	1360 ± 280
Effluent COD (mg/L)	322 ± 94
TC (cfu/100 ml)	None detected
TSS (mg/L)	Below 10 mg/L
Membrane Permeability Reduction	85-90%
Membrane Backflush Interval	30-60 min

Based on these results, metrics for TC and TSS reductions were met. However, optimization of AnMBR performance is required in order to meet the effluent COD target of < 90 mg/L, corresponding to an effluent BOD level of < 30 mg/L (based on correlations between BOD and COD values as measured in effluents during this study). Additionally, reactor equilibration times were about 1 week (for COD removal) and 2 weeks (for gas production).

3.4 Testing AnMBR capabilities for treating highly concentrated FOB wastewater/sludge

3.4.1 Operation at mesophilic temperature (35°C)

A lab-scale continuous AnMBR system for treating highly concentrated FOB wastewater and sludge has been operating at UIUC since August of 2011 to investigate the treatment of high strength wastewater via anaerobic digestion. This system operates at longer HRT and thus requires concentration of the solids prior to utilization, though it could potentially be directly applied to latrine waste at outposts. The goal for this system is to provide a sustainable and energy positive wastewater treatment process for forward operating bases through the conversion of wastewater organics

into renewable methane gas. The main objectives for the AnMBR system were to investigate bioaugmentation as a method to improve substrate conversion to methane, and to begin investigation of the addition of adsorbent materials to improve effluent quality, methane production, and membrane flux. The potential to operate under ambient temperature conditions was also identified as a research topic, as a means to improve the net energy balance of the proposed treatment process.

Original plans for the continuous AnMBR system included operation of the system with bioaugmentation at a higher organic loading rate (OLR) of 5.1 g-COD/L/day until steady-state performance was achieved. However, the high OLR induced significant membrane fouling such that the required effluent flowrate of 1 L/day could not be sustained. During this time, a custom-built Membrana GmbH membrane and a household sediment filter cartridge were concurrently used. According to literature reports of optimal membrane characteristics, the Membrana hollow-fiber membrane was expected to achieve higher fluxes than the sediment filter. However, this was not the case. The Membrana membrane's lower flux was thought to be attributed to poor mixing near the membrane fibers due to the protective enclosure, as well as the tight packing of the fiber bundle, which inhibited solids from being released by daily backwashing. Consequently, the Membrana membrane was replaced with a second sediment filter, and the OLR was reduced to a medium OLR level of 2.5 g-COD/L/day to reduce membrane fouling. The sediment filters were modified into daisy-chained halves thereby halving their height, allowing for a reduction in the methane phase liquid volume to mitigate the change in HRT caused by lowering the OLR.

Under the medium OLR condition, the AnMBR system has been operated over the past year both with and without bioaugmentation, using two different bioculture mixtures. During all periods of operation the AnMBR system was operated at 37 °C and a 12 day HRT. Initial testing with bioaugmentation at a medium OLR began on 25 January 2013 and stopped on 12 March 2013. The bioaugmentation bioculture consisted of a 50:50 VS mixture of dried anaerobic sludge taken from the methane phase reactor of the AnMBR system, and propriety bioculture. The propriety bioculture was provided by Phylein Inc, and consisted of a 1:1:1 VS mixture of citrus-, hog manure-, and cellulosic-based biocultures. This mixture was determined based on batch test results which showed it to provide the most benefit in terms of methane production, soluble COD generation,

and VFA production. The complete bioculture mixture was applied daily to the pre-digestion reactor at a dosage of 3.9% of influent VS.

Preliminary evaluation of bioaugmentation in the AnMBR system indicated that bioaugmentation was beneficial in improving soluble COD (SCOD) and VFA production. However, no significant improvement in methane production was observed. In fact, a slight decrease in methane production compared to operation without bioaugmentation was reported. This was believed to have been caused by an increase in sulfate reducing bacteria in the system due to the recirculation of anaerobic sludge as a component of the bioaugmentation bioculture. Therefore, another investigation of bioaugmentation in the AnMBR system was performed that omitted the anaerobic sludge from the bioaugmentation mixture to better elucidate the effects of bioaugmentation on methane production. Bioaugmentation using a revised bioculture mixture was started on 11 November 2013. The revised bioculture mixture consisted of a 1:1:1 VS mixture of the proprietary citrus-, hog manure-, and cellulosic-based biocultures and was applied daily to the pre-digestion reactor at a dosage of 3.9% of influent VS.

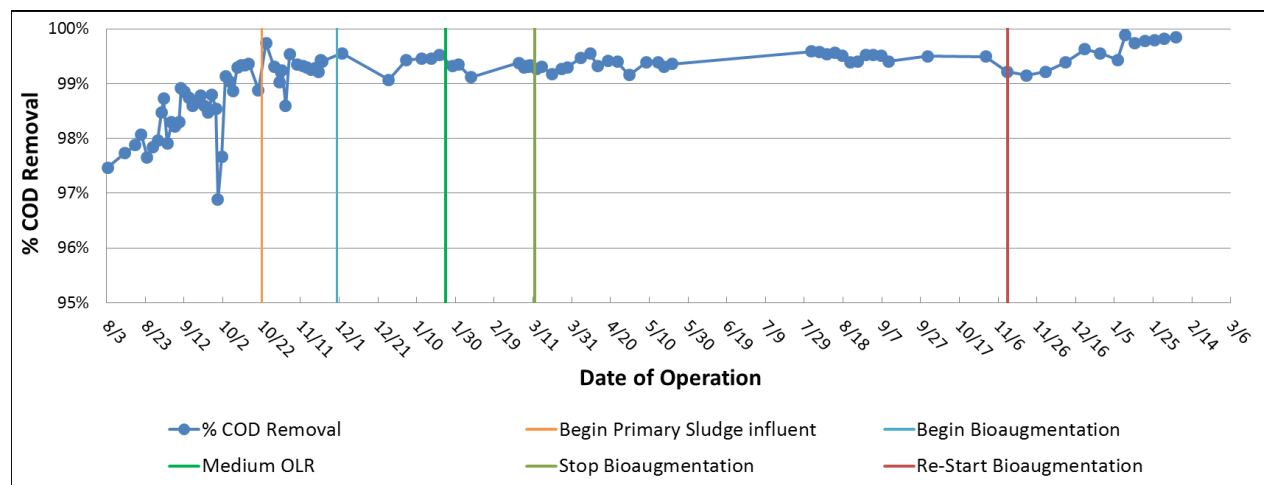
COD removal is a significant indicator of wastewater treatment process effectiveness. The AnMBR system COD removal was calculated as effluent sCOD divided by the feed wastewater total COD (TCOD). It should be noted that effluent TCOD and SCOD only differed by 37.5 mg/L on average, while the feed wastewater was 1 – 2 orders of magnitude greater. Therefore, effluent sCOD and TCOD values can be used interchangeably in this calculation since their difference is negligible. For characterizing MBR effluent, it is believed that SCOD is a better measure, because most commercial MBR systems have a smaller pore size that will only allow SCOD to exit.

As shown in Figure 19, after first reaching steady-state COD removal on day 74, the AnMBR system was able to consistently achieve >99% TCOD removal despite increases and decreases in OLR and both with and without bioaugmentation. AnMBR systems treating municipal wastewater are typically reported to achieve 95% COD reduction. The pilot system's higher COD removal can be explained at least in part by the use of influent with a solids content that is much higher than most other municipal wastewater systems. Nevertheless, this does not diminish the success of the methanogens in removing dissolved organics, i.e., SCOD. The average

COD concentration in the effluent over the last year has been 284 mg/L. This value is slightly above typical regulatory discharge levels of 125 – 250 mg/L (EPA 1997). With the use of a tighter membrane and/or adsorbents in the AnMBR, it is likely that typical discharge limits could be met. However, some additional processing through aerobic biological treatment or other processes may be needed to meet more stringent water quality standards associated with water reuse applications.

The low OLR was established to mimic the conditions expected on an FOB. The high COD removal achieved under the low OLR suggests that a similarly designed and operated AnMBR system is a promising replacement for current FOB wastewater treatment systems. Furthermore, the fact that the AnMBR system was able to maintain more than 98% COD removal directly after a sudden 7x loading increase when switching to the high OLR shows the robustness and stability of the AnMBR process. Note that this work was done with concentrated municipal wastewater rather than real FOB wastewater, which has not been well characterized. Thus, further characterization of the target FOB wastewater is recommend, and it may be constructive to verify AnMBR system performance with FOB wastewater sources.

Figure 19. Percent COD removal in the AnMBR system.



Methane production in the AnMBR system is shown in Figure 20. The upper (red) line in Figure 20 shows a 12 day running average of methane production per gram of VS added over time, which can be compared to the red dashed line showing the theoretical methane production based on elemental CHN analysis. Average methane production during the first period

of operation with bioaugmentation under the medium OLR was 93% of theoretical. This was slightly less than the average methane production seen during the following period of operation without bioaugmentation which was 102.6% of theoretical. During operation with the revised bioculture which began on 11 November 2013 and continues to present, the previously observed negative impact of bioaugmentation on methane production was not evident. With the revised bioculture, average methane production was 128.6% of theoretical methane production. It should be noted that a recent spike in methane production was observed, most likely due to a significant fluctuation that occurred in influent volatile solids and SCOD concentrations. One of the recent batches of influent primary sludge(PS) collected from the Urbana wastewater treatment facility had a significantly higher concentration of SCOD which may have made it more easily digestible, increasing the observed methane production per gram of VS. This batch of influent was fed for a period of 27 days (17 December 2013 to 13 January 2014). Since then, methane production levels have started to re-stabilize near 112% of theoretical maximum. In the future, measures will be taken to maintain more consistency and avoid such large fluctuations in the influent characteristics.

Figure 20. Methane production per gram of VS added (12-day moving average) and theoretical maximum in the AnMBR system.

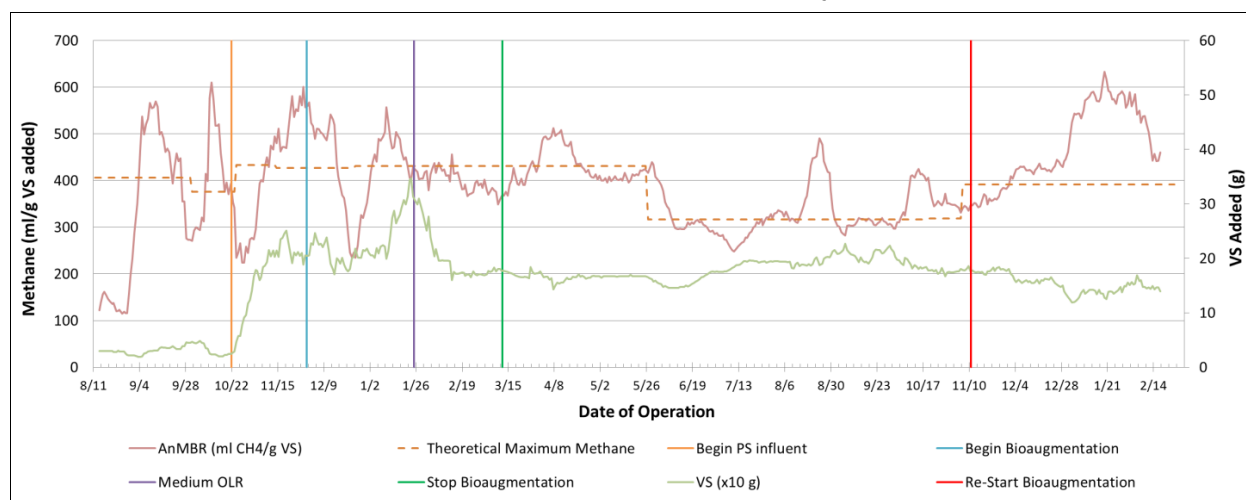
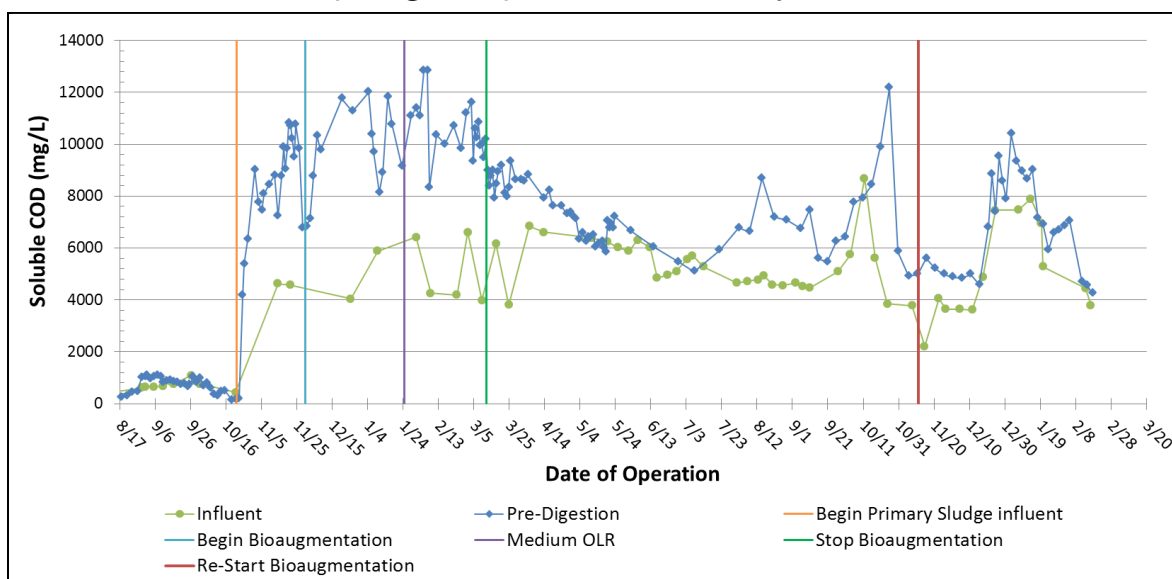


Figure 21 shows soluble COD concentrations in the influent (green) and pre-digestion phase (blue) of the AnMBR system. The recent spike in influent SCOD concentration can be seen in Figure 3 (17 December 2013 to 13 January 2014). In addition, comparing SCOD concentrations during the period of operation with and without bioaugmentation, it can be seen that bioaugmentation with the original bioculture mixture had a positive

effect on SCOD generation in the pre-digestion phase as expected based on preliminary batch test results. During the first period of operation with bioaugmentation a net increase of 5497 mg/L was seen between the pre-digestion phase and influent SCOD concentrations. This was significantly greater than the net increase of 1930 mg/L that was seen during operation without bioaugmentation.

Figure 21. Soluble COD concentrations in the influent and pre-digestion phase of the AnMBR system.



In addition, as expected from preliminary batch test results, bioaugmentation using the initial bioculture mixture also increased VFA concentrations, particularly acetic acid concentrations, in the AP of the AnMBR system. This is significant, as acetate is one of the primary substrates for methanogenesis. During operations with bioaugmentation using the initial bioculture mixture, acetate concentrations in the AP were 879 ± 19 mg/L, which is much higher than the 449 ± 12 mg/L without bioaugmentation. This evidence suggests that bioaugmentation did provide a benefit to substrate hydrolysis. However, contrary to the original expectations, bioaugmentation with the initial bioculture mixture yielded less methane and proportionately more carbon dioxide compared to operation without bioaugmentation. The reason for this contradiction is believed to be that a larger fraction of accumulated VFAs were being diverted to sulfate reduction pathways that result in the production of hydrogen sulfide. It is hypothesized that without bioaugmentation, acetogens and methanogens were able to process substrates as they were being produced, leaving less

available for sulfate-reducers. However, with the bioaugmentation-induced accumulation of VFAs, and the recycling of microorganisms from the methane phase reactor to the pre-digestion phase reactor, sulfate-reducers were given greater opportunity to consume these substrates that could not be converted into methane quickly enough. Since gaseous hydrogen sulfide could not be measured directly with our experimental apparatus, it was measured indirectly by the liquid sulfide (S^{2-}) concentration.

Table 13 below summarizes sulfide concentrations in all phases of the AnMBR system during operation with and without bioaugmentation. Looking at Table 13, it can be seen that during operation with the initial bioculture mixture, which included recycled anaerobic sludge, there was a significantly higher concentration of sulfide in the methane phase, compared to operation without bioaugmentation, supporting the hypothesis that greater sulfate reduction was occurring during operation with bioaugmentation. In addition, with revision of the bioculture, eliminating the recycled sludge from the mixture, the percent increase in sulfide concentrations from the pre-digestion phase to the methane phase is significantly lower than operations with the original bioculture with and without bioaugmentation. This data suggests that the recycled MP sludge in the original bioaugmentation culture did lead to competition between sulfate reducers and methanogens that did result in lower methane production. However, noting that recent sulfide measurements indicate significantly lower concentrations in the influent, pre-digestion, and methane production phases, some further investigation is needed to confirm the effect of bioaugmentation on sulfide levels, which will be conducted in the upcoming year's testing.

Table 13. Average sulfide concentrations in the AnMBR system during operation with and without bioaugmentation.

	Sulfide Concentration (mg/L)				% Increase from Pre-Digestion to Methane Phase
	Influent	Pre-Digestion	Methane Phase	Effluent	
With Bioaugmentation <i>Initial bioculture</i>	25.20 ± 2.24	23.70 ± 1.30	120.96 ± 3.45	0.05 ± 0.01	410
Without Bioaugmentation	31.65 ± 3.21	31.90 ± 2.29	89.25 ± 1.33	0.03 ± 0.00	180
With Bioaugmentation <i>Revised bioculture</i>	9.15 ± 0.21	9.45 ± 2.54	18.7 ± 1.84	0.03 ± 0.06	98

Finally, although operation with the original bioculture mixture had a positive effect on substrate hydrolysis in terms of SCOD generation and VFA production, operation with the revised bioculture did not appear to benefit SCOD generation. Operation with the revised bioculture resulted in a net increase of only 1794 mg/L in the average SCOD concentration between the pre-digestion phase and influent SCOD concentrations. This was similar to the net increase seen during operation without bioaugmentation (1930 mg/L). VFA analysis with the revised bioculture mix is still needed, and more work is needed to better understand why bioaugmentation did not show an advantage for substrate hydrolysis in this case.

Koe and Ang (1989) experienced similarly baffling results when bioaugmenting a semi-continuous anaerobic system treating municipal wastewater PS. A 1x and 10x bioaugmentation loading resulted in lower biogas quality and COD reductions despite higher acetic acid concentrations. In addition, at high feed concentrations, bioaugmentation reduced gas production. However, when the same bioculture was applied to a pilot-scale study and a full-scale treatment facility, notable improvements in volatile solids destruction and biogas production were observed. Other studies using different biocultures have reported cases where a bioaugmented system performed equally well to a non-bioaugmented system. In all of these cases, including Koe and Ang's, the non-bioaugmented system was already achieving a high level of COD destruction and methane production. The current results with a pilot-scale, continuous, two-phase AnMBR system treating PS concur that bioaugmentation will not improve an AD system that is already achieving high performance levels without bioaugmentation. Only during startup or in more stressed conditions may bioaugmentation improve AD performance.

Nevertheless, bioaugmentation may still benefit a full-scale system treating FOB wastewater. Many studies have shown that bioaugmentation can improve AD performance in under-performing systems. If the AnMBR system is operated at higher organic loading rates, or lower HRTs and/or SRTs, such that methane yield is appreciably less than theoretical maximum, bioaugmentation is expected to improve biogas production. Finally, bioaugmentation can help to reduce start-up times by increasing the number of organisms early in the AD reactor life-cycle.

3.4.2 Operation at ambient temperature (20 °C)

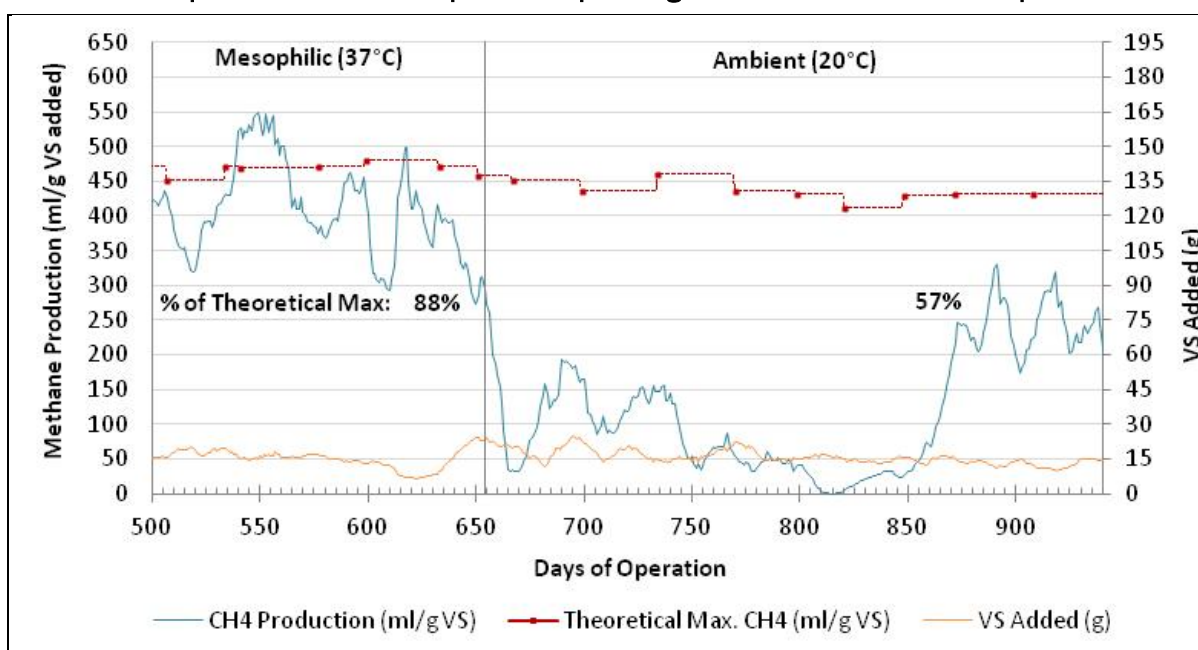
As mentioned previously, conventional anaerobic processes are maintained at temperatures around 35 °C or higher, which is not favorable for processing dilute raw wastewaters. In order to achieve a positive energy balance for anaerobic treatment of wastewaters with a low concentration of organics, the treatment must be conducted at ambient temperature, which eliminates the energy input for heating. Therefore, this study sought to investigate the performance of the pilot AnMBR system under ambient temperature conditions. Primary sludge continued to serve as the substrate during ambient temperature testing in order to provide a consistent basis for comparing the system performance under mesophilic and ambient temperature operating conditions. However, for full-scale operations under ambient temperature, it would be possible to process the whole raw wastewater stream (with a lower influent COD concentration) in the AnMBR system.

On Day 654 of operation, the temperature in the methane phase of the continuous AnMBR system was reduced from mesophilic conditions (37 °C) to ambient (20 °C). Upon switching to ambient conditions a significant reduction in methane production, COD removal, and effluent quality was observed. It was suspected that reducing the acid phase temperature would further negatively impact methane production. Therefore, in order to avoid potential compounded negative effects on system performance and more clearly see the effects of reducing the methane phase reactor temperature, the temperature in the acid phase was maintained at mesophilic conditions during this study. Note that the methane phase reactor accounts for over 90% of the total hydraulic retention time, and thus is responsible for the vast majority of the heat input needed to maintain mesophilic temperatures.

Figure 22 shows methane production in the AnMBR system after the change from mesophilic to ambient temperature in the methane phase reactor. It can be seen that the initial reduction in temperature resulted in a 92% decrease from average in methane production levels during previous operation under mesophilic conditions. Methane production under ambient conditions showed some improvement around Day 682, and began to approach expected production levels (≥ 100 ml/g VS added) based on ambient temperature batch test results. A second decline in methane production was observed beginning around Day 740, which was due to unintended fluctuations in pH resulting from a malfunction of control unit

and operational errors. The stress resulting from these fluctuations combined with the stress of reduced operating temperatures is thought to be the cause of reduced digester performance and eventual reactor failure at around Day 815. Upon re-stabilization of pH around Day 820, there was improvement in methane production. However, to speed up recovery of reactor performance, 30% of the methane phase reactor volume was replaced with fresh mesophilic anaerobic sludge collected from the Urbana Wastewater Treatment Plant. After the addition of fresh anaerobic sludge on Day 835, average daily methane production increased sharply and stabilized at around 57% of theoretical maximum, (246 ml/g VS_{added}).

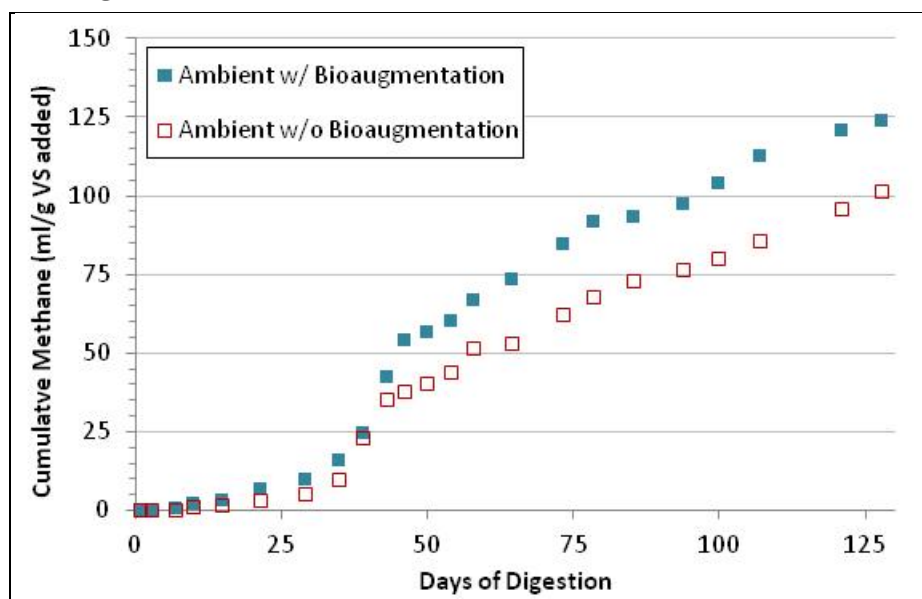
Figure 22. Methane production levels in the AnMBR system upon switching from mesophilic to ambient temperature operating conditions in the methane phase.



Methane production from an ambient temperature batch test is shown in Figure 23. The batch test was performed using anaerobic sludge collected from the continuous AnMBR system during mesophilic operation. Prior to batch testing the anaerobic sludge was acclimated to ambient temperature conditions for 200 days. For all conditions an equal volume of anaerobic sludge and primary sludge were added to 175 ml serum bottles, sealed, and digested under ambient temperature conditions. In the bioaugmentation condition, the proprietary bioculture mixture was also added at a dosage of 3.9% of the primary sludge VS. Methane production for all batch test conditions was between 100-150 ml per gram of VS added, which provided some expectation for methane production levels in the continuous

AnMBR. Results also indicated that bioaugmentation had a positive effect on ambient temperature digestion resulting in a 23% increase in methane production after 128 days of digestion.

Figure 23. Ambient temperature batch test methane production.



3.4.3 AnMBR energy analysis

The resulting potential energy recovery under mesophilic and ambient temperature operation with and without bioaugmentation was evaluated and compared based on the average methane production values for each condition as determined from this study, and considering the input of energy required to heat the wastewater in the case of mesophilic operation (from 20-37 °C). Table 14 summarizes the relevant values used in the energy balance calculations and the resulting net energy recovery (energy out) for each of the four process scenarios. All methane production values were normalized to a theoretical maximum of 450 ml/g VS added. Methane production at ambient temperature (20 °C) without bioaugmentation condition was assumed to be 23% less than methane production under ambient conditions with bioaugmentation, based on the batch test results. An influent VS concentration of 20 g/L was assumed, which is the average VS concentration of the five batches of primary sludge that were used in this study.

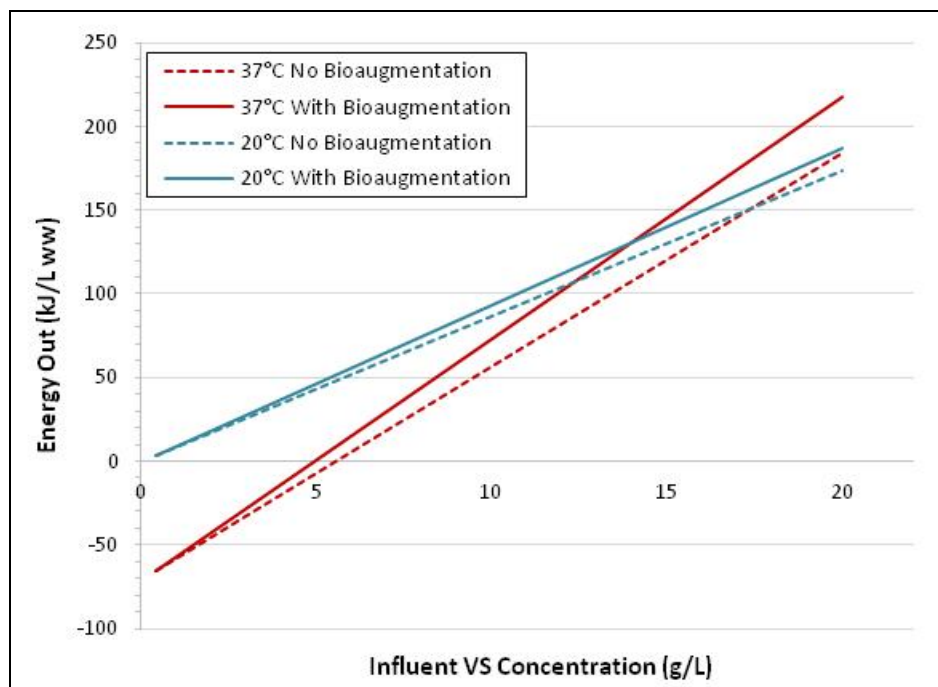
Table 14. Energy balance calculation values and resulting estimated kJ of net energy recovery (energy out) per liter of wastewater treated under four different operating scenarios: mesophilic operation (37 °C) with or without bioaugmentation, and ambient temperature (20 °C) operation with or without bioaugmentation.

	Methane Produced (L/g VS)	Influent VS (g/L)	Methane Heat of Combustion (kJ/L)	Energy In for Heating* (kJ/L ww)	Energy Out (kJ/L ww)
37 °C With Bioaugmentation	0.396	20	36.4	71	183.9
37 °C No Bioaugmentation	0.351	20	36.4	71	216.6
20 °C With Bioaugmentation	0.257	20	36.4	--	186.6
20 °C No Bioaugmentation	0.239	20	36.4	--	176.5

*Calculated as amount of heat required to heat 1 kg of water from 20-37 °C, using $Q = mC_p(T_2 - T_1)$

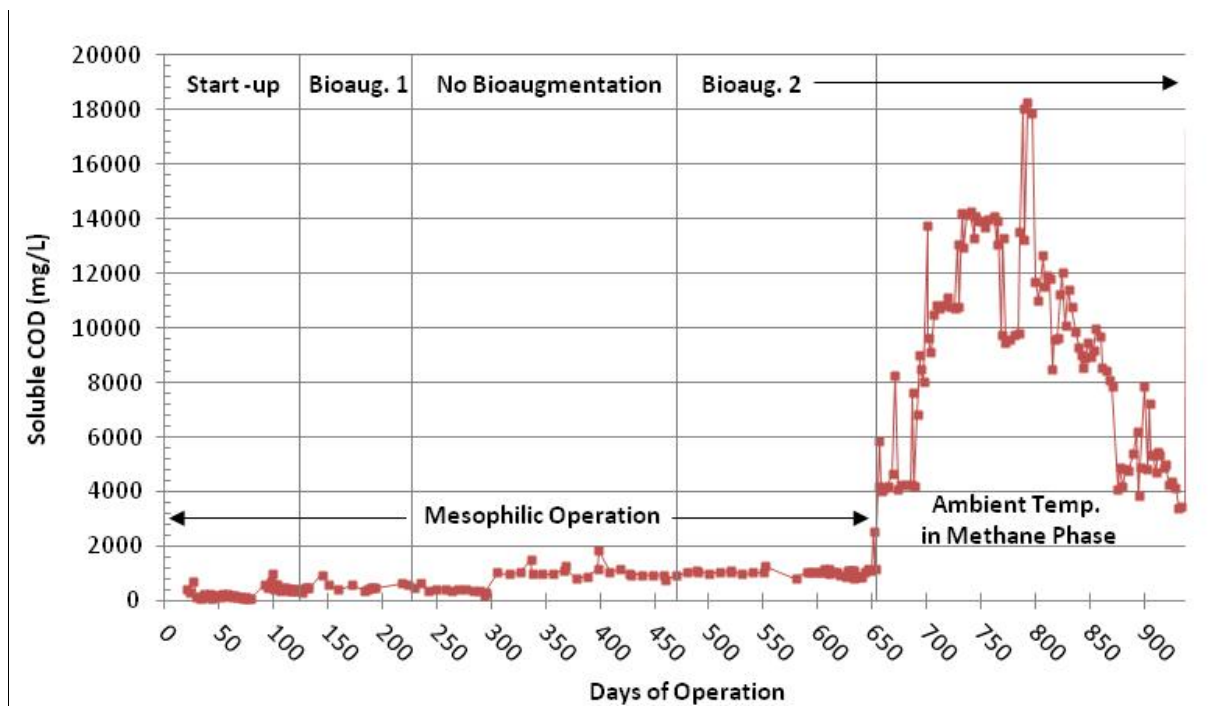
Results from Table 14 indicate that for the high strength wastewater used in this study, mesophilic operation has the potential to provide a positive energy balance since more energy can be recovered as methane than would be required for heating the wastewater. Mesophilic operation with bioaugmentation appears to be the best option for energy recovery from the high strength waste water used in this study. However, ambient temperature operation can provide a similar energy balance to mesophilic operation without bioaugmentation, which would reduce cost. In addition, typical raw municipal wastewater has a much lower VS concentration around 0.4 g/L (Metcalf and Eddy, 2004). In this case, mesophilic operation does not have the potential to provide a positive energy balance, as the amount of energy needed to heat the more dilute wastewater would outweigh the amount of recoverable methane energy. Figure 24 shows the estimated net energy recovery (energy out) per liter of wastewater treated via each of the four process scenarios for different influent VS concentrations ranging from 0.4 to 20 g/L. It can be seen that for wastewaters with a concentration of less than around 5 g/L VS, mesophilic operation does not have the potential to provide a positive energy balance, while ambient temperature operation does. In fact, ambient temperature operation may be able to provide a better energy balance than mesophilic operation for wastewaters with concentrations up to 13-14 g/L VS. Further investigations in this area to verify the methane production potential of lower strength wastewater under ambient temperature conditions with and without bioaugmentation in the proposed AnMBR system would be beneficial.

Figure 24. Estimated net energy recovery (energy out) per liter of wastewater treated via four different process scenarios for influent VS concentrations ranging from 0.4 to 20 g/L.



The lower methane production resulting from the initial switch to ambient temperature led to a build up of undigested soluble organics in the methane phase reactor and effluent. Figure 25 shows sCOD concentrations over time in the methane phase of the AnMBR system. As the reactor stabilized and methane production improved over time, soluble COD levels in the AnMBR similarly improved and stabilized near 4000 mg/L. However, this was still higher than previous levels observed under mesophilic operation (average 677 mg/L). Therefore, due to the lower conversion of organics to methane under ambient temperature conditions, the improvement in energy balance appears to come at the sacrifice of effluent quality. To address this issue, the addition of adsorbent materials was investigated as a means for improving effluent quality under ambient temperature conditions.

Figure 25. Soluble COD concentrations in methane phase of the continuous AnMBR system over time.



Thus, reducing operating temperature to ambient (20 °C) conditions in the methane phase of the continuous AnMBR system decreased organics removal, methane production, and effluent quality compared to operation under mesophilic conditions (37 °C). Average methane production under ambient operating conditions stabilized near 246 ml/g VS_{added}, or 57% of theoretical maximum. For the high strength wastewater substrate used in this study, energy balance estimates indicated that a positive energy balance could be achieved under both mesophilic and ambient operating conditions with mesophilic operation offering a greater net energy recovery than ambient temperature operation. However, for lower strength wastewaters, less 14 g/L VS, ambient temperature operation has the potential to provide greater net energy recovery than mesophilic operation, and for wastewater with less than 5 g/L VS, only ambient temperature operation has the potential to be net positive due to the energy input required for heating in the case of mesophilic operation. Results from this study warrant further investigation to verify the methane production potential of lower strength wastewater under ambient temperature conditions with and without bioaugmentation in the proposed AnMBR system.

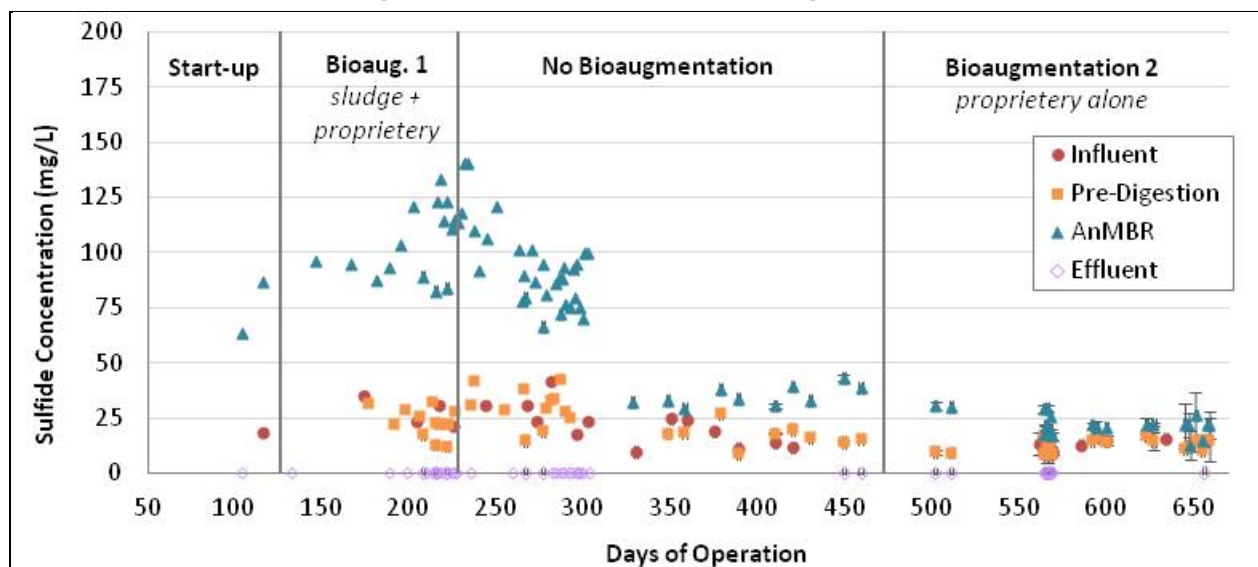
3.4.4 Optimizing AnMBR performance.

3.4.4.1 Bioaugmentation

Based upon the results of initial batch experiments to find the most effective bioculture (data not shown), the initial bioculture used in this study consisted of roughly half anaerobic sludge (recycled from the methane phase reactor) and half dry bioculture blend, on a VS basis. The dry bioculture blend was a 1:1:1 VS mixture of three proprietary biocultures previously created to augment anaerobic digestion of citrus wastes, hog manure, and cellulosic wastes as obtained from Microbial Energy Systems, Inc. Each of the three proprietary biocultures contained 5-10 facultative bacterial species that had shown improved acid production in lab experiments. The final bioculture mixture was used for routine bioaugmentation, entailing daily additions to the acid phase reactor. The bioculture mixture was added at a dosage of 3.9% (dry basis) of the influent VS to the acid phase.

During the first period of bioaugmentation testing in the continuous AnMBR system, elevated sulfide concentrations (up to 440 mg/L) in the methane phase (AnMBR) were observed in the system. These levels were 10 times higher compared to sulfide concentrations during operation without bioaugmentation. Figure 26 shows sulfide concentrations in the different phases of the continuous AnMBR system over time. It was suspected that recirculation of the anaerobic sludge as a component of the bioaugmentation bioculture contributed to an accumulation of sulfate reducing bacteria in the system. Therefore, a second round of bioaugmentation was investigated, this time eliminating the anaerobic sludge component and using only the proprietary bioculture blend. Bioaugmentation with the proprietary bioculture alone successfully maintained sulfide concentrations below 40 mg/L, while providing similar benefits to system performance as seen during the first round of bioaugmentation, which are discussed in the following sections.

Figure 26. Sulfide concentrations in AnMBR system over time during operation with and without bioaugmentation.



Bioaugmentation in the acid phase was found to improve substrate hydrolysis and acetogenesis as indicated by increased soluble COD and VFA concentrations. Table 15 summarizes the resulting soluble COD and VFA concentrations in the acid phase during periods of operation with and without bioaugmentation. Bioaugmentation resulted in a 4-56% increase in soluble COD and a 49-113% in total VFA concentrations during both periods of operation with bioaugmentation, compared to operation without. Acetic acid specifically increased by 96-140% as a result of bioaugmentation.

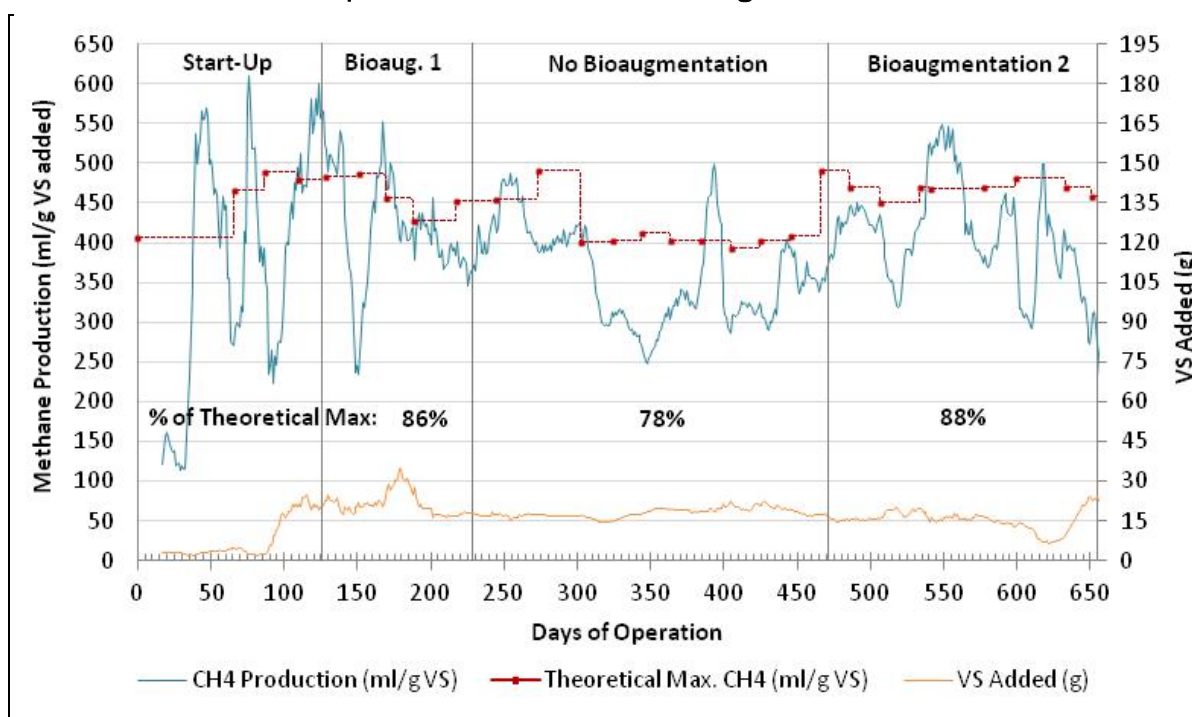
Table 15. Average soluble COD and VFA concentrations in acid phase during operation with and without bioaugmentation.

(mg/L)	Bioaugmentation 1 <i>Sludge + Proprietary</i>	No Bioaugmentation	Bioaugmentation 2 <i>Proprietary Only</i>
Soluble COD	9946	6390	6629
Acetic Acid	879	449	1080
Total VFA	3134	1614	3438

The benefits of bioaugmentation on substrate hydrolysis and acetogenesis subsequently contributed to improvements in methane production. Figure 27 shows average methane production per gram of volatile solids added in the AnMBR system during operation with and without bioaugmentation.

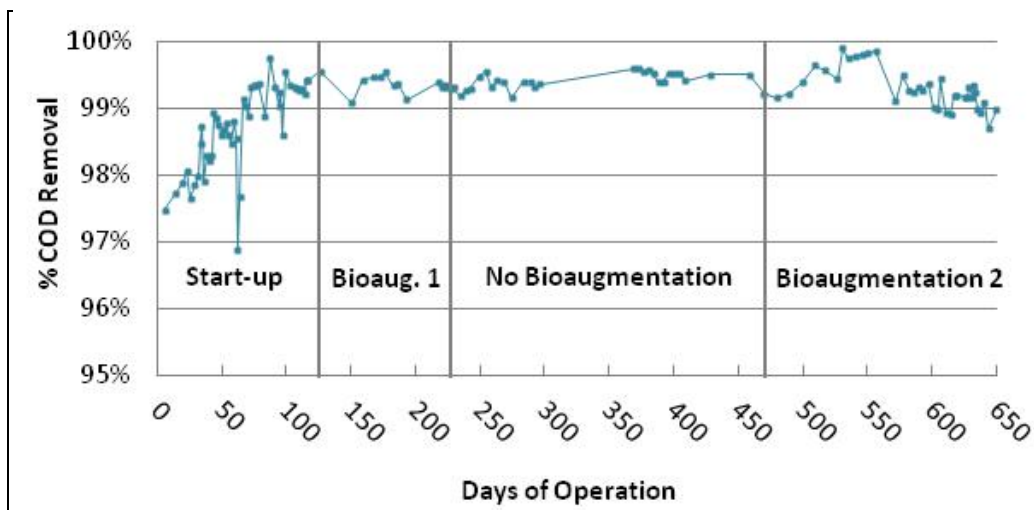
Overall, operation with bioaugmentation was found to have a positive impact on methane production compared to operation without bioaugmentation. Average methane production during the first and second periods of operation with bioaugmentation were 396 and 414 ml/g VS_{added} respectively, corresponding to 86% and 88% of theoretical maximum methane production. This was an 8-10% increase in methane production compared to operation without bioaugmentation which yielded an average of 331 ml/g VS_{added}, or 78% of theoretical maximum.

Figure 27. Methane production in the continuous AnMBR system over time during operation with and without bioaugmentation.



During all periods of operation with and without bioaugmentation, under mesophilic operating temperature, the AnMBR system was able to consistently achieve >98% total COD removal, as shown in Figure 28. The average COD concentration in the effluent during the bioaugmentation study under mesophilic temperatures (37 °C) was 232 mg/L. This value is within the range of typical regulatory discharge levels of 125 – 250 mg/L (EPA 1997), although it is on the higher end of the range. With the use of a tighter membrane and/or adsorbents in the AnMBR, it is quite likely that even lower effluent COD levels could be met.

Figure 28. Chemical oxygen demand (COD) removal in the AnMBR system over time during operation with and without bioaugmentation.



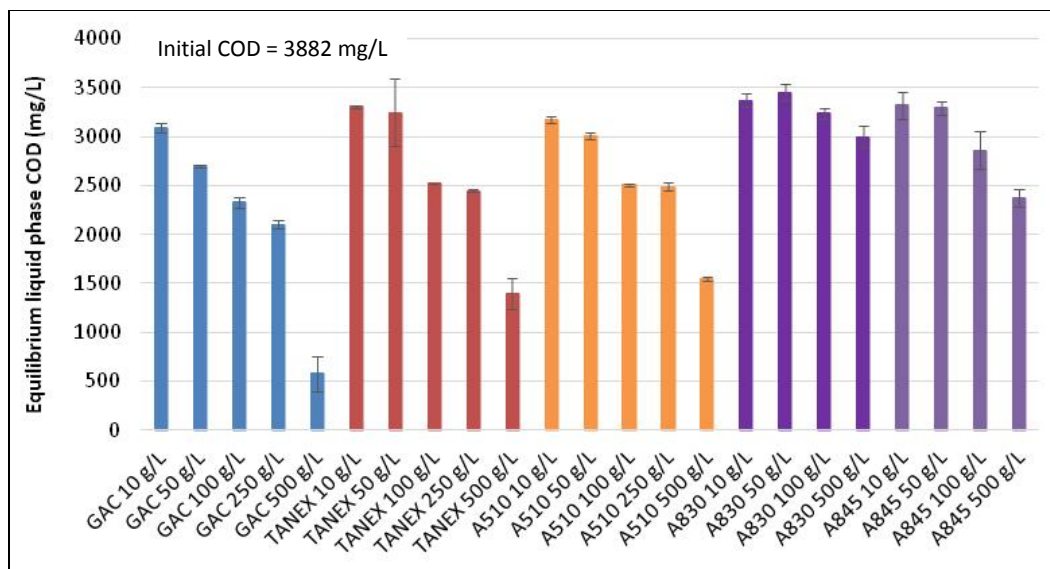
Bioaugmentation in the acid phase of the AnMBR system was found to positively impact anaerobic process performance. The targeted rate-limiting steps of hydrolysis and acetogenesis were improved as indicated by increased soluble COD (+4% to +56%) and acetic acid (+96% to +140%) concentrations compared to operation without bioaugmentation. This led to a subsequent increase in mesophilic methane production with bioaugmentation resulting in total methane production that was 86-88% of the theoretical maximum for the primary sludge influent feedstock. Although bioaugmentation with recycled anaerobic sludge + proprietary bioculture resulted in a slightly greater increase of acid phase soluble COD and overall methane production compared to bioaugmentation with the proprietary bioculture alone, it also led to an undesirable build-up of sulfide in the system. Therefore, the recommended bioaugmentation strategy would be application of the proprietary bioculture alone without recycling of the anaerobic sludge in order to maintain low sulfide concentrations while still achieving improved hydrolysis, acetogenesis, and methane production.

3.4.4.2 Adsorption

All five adsorbents were initially loaded into serum bottles containing filtered AnMBR effluent. Adsorbent dosages of 10, 50, 100, 250 and 500 g/L were tested. The removal of soluble COD from the liquid phase was measured overtime for all condition and the resulting equilibrium liquid phase soluble COD after 16 days of contact time for the five candidate adsorbents is shown in Figure 29 . The initial soluble COD concentration of the liquid

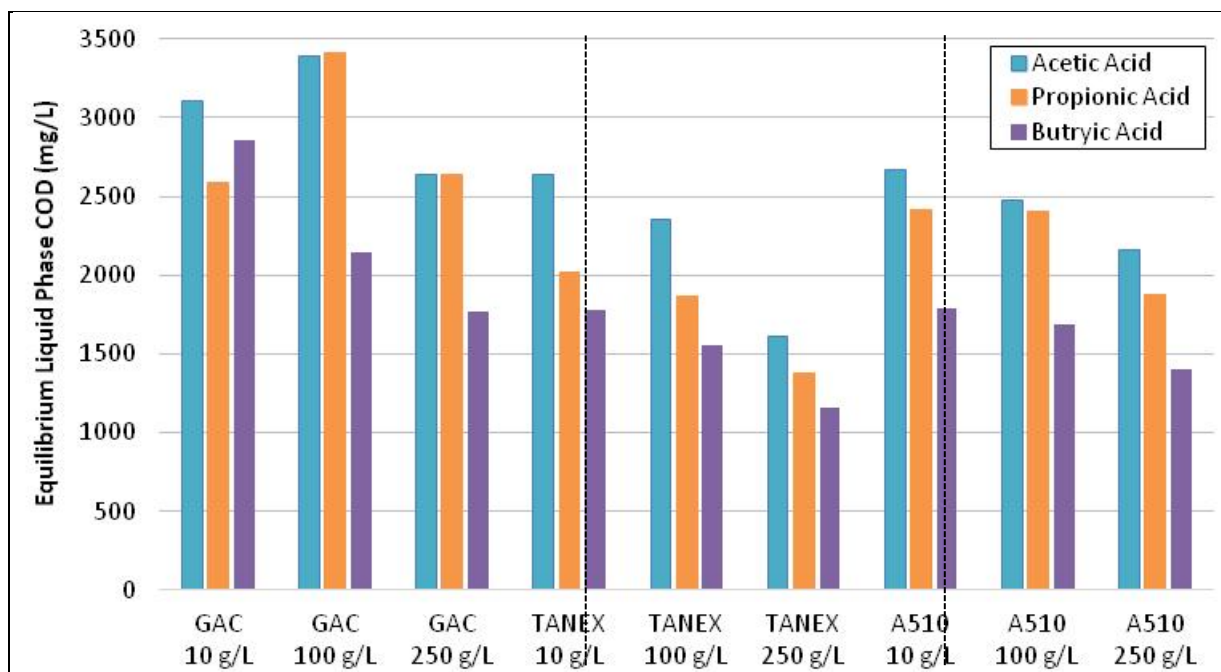
phase was of 3882 mg/L. From Figure 29 it can be seen that GAC provided the best adsorption of soluble COD followed by the two strong-base anion-exchange resins (Tanex and A510) and the two weak-base anion-exchange resins (A845 and A830) provided the least COD adsorption.

Figure 29. Equilibrium liquid phase COD concentrations for candidate adsorbents and ion-exchange resins showing after 16 days of contact time in filtered AnMBR effluent (initial liquid phase COD = 3882 mg/L).



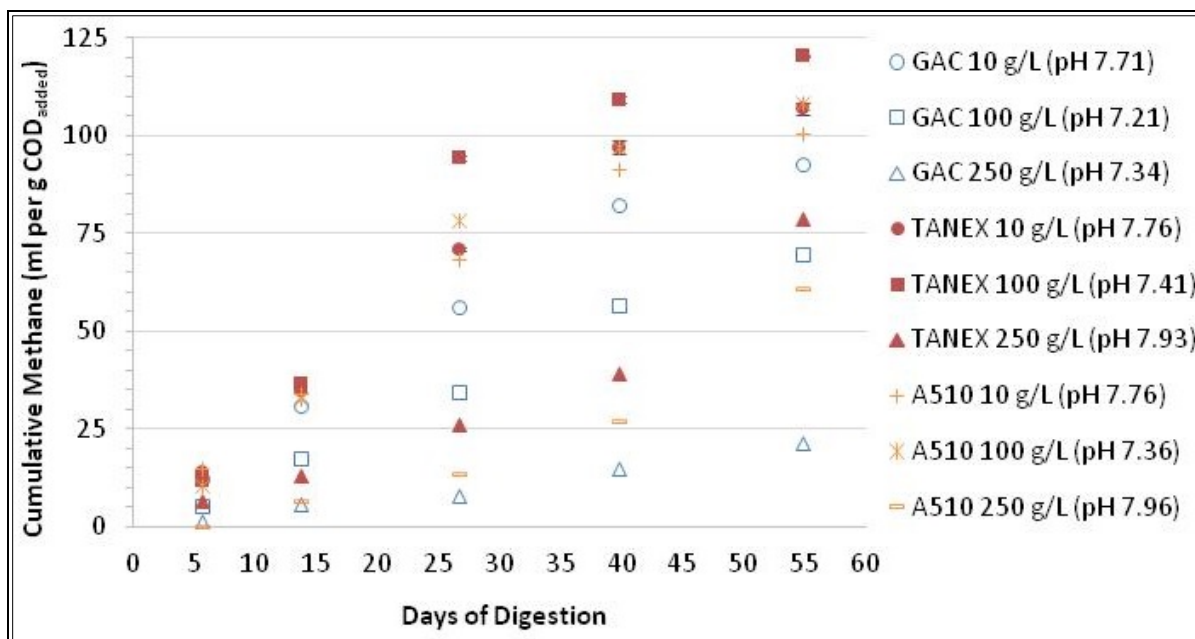
Although GAC was able to adsorb the greatest amount of soluble COD, Tanex provided the greatest adsorption of VFAs. The ability of GAC, Tanex and A510 to adsorb specific VFAs was investigated by measuring the amount of VFA remaining the liquid phase after 27 days of contact time. Figure 30 shows the concentration of acetic, propionic, and butyric acid remaining in the liquid phase for adsorbent dosages of 10, 100, and 250 mg/L.

Figure 30. Equilibrium liquid-phase concentrations of volatile fatty acids after 27 days contact time with various dosages (10, 100 and 250 g/L) of GAC, Tanex resin, and A510 resin in filtered AnMBR effluent.



After loading the adsorbent materials (GAC, Tanex, and A510) with liquid phase COD, anaerobic seed sludge was added to each condition (10% v/v) to evaluate the potential for the various adsorbent materials to benefit methane production. Figure 31 shows methane production with each adsorbent condition after 40 days of batch digestion under ambient temperature. It shows that the strong-base anion-exchange resin with 10 g/L and 100 g/L resulted in greater methane production than GAC. The 250 g/L resin conditions produced the least amount of biogas, which is likely due to the increased pH levels that were observed in these conditions. The legend in Figure 31 includes the measured pH value for each condition on the last day of digestion. Overall, Tanex was determined to be the best candidate adsorbent material for application in the AnMBR reactor.

Figure 31. Biogas production per gram of COD_{added} from batch test digestion of filtered AnMBR effluent with various adsorbent (GAC, Tanex, and A510), dosages (10, 100 and 250 g/L).



3.5 Organic sequestration experiments

An initial round of organic sequestration experiments were performed using the wastewater described above. The sequestration strategy used was adsorption with Purolite Tanex, an organic ion-exchange resin. 200-mL batch reactors containing wastewater were dosed with between 1 and 64 mL of Tanex resin and stirred magnetically. The COD value of the water was measured before and after dosing, and settling of the IX resin (Figure 32). The reactor solution went from brown to clear for low IX doses. Pulverization of IX resin was observed due to the magnetic stirring, with solutions becoming turbid white at IX doses higher than 4 mL. Therefore, effluent COD was only measured in controls and low-dose reactors. It is likely that this pulverization added some COD to the treated samples. However, a marked decrease in total COD was still observed, as shown in Table 16.

Figure 32. The addition of Tanex to a high-throughput AnMBR bioreactor may aid in sequestering organic contaminants during reactor startup to promote high organic levels in the reactor which can promote anaerobic culture maturation.

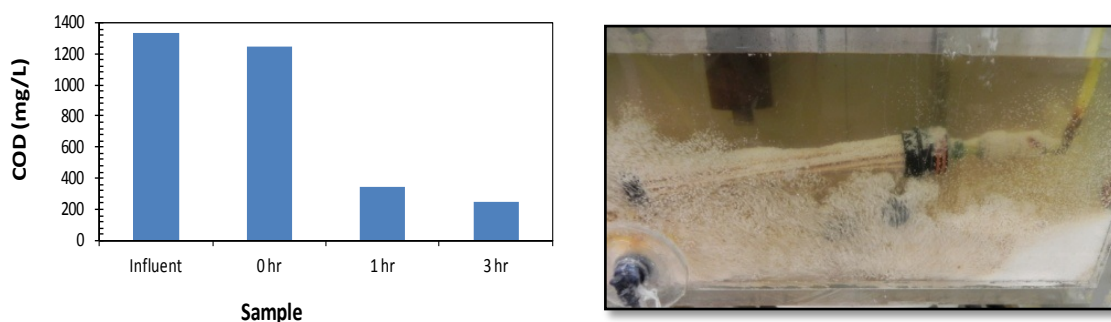


Table 16. Reduction in organic matter content of wastewater, as measured by COD analysis, due to exposure to varying dose of ion-exchange resin.

IX Dose (ml)	Final COD	% Reduction
0-control	1200	4
1	220	82.4
2	168	86.56
4	160	87.2

In order to further evaluate the benefits that addition of Tanex resin to the AnMBR system could provide in terms of reactor stability and recovery after shock-loading, an intentional shock-load event was carried out in the AnMBR system prior to the addition of the resin. Figure 33 shows soluble COD concentration in the methane phase of the continuous AnMBR system before and after shock-loading with and without the addition of Tanex resin under ambient temperature operation. The first shock-load to the system occurred on Day 938 and consisted of the addition of 16,000 mg/L of acetic acid to the methane phase of the AnMBR system. This dosage corresponded to approximately twice the regular daily input of soluble COD to the methane phase reactor. On Day 1004, 1100 g of Tanex resin (corresponding to a dosage of 100 g/L), distributed among three mesh bags (see Figure 34), was added to the methane phase reactor. Subsequently, a second shock-loading event of 16,000 mg/L acetic acid was added to the system on Day 1009.

Figure 33. Soluble COD concentration in the methane phase of the continuous AnMBR system before and after shock-loading with and without the addition of Purolite® Tanex under ambient temperature operation.

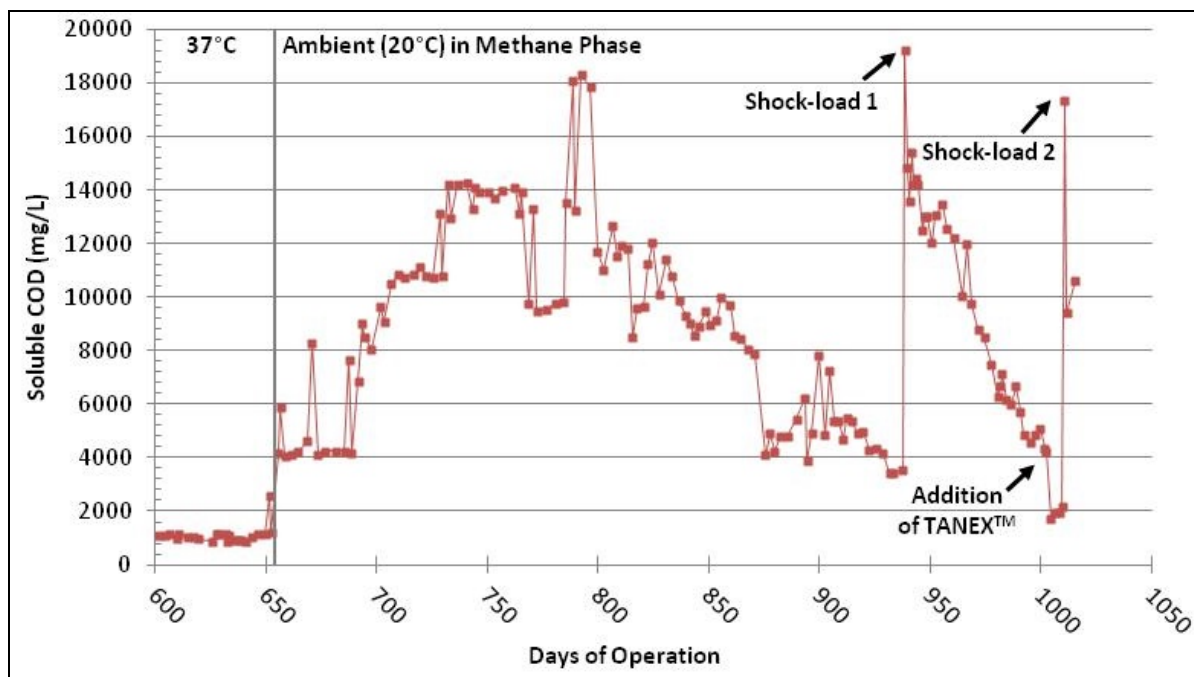


Figure 34. One of three mesh bags that were deployed into the continuous AnMBR system containing approximately 370 g of Purolite® Tanex each.



As shown in Figure 35, the recovery of the soluble COD concentration in the AnMBR to the levels before the shock-loading took more than 50 days

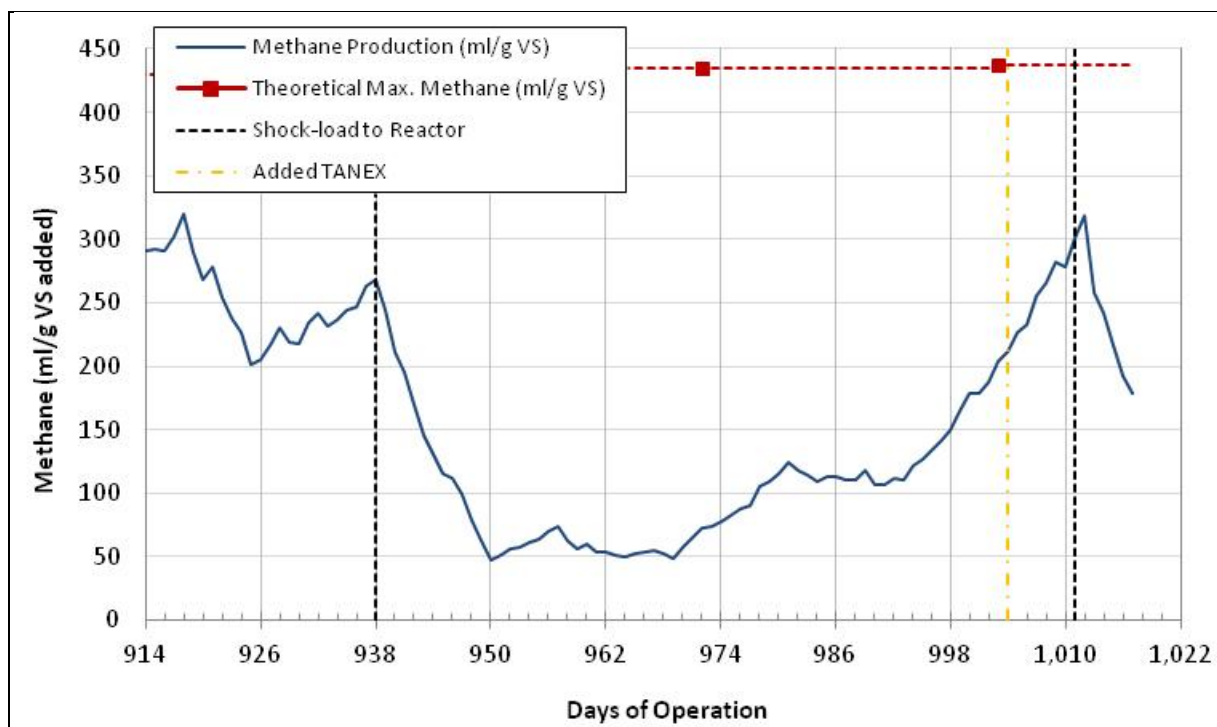
after the first shock-load event. After this recovery, 100 g/L of Tanex resin was added to the reactor. Addition of the resin provided an immediate benefit, reducing soluble COD levels from 4246 mg/L to 1687 mg/L over the first 3 days of deployment. This COD removal was in line with the expected soluble COD removal based on initial batch adsorbent testing in which a dosage 100 g/L of Tanex had been shown to reduce liquid-phase soluble COD from 3882 to 2519 mg/L. The continuous reactor results were somewhat better than the batch test results because the continuous AnMBR had simultaneous adsorptive removal and biological removal mechanisms, but the batch test separated these two removal mechanisms. Soluble COD levels in the AnMBR remained near 2000 mg/L until the second shock-load event. The second shock-load event resulted in a similar initial spike in the AnMBR soluble COD. However, with the Tanex resin present in the reactor, soluble COD levels were decreasing faster, and were reduced by nearly 40% (17364–10622 mg/L) within just 3 days after shock-loading. Without the resin, it took approximately 20–30 days for the soluble COD to be reduced by 40% after the shock-loading event. Therefore, addition of the resin appears to have provided the expected benefit for reactor stability in terms of providing adsorption of excess soluble organics. Further monitoring will reveal whether this benefit translates into increased methane production.

During both shock-load events pH control was turned off for the first 5 days to compare the effect of shock-loading on pH with and without the Tanex resin present. In the case of the first shock-load without Tanex, pH in the methane phase dropped to a minimum of 5.18 within the first hour. Over the next 5 days, the pH only came back up to as high as 5.35. At that point, pH control was turned back on and pH was maintained at 7.40. In the case of the second shock-load, when the Tanex resin was present in the reactor, pH in the methane phase dropped to a minimum of 4.17 within the first hour, and came up to as high as 5.37 in the 5 days after that, before restarting automatic pH control. Thus, for the given shock-load and resin dosage, the Tanex resin did not provide significant stabilization in terms of pH.

The significant drop in pH is the likely cause for the reduced methane production that was observed directly after both shock-load events. Figure 35 shows the methane production in the continuous AnMBR system after the two shock-load events. The first shock-load resulted in an 80% decrease in average methane production within 12 days. (It should be noted that this

value assumes 71% methane in the biogas, which was the average percent methane measured prior to shock-loading. Around the time that we initially shock-loaded the system, our GC became inoperable and thus biogas quality analysis has been outsourced and is still pending.) By about 36 days after the first shock-loading without resin, methane production began to improve and return to similar average levels as were observed prior to the shock-load event. The second shock-load also resulted in a decrease in methane production, but the reactor has not had sufficient time to recover. It is expected that the magnitude of this decrease will be less with the Tanex resin present, and recovery to normal levels of methane production will occur more quickly, but this needs to be confirmed over the next few weeks of continuing operation.

Figure 35. Methane production in the continuous AnMBR system before and after shock-loading with and without the addition of Purolite® Tanex under ambient temperature operation.



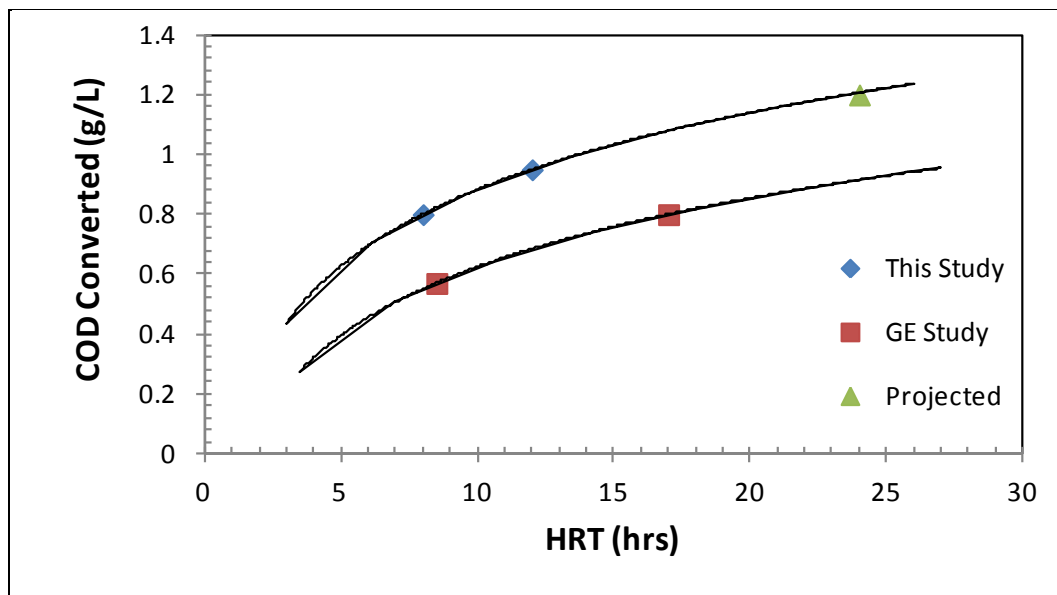
Five candidate adsorbent materials were evaluated based on their ability to adsorb soluble COD and VFAs, as well as their benefit on methane production during batch testing. While GAC was found to provide the best adsorption of soluble COD, Tanex, a commercially available strong base anion-exchange resin, proved to be the best for adsorption of VFAs and improving methane production. Based on these results, Tanex was deployed in the continuous AnMBR system and reactor stability and recovery

after a shock-load event with and without the addition of Tanex to the system was investigated. Results indicated that the addition of the resin to the AnMBR system provided an initial benefit of reduced soluble COD concentrations. Upon shock-loading, although the resin did not provide a significant stabilization in terms of pH, the resin did appear to benefit reactor stability in terms of providing adsorption of excess soluble organics. With addition of the resin, 38% recovery to the previous soluble COD levels was achieved within 3 days after shock-loading, compared to 20-30 days without the resins.

3.5.1 AnMBR optimization via design modification

Because the high-throughput MBR performance was not sufficient for long periods of operation, several design improvements have been made. A physical improvement was the addition of an intermittently operated BAC filter to polish the effluent and help improve performance during times when the AnMBR is starting up or not running at optimal performance due to variable use, spikes in organic loads, or reactor poisoning. This modification adds a 10% space requirement to the design. An operational improvement is the increase to the HRT of the AnMBR, allowing more time for biodegradation to occur. The HRT is being stepped up in 4 hour increments to facilitate improved organics removal. Based on projections based on data from this study and published pilot scale data (Cumin *et al.*, 2012), an organic loading rate of 1200 mg COD/L/day should be feasible (Figure 36). Confirmatory experiments are ongoing. Experiments are also being performed that simulate repurposing the amount of waste heat from co-gen processing of the methane to increase reactor temperature and reduce the HRT, but such an approach could be reserved for cool weather operating conditions.

Figure 36. Relationships between COD conversion in an AnMBR for two different reactors. The blue diamonds represent data collected in the current study for treating FOB-representative waste water (influent COD 1300) and using adsorbent augmentation in the high throughput AnMBR at ERDC. The red squares represent data collected in pilot-scale studies on a commercial system treating less concentrated wastewater (influent COD 300-550 mg/L). Based on these data, the projected HRT required for treating FOB-representative wastewater is 24 hours.



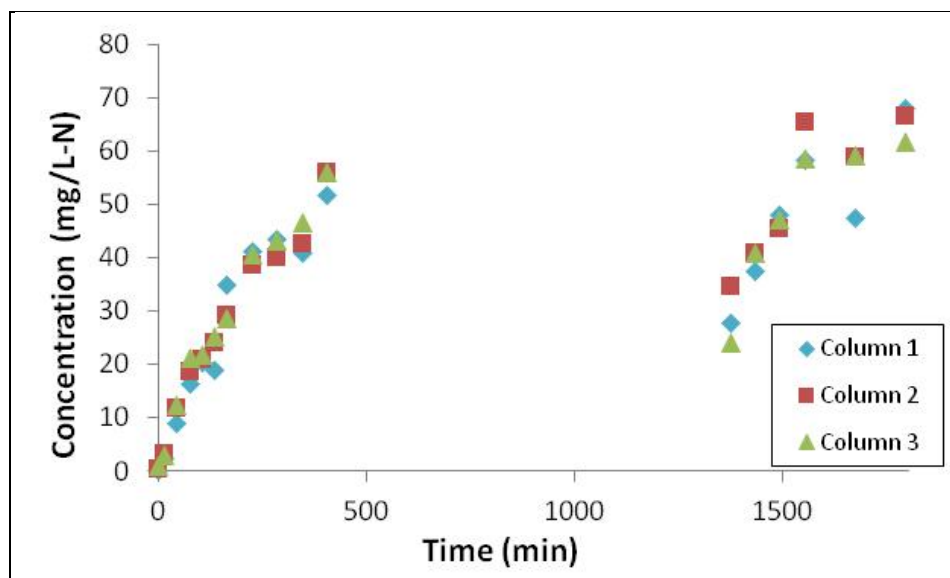
Thus, to treat 10 kgpd (enough to support 1000 PAX) of FOB-representative wastewater at an HRT of 24 hours, the AnMBR reactor size will need to be closer to 30 m³, which will require its own 20 ft ISO container. Thus, the resultant AnMBR reactor size will be about 2X larger than the original ACE concept design. However, given that this new approach does not involve heating the water above ambient temperature, the associated logistics savings (in terms of fuel costs) will be substantial. Thus, the final ACE system will need to be housed in a 40 ft shipping container, or in a 20 ft ISO plus one Tricon.

3.5.2 Ammonia sequestration on clinoptilolite

The original clinoptilolite media chosen for ammonia uptake experiments was AmmoChips by API. AmmoChips were chosen primarily for their ease of purchase at local pet shops and online. The particles were roughly 8 mm in size. Do to the relatively large diameter, the AmmoChips allowed the solution to flow freely around the particles thus not creating significant back-pressure. Successful ammonia sequestration was possible using this media. However, breakthrough was reached after a relatively short period

of time. Also, as seen in Figure 37, when the flow was stopped overnight, the capacity of the clinoptilolite appears to have increased.

Figure 37. AmmoChip loading runs at 60 mL/min. Initial concentration = 85 mg/L-N.

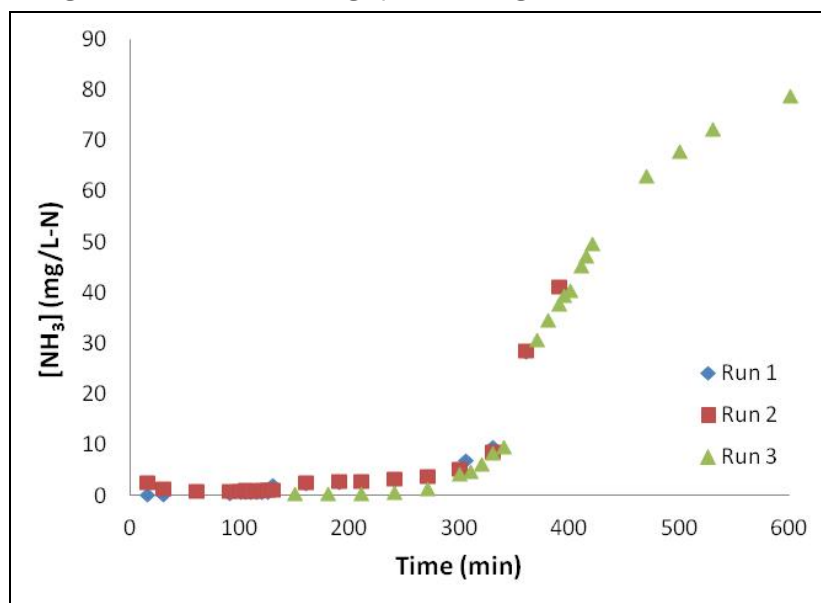


During regeneration, ammonia slowly leached off the media resulting in a dilute brine not ideal for subsequent electrolysis. We believe that during loading, ammonia diffuses into the particle. When the flow is stopped for a period of time, the interior diffusion leaves active sites available on the surface resulting in observed performance improvements when the system is restarted. Since significant ammonia is inside the particle, long regeneration times are required to allow for diffusion out to the surface before ammonia is released into the brine.

Zeobest is another commercially available product though not as common in the market. The Zeobest particle size is significantly smaller than AmmoChips with an average diameter around 1 mm. The smaller particle size packs more efficiently in the column, restricting flow, and creating back pressure that required a pump upgrade to overcome. Additionally, particle retention within the column was more complicated requiring a filter to prevent the media from sliding down into the tubing. Since most of the active sites were not located at the surface of the particle, Zeobest was extremely effective at sequestering ammonia. With 480 g of Zeobest clinoptilolite, breakthrough was not observed for 33 days. Similarly, 250 g showed no sign of breakthrough for 16.7 days. The amount of media was

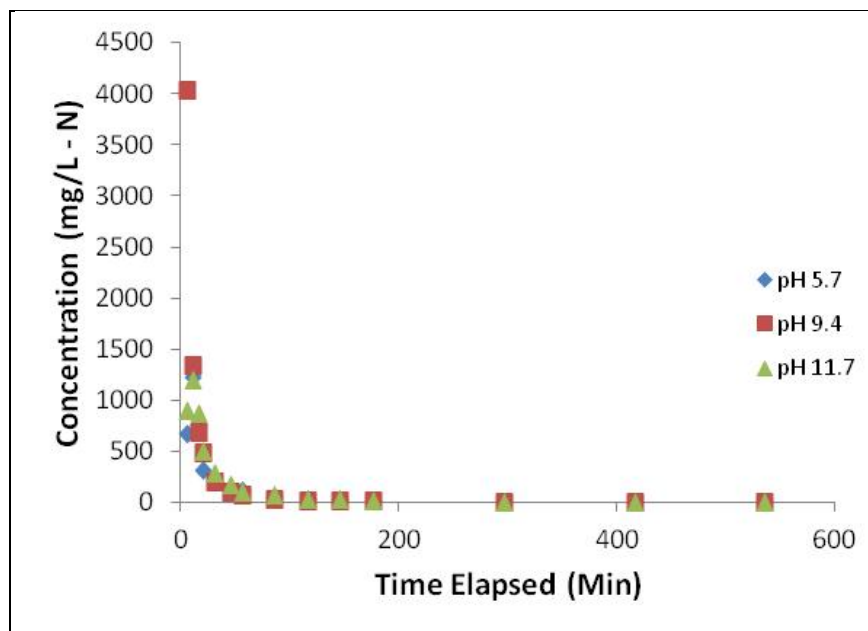
reduced to 75 g to enable reasonable loading and regeneration times. Repeat loading and regeneration cycles showed no degradation in the ability of clinoptilolite to sequester ammonia (Figure 38).

Figure 38. Repeat loading cycles on regenerated clinoptilolite.



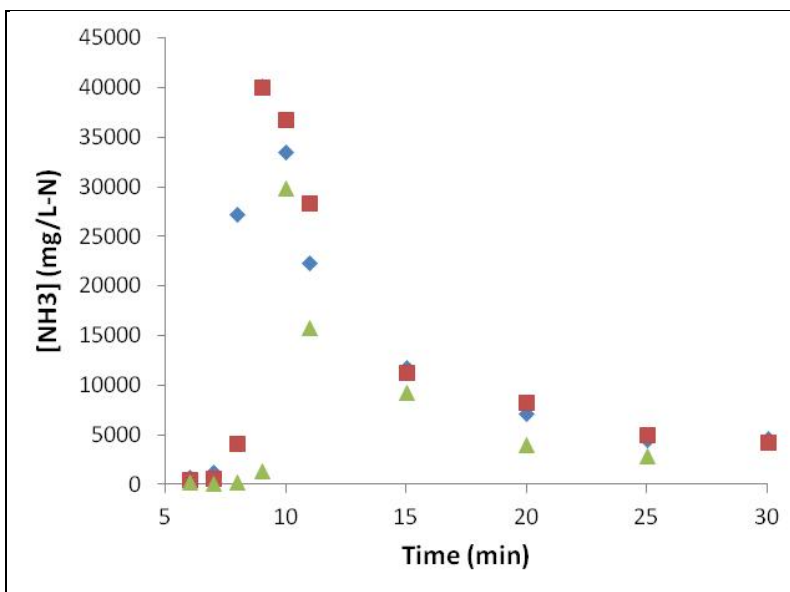
Under ideal conditions, the addition of NaOH to the regenerant would increase the maximum concentration of ammonia recovered. In theory, the higher pH would favor neutral NH_3 over cationic NH_4^+ . The neutral species would not be attracted to the negative sites on clinoptilolite thus driving the equilibrium to ammonia desorption. However, as seen in Figure 39, the increase in pH through NaOH addition did not have an effect on clinoptilolite regeneration. While no positive affect was observed as hoped, there was no detrimental effect either. Since the regenerant solution will be caustic to meet the needs of ammonia electrolysis, the clinoptilolite will have to be stable in that environment.

Figure 39. Regeneration of saturated clinoptilolite at pH 5.7, 9.4, and 11.7.



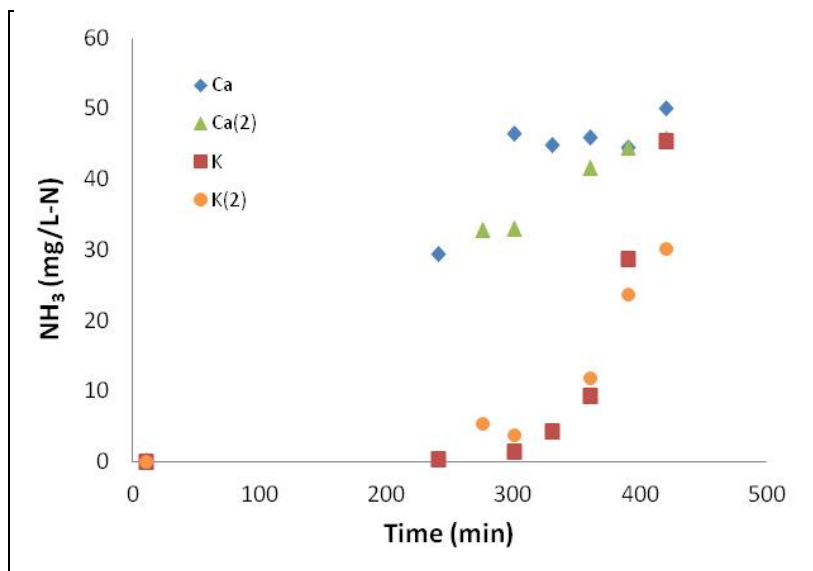
One of the critical process adaptations implemented to increase compatibility of ammonia sequestration with ammonia electrolysis was a stop-flow regeneration method. In this method, the column was filled with the 10% NaCl regenerant solution, then flow was stopped. During this time, the NH_4^+ ions sorbed to the clinoptilolite surface would be released within a smaller volume of solution than if the flow were continuous. When the flow was restored, peak ammonia concentrations were measured around 38,000 mg/L (Figure 40) compared to 6,000 mg/L under continuous flow regeneration (Figure 39). As ammonia electrolysis is more efficient at higher ammonia concentrations, the ability to generate a more concentrated ammonia brine following regeneration better integrated the two technologies.

Figure 40. Clinoptilolite regeneration using a stop-flow method.



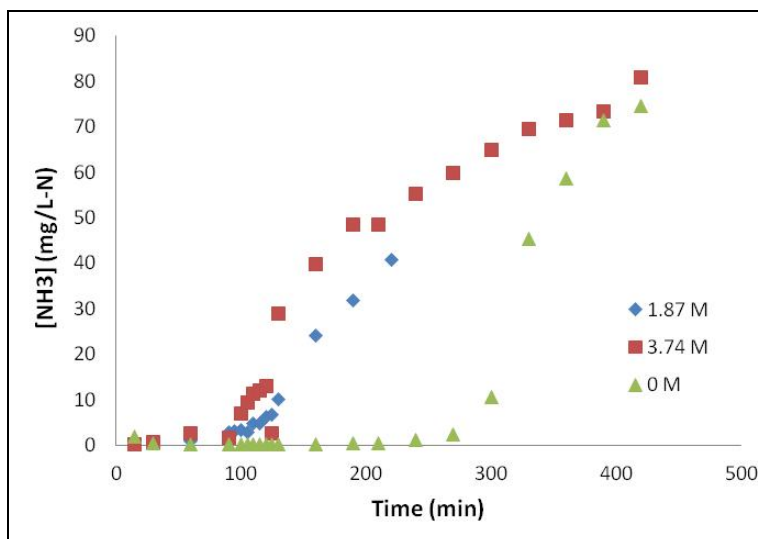
Competing ions are a potential complication when using real water in the clinoptilolite influent stream. While clinoptilolite is generally selective for ammonia based on charge and size, other ions could also adsorb to the negative binding sites reducing the capacity for ammonia adsorption. The two ions expected to result in reduced capacity were calcium (Ca^{+2}) because of its relatively high concentration in common waters and potassium (K^{+}) since it is preferred over NH_4^{+} . We selected test values of 3.75 mM Ca^{+2} or 1.02 mM K^{+} to represent what might be found in moderately strong wastewater. Figure 41 shows the results. Potassium has minimal effect at these concentrations. Calcium, however, does have an effect. Significant breakthrough is observable by the time monitoring is begun. Following a regeneration cycle, a second ammonia loading with calcium displays the same behavior without compounded detrimental effects.

Figure 41. Effect of competing ions on ammonia sequestration (3.75 mM Ca^{+2} or 1.02 mM K^{+}).



Further analysis on calcium ion competition was performed to see if lower concentrations corresponded to improved performance. The clinoptilolite column was loaded with ammonia for approximately 420 minutes. The influent solution also contained Ca^{2+} in the form of aqueous CaCl_2 . The calcium concentrations for the experiments were at 1.87 mM and 3.74 mM (Figure 42). These concentrations represent average wastewater hardness for various testing locations. Hard water is usually listed with calcium concentration of 5 mM and domestic soft water is between 0.15-0.4 mM of Ca^{2+} . Capacity for ammonia sequestration was restored following a regeneration cycle.

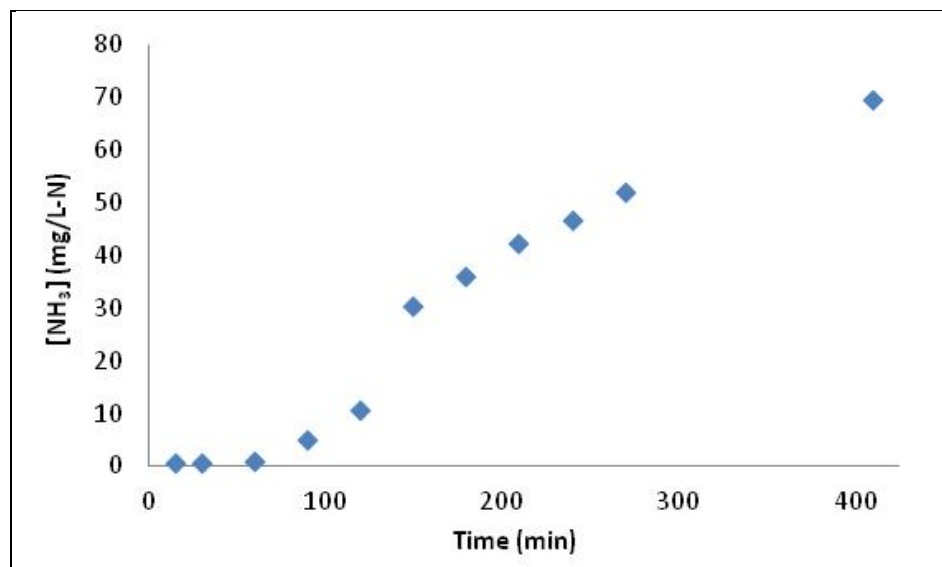
Figure 42. Ammonia breakthrough at 1.87 mM, 3.74 mM, and 0 mM Ca^{2+} levels. The 0 mM run followed regeneration of the column after the calcium runs demonstrating restored capacity.



The data suggests that the presence of calcium decreases the effectiveness of the clinoptilolite in regards to ammonia removal. Reducing the calcium levels by 50% has only a marginal effect in restoring capacity. However, as can be seen in Figure 42, ammonia removal capacity was restored with regular regeneration with NaCl and removal of the calcium source. At FOBs with tactical water purification systems (TWPS) or reverse osmosis purification units (ROPU), the calcium levels of supply waters are expected to be very low. Unless a large influx of calcium is introduced prior to waste water treatment, calcium levels are not expected to reach problematic levels. If a one-time calcium event were to occur, the columns would return to a fully functioning state following a regeneration cycle. In cases where calcium is present continually at higher concentrations, the load-regeneration program times or clinoptilolite volumes could be adjusted to account for reduced capacity.

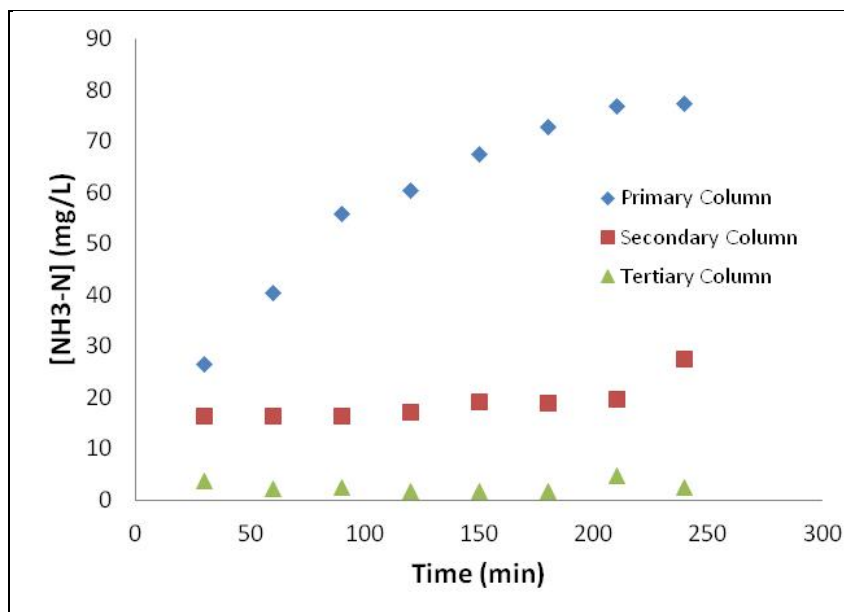
To see how real waters would affect the performance of the clinoptilolite, waste water was obtained following primary treatment. The ammonia levels in the water were increased to 80 mg/L by adding ammonium chloride so the results could be compared to previous experiments. The results are shown below in Figure 43. The real water breakthrough behavior is nearly identical to that observed for calcium containing waters. As before, capacity was restored by regeneration using the 10% NaCl solution.

Figure 43. Ammonia loading experiment data for real waste water.



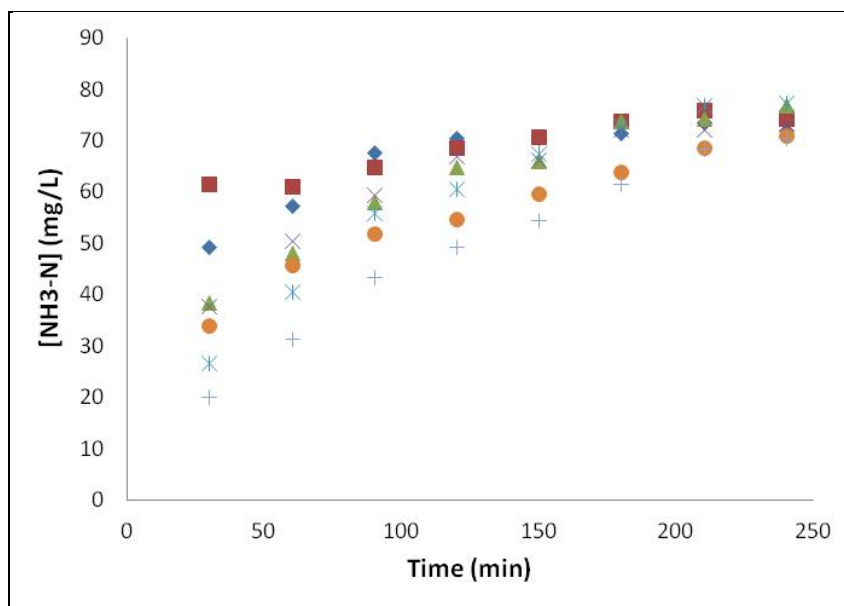
The most effective coupling of ammonia sequestration and ammonia electrolysis occurs when the ammonia concentration in the regenerant brine is maximized. Significant increases were gained by modifying the regeneration procedure to a stop-flow method. Additional gains could be made if the columns were fully loaded (100% breakthrough) prior to regeneration. Since breakthrough occurs over a period of time before reaching saturation, fully loading a single column would release more ammonia into the treated water stream than allowed. The solution was to develop a system of clinoptilolite that operates in series. Each subsequent column would collect breakthrough allowing the first column to be fully loaded without releasing ammonia into the treated water effluent. The serial operation of ammonia sequestration columns will become even more crucial in places where calcium or other compounds decrease capacity and lengthen breakthrough times. Figure 44 represents the ammonia concentrations measured exiting each of the three columns in series.

Figure 44. Ammonia breakthrough observed in three serially operated load columns.



Additional functionality was introduced by automating steps of the process. Solenoid valves controlled the flow to the three load columns and a fourth column undergoing regenerations. An operational schedule of four hours run time was implemented at a flow rate of 75 mg/L. Figure 45 shows multiple loadings of the primary column. While the effluent flow began at varying concentrations, the column was fully loaded at the end of four hours. Regeneration was performed by manually starting and stopping the pump to allow for the hour long soak period.

Figure 45. Repeat loading of the primary column in multi-column operation.

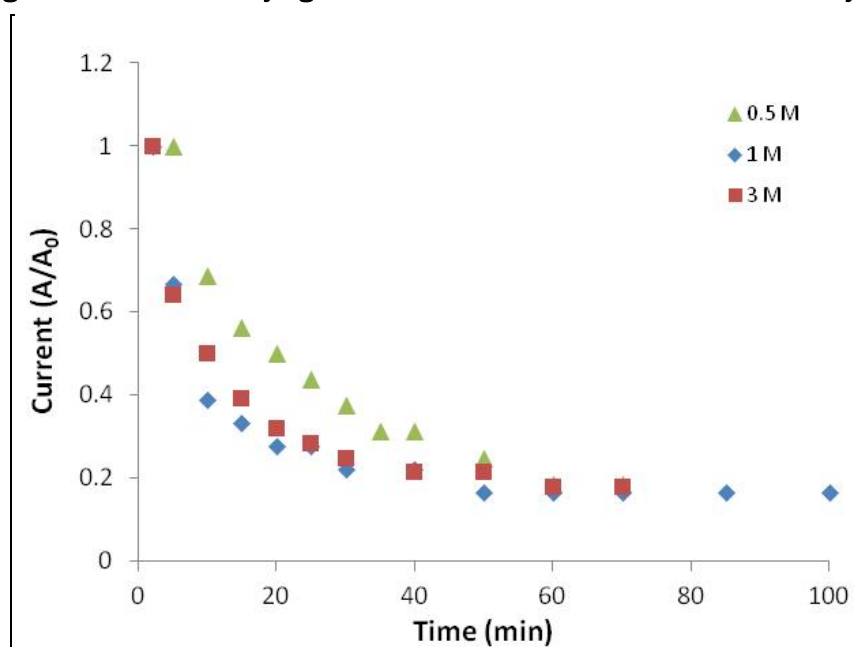


3.5.3 Ammonia electrolysis

Since ammonia electrolysis has already been demonstrated, the focus was on identifying optimal operating conditions for ammonia electrolysis. Both effective operation and safe operation were considered. Additionally, the traditional KOH carrier solution was being changed to NaOH to be compatible with the clinoptilolite regenerant brine. Since potassium is preferred over ammonia, we didn't want to introduce KOH to the regenerant. Thus, baseline measurements for NaOH-based operation were needed.

The recommended operating parameters used a 5M NaOH solution. From both a material consumption and safety standpoint, this level of concentration was not desirable. The experiment was repeated with NaOH concentrations of 0.5M and 3M. As seen in Figure 46, the behavior of the system did not vary greatly. Starting currents were also fairly constant, falling between 1.2-1.8A for these runs.

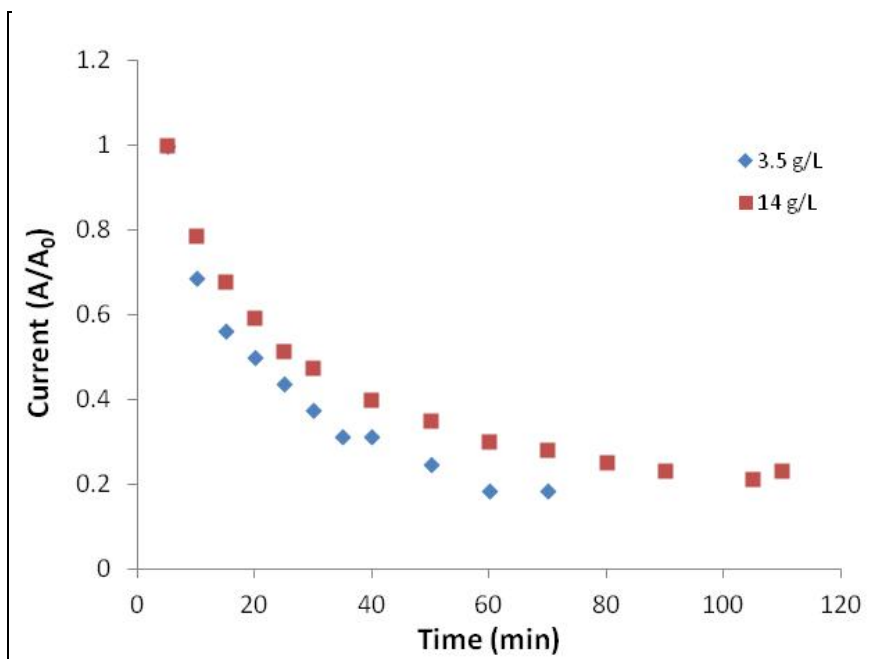
Figure 46. Effect of varying NaOH concentrations on ammonia electrolysis.



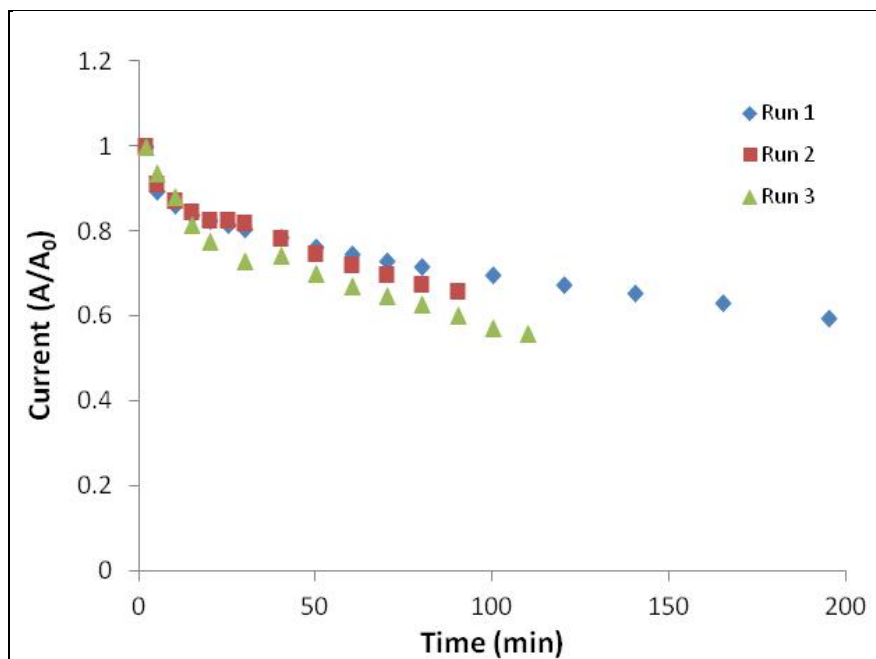
The relatively low ammonia concentration used (3.5 g/L) is representative of what could be achieved currently during clinoptilolite regeneration. However, with refined methods, the ammonia concentration in the regenerant brine was greatly increased. Thus, the system was also run at 14 g/L and 20 g/L. The results for the 14 g/L NH_4Cl run compared to an earlier 3.5 g/L run are shown in Figure 47. The behavior of the two systems is

comparable; however, the starting current values increased to 10.3A with the increase in ammonia concentration.

Figure 47. Effect of varying ammonia concentrations on ammonia electrolysis ($A_0 = 1.4$ A for 18g/5L; 10.3 A for 70g/5L).

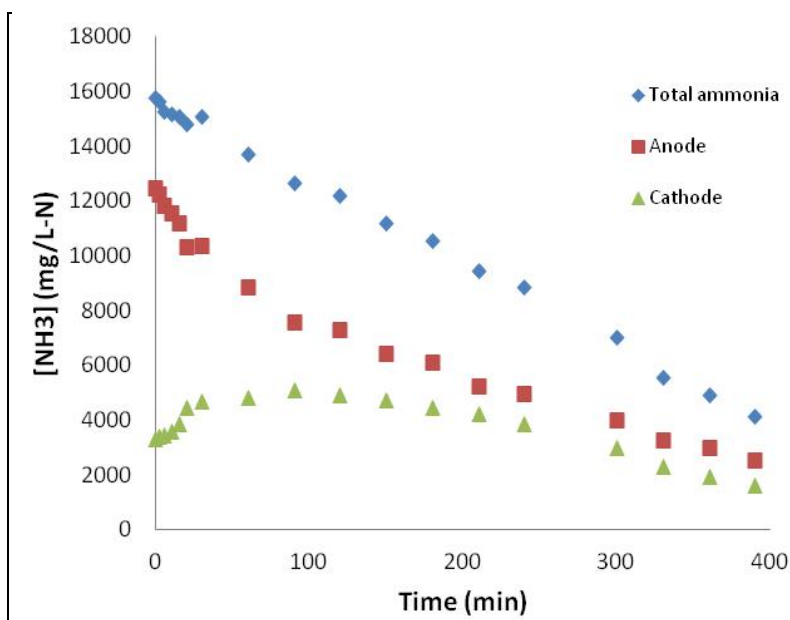


Repeat runs were made for 20 g/L at $[\text{NaOH}] = 0.5\text{M}$ (Figure 48). The data sets are fairly consistent in behavior with starting currents of 21-24A. However, it is worth noting that the current decays more slowly than the 3.5 g/L and 14 g/L runs. Modeling efforts at Ohio University suggest that a low $[\text{OH}^-]/[\text{NH}_3]$ ratio could impede performance. While the addition of other catalytic metals to the palladium is believed to help alleviate this problem, it may be challenging the system once it approaches a 1:1 ratio. However, it is believed that the concentration of NaOH would need to be increased given the maximum ammonia concentrations it is able to achieve during clinoptilolite regeneration.

Figure 48. Ammonia electrolysis runs at 20 g/L NH_4Cl . $A_0 = 22$ A.

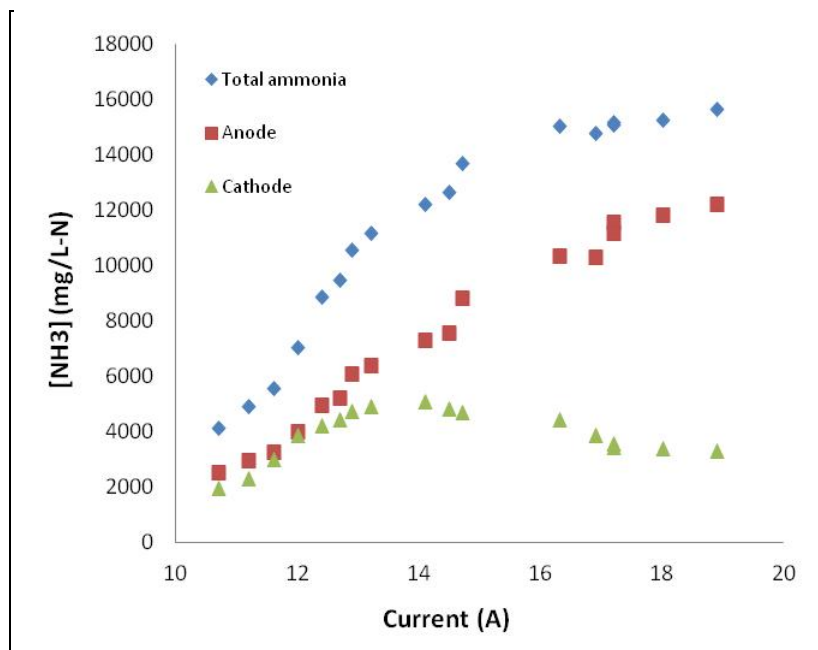
One of the biggest practical hurdles to overcome in the ammonia electrolysis design was how to sample the solutions for ammonia concentration. With variable flow potentials and the presence of gas bubbles, sampling from the lines was not ideal. The best option was determined to be sampling directly from the reservoir. While this would not give specific ammonia values throughout the system, the reservoir values were the concentrations being fed into the catalytic cells resulting in the observed currents. Once a sampling method was established, it was discovered that even though the ammonia solution was only introduced on the anode side, significant ammonia readings were recorded for the cathode solution as well (Figure 49). After discussing with E3, it was believed this was due to the similar shape and size of ammonia to water molecules. Since the membrane is water permeable, ammonia may also be passing through the membrane. With respect to ammonia conversion, the transport of ammonia does not appear to be a concern as ammonia levels decrease in both solutions as the run progresses.

Figure 49. Ammonia levels measured in anode and cathode solutions during an electrolysis experiment. Total ammonia is the sum of the measured concentrations.



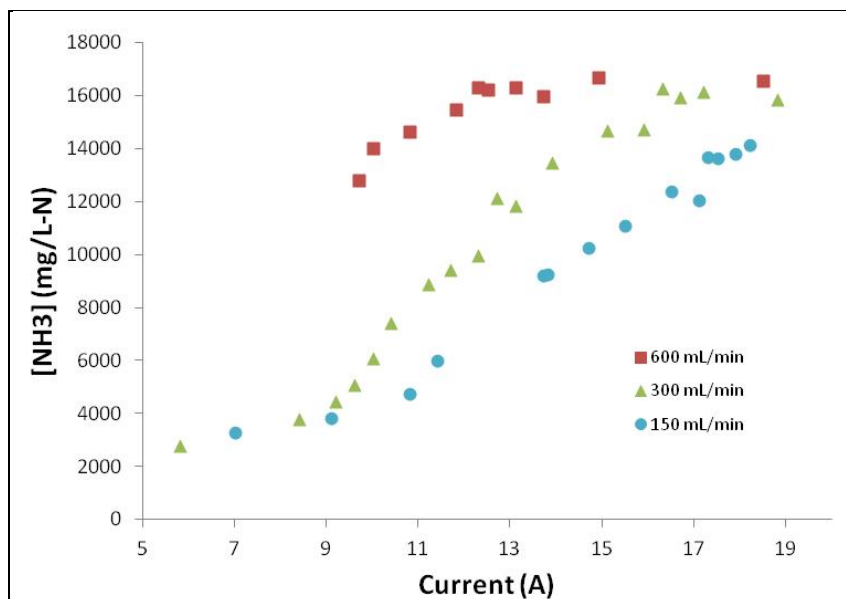
The ability to measure ammonia concentrations also allowed plotting of current vs. concentration (Figure 50). As a result, some insight was gained into the lower observed decay rate in the current at high ammonia concentrations. The initial concentrations of ammonia (15 g/L-N) do not vary significantly even as the current drops from 20 A to 16 A. It is believed that the catalyst surface is being poisoned by the abundance of ammonia molecules. As the ammonia molecules adsorb to the surface, additional free sites are unavailable for subsequent intermediates to bind and react. This hypothesis is supported by modeling results shown in the next section (see section 3.5.4, Figure 54).

Figure 50. Comparison of current readings to ammonia concentrations of the anode, cathode, and total solution.

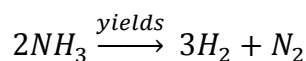


Flow rates of 300 mL/min and 150 mL/min were chosen to study the impact of flow rate on current output (Figure 51). With the lower flow rate, the region of saturation is reduced. Additionally, more current is produced for the same concentration values. Once the flow rate through the catalytic cell is slowed, a better balance is achieved between surface reaction rates and diffusion of ammonia molecules to the surface. Lower flow rates have the added benefit of reducing the energy consumption of the pumps.

Figure 51. Impact of flow rate on ammonia electrolysis performance.



Hydrogen and nitrogen are produced in a 3:1 molar ratio as per the simplified chemical reaction below.



Gas production was approximated during experimentation using wet tip meters attached to the gas separators. Table 17 shows the measured volumes of hydrogen and nitrogen from one such experiment. Since gas volumes are being measured in discrete 100 mL increments, measuring exact ratios is not possible. However, the obtained ratios are in general agreement with the expected 3:1 hydrogen:nitrogen. Gas chromatography of a hydrogen sample revealed pure hydrogen within error due to atmospheric contamination. The purity of the gas is compatible with fuel cell operation or combustion to generate electricity.

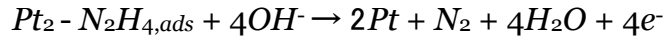
Table 17. Experimental values of hydrogen and nitrogen production.

Hydrogen (mL)	Nitrogen (mL)	Hydrogen:Nitrogen
0	0	-
100	0	-
300	100	3
800	300	2.66666667
2700	1000	2.7
5700	2000	2.85
8500	3000	2.83333333

Hydrogen (mL)	Nitrogen (mL)	Hydrogen:Nitrogen
11100	4000	2.775
13500	4900	2.75510204

3.5.4 Ammonia electrolysis model

The overall reaction kinetics for ammonia electrolysis do not follow the Butler-Volmer equation. Thus, the reaction path presented by Rosca and Koper was used in the analysis (Gootzen et al. 1998).



Each of these single reactions can be considered as elementary and governed by Butler-Volmer equations. The adsorption of ammonia to the platinum surface is taken to be the rate limiting step with the maximum impact on reaction kinetics.

The microkinetics model developed for ammonia electrooxidation at the anode is fully explained in Diaz and Botte (2015). The current density is dependent on the number of electrons transferred (n), species concentration (c), reference potentials (U_{ref}), anode voltage (V_a), cell potential (ϕ), Faraday's constant (F), equilibrium constants (K), and rate constants (k) and is given by:

$$i = \frac{n_a \cdot F \cdot k_{2f,a} \cdot K_{1,a}^2 \cdot c_{NH_3}^2 \cdot c_{OH^-}^2 \cdot \exp\left(\frac{2F(V_a - \phi - U_{ref_{a1}})}{RT}\right)}{\left(1 + K_{1,a} \cdot c_{NH_3} \cdot c_{OH^-} \cdot \exp\left(\frac{F(V_a - \phi - U_{ref_{a1}})}{RT}\right) + K_{1,a} \cdot K_{4,a} \cdot c_{NH_3} \cdot c_{OH^-}^2 \cdot \exp\left(\frac{F(2V_a - 2\phi - U_{ref_{a1}} - U_{ref_{a4}})}{RT}\right) + K_{1,a} \cdot K_{4,a} \cdot K_{5,a} \cdot c_{NH_3} \cdot c_{OH^-}^3 \cdot \exp\left(\frac{F(3V_a - 3\phi - U_{ref_{a1}} - U_{ref_{a4}} - U_{ref_{a5}})}{RT}\right)\right)^2} \quad (6)$$

On the cathode side of the electrochemical cell, kinetics for hydrogen evolution reactions (HER) during the reduction of water needed to be established. Appropriate description of HER kinetics must include the reaction mechanism and surface coverage of adsorbed hydrogen. The latter quantity is of fundamental importance in describing electro-catalytic reactions.

The kinetics for the hydrogen evolution reaction at the cathode was based on a combination of the Volmer and Tafel elementary reactions as explained in Estejab *et al.* (2015). The current density is dependent on number of electrons transferred (n), the species concentration (c), reference potentials (U_{ref}), cathode voltage (V_c), cell potential (ϕ), Faraday's constant (F), symmetry factor (β), and rate constants (k) and is given by:

$$i = \frac{2n_c F k_{3f,c} \left(k_{1f,c} \exp\left(\frac{-\beta F (V_c - \phi - U_{ref,c})}{RT}\right) - k_{1b,c} c_{OH^-} \exp\left(\frac{(1-\beta) F (V_c - \phi - U_{ref,c})}{RT}\right) \right)}{k_{1f,c} \exp\left(\frac{-\beta F (V_c - \phi - U_{ref,c})}{RT}\right) + k_{1b,c} c_{OH^-} \exp\left(\frac{(1-\beta) F (V_c - \phi - U_{ref,c})}{RT}\right) + 4k_{3f,c}} \quad (7)$$

Table 18. Optimum parameters for Equations 6 and 7 generated from experimental measurements for the conditions tested in Table 9 (Estejab *et al.* 2015).

Parameter	Value
$k_{2f,a}$	2.3×10^{-10}
$K_{1,a}$	10.0
$K_{4,a}$	8.6
$K_{5,a}$	2.24×10^{-2}
$U_{ref,a1}$	-0.83
$U_{ref,a4}$	-0.30
$U_{ref,a5}$	-0.18
$k_{1f,c}$	4.2×10^{-7}
$k_{1b,c}$	9×10^{-8}
$k_{3f,c}$	4.7×10^{-7}
β	0.24

Parameters were generated for the aforementioned kinetics (Equation 6 and Equation 7) based on experimental values collected in this project and are provided in Table 18. The semi-empirical model developed using the

parameters showed good agreement with the current density generated based on the high and low concentrations of ammonia examined in Table 11 (Figure 52 and Figure 53).

Figure 52. Calculated and measured current density versus cell voltage at low concentrations of NH_4Cl and KOH : $1 \times 10^{-5} \text{ mol cm}^{-3}$ and $1 \times 10^{-4} \text{ mol cm}^{-3}$ respectively. The decrease in conversion at higher cell voltages can be attributed to depletion of reactant and/or electrode poisoning (Estejab et al. 2015).

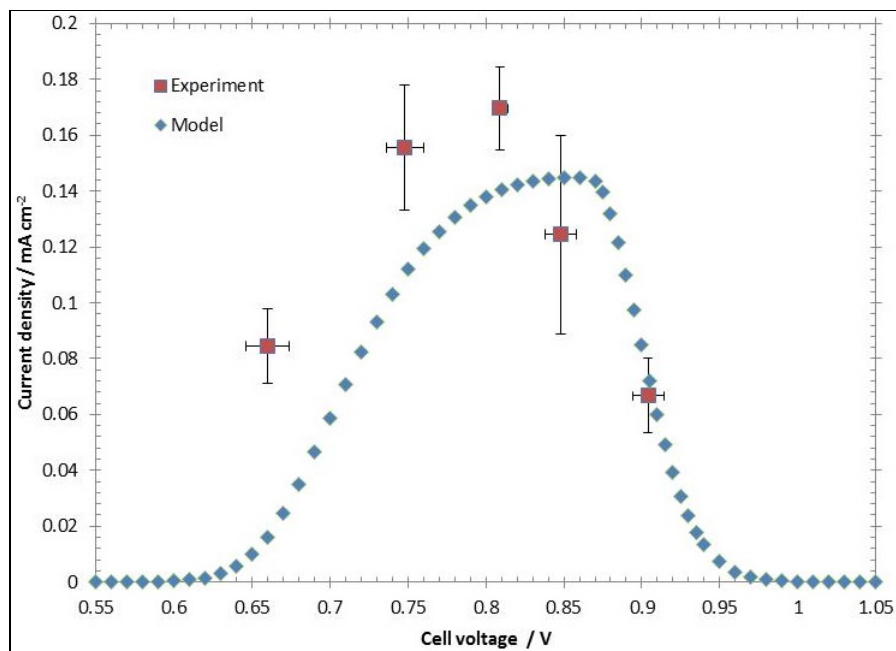
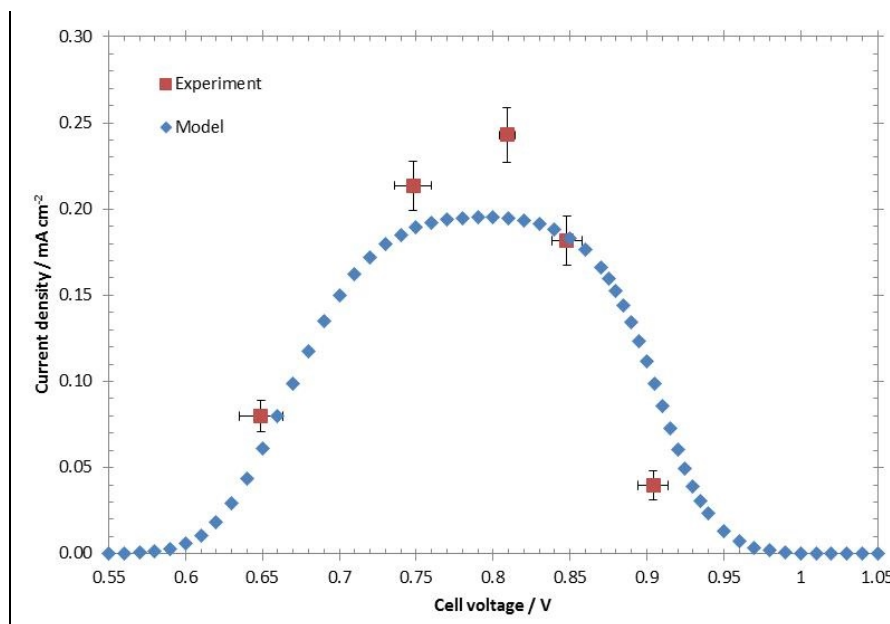
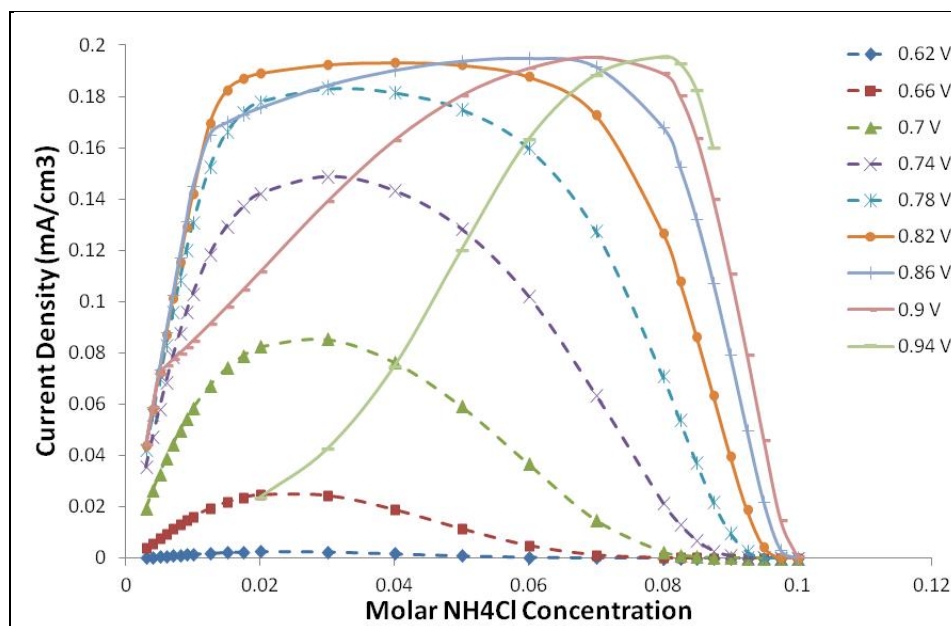


Figure 53. Calculated and measured current density versus cell voltage at high concentrations of NH_4Cl and KOH : $7 \times 10^{-5} \text{ mol cm}^{-3}$ and $1.5 \times 10^{-4} \text{ mol cm}^{-3}$ respectively. The decrease in current density at higher cell voltages can be attributed to electrode poisoning (Estejab et al. 2015).



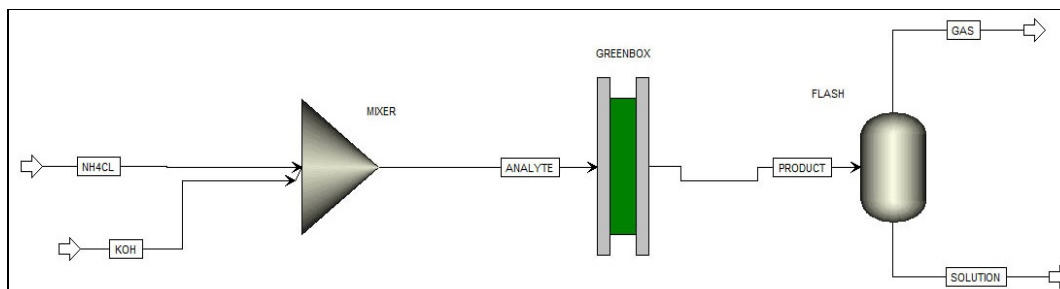
The model therefore suggested that for optimum kinetics at these fixed concentration values, the cell should be operated close to 0.80 V for palladium-nickel catalyst cells. Further analyses indicated that there is a complex correlation between the inlet concentrations, cell conditions, and cell performance (Figure 54). Although it is expected that increasing initial concentration and voltage would increase the electrolyzer performance, this is not always the case. As an example, higher concentrations of the ammonium ion (at a fixed hydroxide ion concentration) indicate the higher potentials will go from a positively-skewed current density relationship to a negatively-skewed current density relationship i.e., the concentration range over which the current density is maximum decreases.

Figure 54. Predicted current density as a function of NH_4Cl concentration for different cell voltages and 0.1M KOH concentration. Right axis is the ratio of hydroxide ion to ammonia concentration at the anode. For voltages below 0.80 V (dashed lines) increasing reactant concentration to more than 0.0295M NH_4Cl causes $[\text{OH}^-]/[\text{NH}_3]$ to be less than 3 and current density decreases. For voltages above 0.80 V (solid lines) catalyst poisoning is the reason for the decrease of the current density (Estejab et al. 2015).



This complex interplay could be ameliorated by creating a user-friendly interface to provide flexibility for performing multi-variate analysis. For this flexibility, an ASPEN Plus interface was built based on the aforementioned FORTRAN subroutine for describing the electrolytic reactions. This ASPEN Plus setup included the electrolytic cell combined additional unit operations for mixing and gas-liquid separations (Figure 55). These additional unit operations will be modified to include actual units in this project i.e., ion exchange columns and bioreactors.

Figure 55. ASPEN Plus schematic for the simulation of the ammonia GreenBox and its adjacent unit operations. The inlet stream to the GreenBox will be the outlet from the ion-exchange membrane and will contain ammonium ions, hydroxide ions, ammonia and water in equilibrium. The outlet streams from the FLASH represent an instantaneous gas-liquid phase separation.



The ammonia electrolytic cell can be operated at optimum conditions dependent on the cell voltage and inlet concentrations of ammonium and hydroxide ions. This optimum condition is also affected by reactant depletion at the electrode surface (low inlet concentrations) and catalytic poisoning (high inlet concentrations). The use of ASPEN Plus provides the opportunity to use equilibrium constants and physical properties developed for electrolyte-based systems as well as a user-friendly interface for general use.

The developed model is the first of its kind for ammonia electrolysis and provides an opportunity to simulate realistic conditions for stand-alone cell operation and deployment in municipal wastewater treatment facilities. Specific to this project, this model combined with the ion-exchange columns and anaerobic digesters will be useful in examining a comparison between this sustainable method of wastewater treatment and a standard treatment plant. Finally, the hydrogen generated from this treatment method can be evaluated for use in improving plant efficiency through the use of a hydrogen fuel cell for supplementary power generation.

4 Conclusions and Implications for Future Research/Implementation

Overall, the findings of this study are generally supportive of continued development of the ACE approach. While the original operating concept was modified slightly, the general approach of combining AnMBR with clinoptilolite ion exchange and ammonia electrolysis should be studied further at pilot-scale using design parameters identified in this study. For AnMBR treatment, an ambient temperature mode of operation was evaluated with augmentation by adsorbents and biocultures. The ambient temperature mode of operation will require longer HRTs than mesophilic operation, which will decrease the volumetric loading capacity of the design, but detailed energy analysis indicated that the mesophilic approach was not favorable. However, processing of sludge and other concentrated organic waste streams using AnMBR could be performed at mesophilic temperatures with a positive energy balance. In either case, the AnMBR technology demonstrated sustained organics removal capability as well as conversion of the organic nitrogen to ammonium ions, which was important for combining this approach with clinoptilolite ion exchange. Additionally, the AnMBR ultrafiltration membrane presents a robust barrier against suspended solids (SS) and pathogens.

Ammonia sequestration with clinoptilolite was successfully demonstrated. A balance between efficient ion exchange and operational backpressure was found with particles roughly 1 mm in diameter. A multiple column design optimized ammonia sequestration performance. The additional columns collected breakthrough while allowing the primary column to be fully saturated with ammonia. The result was a more concentrated ammonia brine for ammonia electrolysis. Ammonia concentrations were also increased through the development of a stop-flow regeneration procedure. Calcium in the influent wastewater stream has the ability to reduce the capacity of the clinoptilolite media for ammonia sequestration. However, the detrimental effect is reversible upon regeneration and can be compensated for by adjusting load cycle times.

The ammonia electrolysis operational procedures were modified to reduce flow rate and sodium hydroxide concentrations. The result is a system that is more efficient, requires less energy input, and is safer to operate. Since

only a fraction of ammonia is removed during each pass, the ammonia solution will need to be recycled through the system. Brine that has been treated to remove the ammonia can be returned to regenerate additional clinoptilolite media, reducing the chemical input of the coupled ammonia sequestration/ammonia electrolysis processes. Hydrogen gas produced by the electrolysis of ammonia was demonstrated as having minimal contaminants, making it suitable for fuel cells or combustion-based energy generation. Initial calculations indicate that the current 30 W GreenBox has sufficient capacity for treating waste water at a 500 PAX base.

The individual component technologies of the ACE wastewater treatment system have been optimized and integration potential demonstrated. The next phase would be the assembly and demonstration of a full-scale unit. A conceptual design of a full-size ACE system is shown in Chapter 3, Figure 18. By housing the equipment in standard shipping containers, the ACE system remains portable for contingency operations. The overall result is an efficient system for onsite treatment that supports self-sufficient FOB design goals.

Literature Cited

- Akram, A. and D.C. Stuckey. 2013. Mitigation of shock-loads using ion-exchange resins in a submerged anaerobic membrane bioreactor (SAMBR). IWA 13th World Congress on Anaerobic Digestion Conference Proceedings.
- Amani, T., M. Nosrati, S.M. Mousav, R.K. Kermanshahi. 2011. "Study of syntrophic anaerobic digestion of volatile fatty acids using enriched cultures at mesophilic conditions." *International Journal of Environmental Science and Technology* 8 (1): 83-96.
- Aspen Technology Inc. 2012. *Aspen Plus v8.0 - Getting Started Modeling Processes with Electrolytes*. Burlington, MA: Aspen Technology Inc.
- Bérubé, P. R; Hall, E. R; and Sutton, P. M. 2006. "Parameters Governing Permeate Flux in an Anaerobic Membrane Bioreactor Treating Low-Strength Municipal Wastewaters: A Literature Review." *Water Environment Research* 78 (8): 887-896.
- Boggs, B.K. and G.G. Botte. 2010. "Optimization of Pt-Ir on carbon fiber paper for the electro-oxidation of ammonia in alkaline media." *Electrochimica Acta* 55: 5287-5293.
- Bonnin, E.P., E.J. Biddinger, and G.G. Botte. 2008. "Effect of Catalyst on Electrolysis of Ammonia Effluents." *Journal of Power Sources* 182: 284-290.
- Botte, G.G. 2005. "Modeling volume changes due to lithium intercalation in a carbon fiber." *Electrochimica Acta* 50: 5647-5658.
- Botte, G.G. 2010. Electro-catalysts for the oxidation of ammonia in alkaline media. U.S. Patent No. 7,803,264, Ohio University.
- Botte, G.G. 2012. Electrochemical method for providing hydrogen using ammonia and ethanol. U.S. Patent No. 8,221,610, Ohio University.
- Botte, G.G. 2012. Layered electrocatalyst for oxidation of ammonia and ethanol. U.S. Patent No. 8,216,956, Ohio University.
- Botte, G.G. 2012. Layered electrocatalyst for oxidation of ammonia and ethanol. U.S. Patent No. 8,613,842, Ohio University.
- Chen, Y., J.J. Cheng, K.S. Creamer. 2008. "Inhibition of anaerobic digestion process: A review." *Bioresource Technology* 99 (10): 4044-4064.
- Choo, K.H., I.J. Kang, S.H. Yoon, H. Park, J.H. Kim, S. Adiya, and C.H. Lee. October 2000. "Approaches to Membrane Fouling Control in Anaerobic Membrane Bioreactors." *Water Science and Technology* 41: 363-371.
- Diaz, L.A. and G.G. Botte. 2015. "Mathematical modeling of ammonia electrooxidation kinetics in a Polycrystalline Pt rotating disk electrode," *Electrochimica Acta* 179: 519-528: doi.org/10.1016/j.electacta.2014.12.162.

- Environmental Protection Agency (EPA) .1997. *Waste Water Treatment Manuals: Primary, Secondary, and Tertiary Treatment*. Wexford, Ireland: EPA.
<http://www.epa.ie/pubs/advice/water/wastewater/wastewatertreatmentmanuals-primarysecondarytertiarytreatment.html>.
- Estejab, A., D.A. Daramola, and G.G. Botte. 2015. "Mathematical Model of a Parallel Plate Ammonia Electrolyzer for Combined Wastewater Remediation and Hydrogen Production." *Water Research* 77: 133-145.
- Fountoulakis, M., P. Drillia, K. Stamatelatou, and G. Lyberatos. 2004. "Toxic Effect of Pharmaceuticals on Methanogenesis." *Water Science and Technology* 50 (5): 335-340.
- Gootzen, J. F. E., A.H. Wonders, W. Visscher, R.A. van Santen, and J.A.R. van Veen. 1998. "A DEMS and cyclic voltammetry study of NH₃ oxidation on platinized platinum," *Electrochimica Acta* 43: 1851-1861.
- Hai, F.I., K. Yamamoto, K. Fukushi. 2005. "Different fouling modes of submerged hollow-fiber and flat-sheet membranes induced by high strength wastewater with concurrent biofouling." *Desalination* 180: 89-97.
- Hegger, K.J. 2010. "Wastewater treatment by novel hybrid biological-ion exchange processes." PhD diss., University of Illinois at Urbana-Champaign.
- Hernandez, J.E., and R.G.J. Edyvean. 2011. "Comparison between a two-stage and single-stage digesters when treating a synthetic wastewater contaminated with phenol." *Water S.A.* 37: 1-6.
- Hu, A.Y and D.C. Stuckey. 2006. "Treatment of Dilute Wastewaters Using a Novel Submerged Anaerobic Membrane Bioreactor." *Journal of Environmental Engineering-ASCE* 132 (2): 190-198.
- Kang, I.-J., S.-H. Yoon, and C.-H. Lee. 2002. "Comparison of the filtration characteristics of organic and inorganic membranes in a membrane-coupled anaerobic bioreactor." *Water Research* 36: 1803-1813.
- Kim, T., Y. Nam, C. Park and M. Lee. 2009. Carbon source recovery from waste activated sludge by alkaline hydrolysis and gamma-ray irradiation for biological denitrification, *Bioresource Technology* 100: 5694-5699.
- Koe, L.C.C., F.G. Ang. 1989. "Biocatalytic addition: Does it aid anaerobic digestion?" *Water Research* 23: 1455-1459.
- Mader, M.J., C.W. Walton, and R.E. White. 1986. "Parallel Plate Electrochemical Reactor Model: Material Balance Closure and a Simplification." *Journal of the Electrochemical Society* 133: 1124-1130.
- Metcalf and Eddy Inc. 1991. *Wastewater Engineering: Treatment, Disposal, and Reuse*, 3rd Ed. New York, NY: McGraw Hill.
- Metcalf and Eddy Inc. 2004. *Wastewater engineering: treatment and reuse*, 4th Ed., Chap. 10, 983-1035. New York, NY: McGraw-Hill International Editions.

- Mignone, N.A. 2005. *Biological Inhibition/Toxicity Control in Municipal Anaerobic Digestion Facilities*. November 3, 2011.
<http://www.awpca.net/Biological%20Inhibition.pdf>
- Nair, S., Y. Kuang, P. Pullammanappallil. 2005. "Enhanced degradation of waste grass clippings in one and two stage anaerobic systems." *Environmental Technology* 26 (9): 1003-1011.
- Newman, J.S. and K.E. Thomas-Alyea. 2004. *Electrochemical Systems*. New York, NY: John Wiley & Sons.
- Noblis. 2010. SERDP Report on Sustainable Forward Operating Bases (May 2010). Falls Church, VA: Noblis.
- Nwuche, C. O. and E.O. Ugoji. 2008. "Effects of heavy metal pollution on the soil microbial activity." *International Journal of Environmental Science and Technology* 5 (3): 409-414.
- Nwuche, C. O. and E.O. Ugoji. 2010. "Effect of co-existing plant specie on soil microbial activity under heavy metal stress." *International Journal of Environmental Science and Technology* 7 (4): 697-704.
- Office of the Undersecretary of Defense for Acquisition, Technology, and Logistics. (2007). *Overseas Environmental Baseline Guidance Document*. DoD 4715.05-G.
- Parawira, W., M. Murto, J.S. Read, and B. Mattiasson. 2004. "Volatile fatty acid production during anaerobic mesophilic digestion of solid potato waste." *Journal of Chemical Technology and Biotechnology* 79 (7):673-677.
- Park, C., C. Lee, S. Kim, Y. Chen, and H.A. Chase. 2005. "Upgrading of anaerobic digestion by incorporating two different hydrolysis processes." *Journal of Bioscience and Bioengineering* 100 (2): 164-167.
- Ryan, P., C. Forbes, S. McHugh, C. O'Reilly, G.T.A. Fleming, and E. Colleran. 2010. "Enrichment of acetogenic bacteria in high rate anaerobic reactors under mesophilic and thermophilic conditions." *Water Research* 44 (14): 4261-4269.
- Singhania, R.R., Christophe, G., Perchet, G., Troquet, J., and Larroche, C. (2012). Immersed membrane bioreactors: an overview with special emphasis on anaerobic bioprocesses. *Bioresource Technology* 122: 171-180.
- Skouteris, G., D. Hermosilla, P. López, C. Negro, and Á. Blanco. 2012. "Anaerobic membrane bioreactors for wastewater treatment: a review." *Chemical Engineering Journal* 198: 138-148.
- United States Environmental Protection Agency. February 2008. *Emerging Technologies for Wastewater Treatment and In-Plant Wet Weather Management*. EPA 832-R-06-006. Washington, DC: USEPA Office of Wastewater Management.
- Vitse, F.; M. Cooper and G.G. Botte. 2005. "On the Use of Ammonia Electrolysis for Hydrogen Production." *Journal of Power Sources* 142: 18-26.

- Wallis-Lage, C.L. and S.D. Levesque. 2009. Cost Effective and Energy Efficient MBR Systems. Black & Veatch. Obtained at <http://www.bvwater.com> on January 5, 2010.
- White, R.E., M. Bain, and M. Raible. 1983. "Parallel Plate Electrochemical Reactor Model." *Journal of the Electrochemical Society* 130: 1037-1042.
- Yoo, R., J. Kim, P. McCarty, and J. Bae. 2012. "Anaerobic treatment of municipal wastewater with a staged anaerobic fluidized membrane bioreactor (SAF-MBR) system." *Bioresource Technology* 120: 133-139.

Appendix A: Publications Produced by this Study

Articles in peer-reviewed journals

Estejab, A.; Daramola, D.A.; and Botte, G.G. (2015). Mathematical Model of a Parallel Plate Ammonia Electrolyzer for Combined Wastewater Remediation and Hydrogen Production. *Water Research* 77: 133-145.

Conference abstracts

227th Electrochemical Society Meeting in Chicago, Illinois (May 24 – 28, 2015): Optimized Performance of a Scale-up Ammonia Electrolyzer for Combined Wastewater Remediation and Hydrogen Production (Oral Presentation).

2013 AIChE Annual Meeting in San Francisco, California (November 3 – 8, 2013) Mathematical Model and Validation of Parallel Plate Water Electrolyzers (Poster Presentation).

2012 AIChE Annual Meeting in Pittsburgh, Pennsylvania (October 28 – November 2, 2012) Computer Simulation of Water and Ammonia Electrolysis (Poster Presentation).

222nd Electrochemical Society Meeting in Honolulu, Hawaii (October 7 – 12, 2012): A Semi-Empirical Model of Ammonia Electrolysis in Comparison to Water Electrolysis (Poster Presentation).

Appendix B: Supplemental Information for Table 1

Table 1 in the main report body (see section 1.3.3) shows estimated energy savings, water demand reduction, and sludge reductions for the proposed wastewater treatment system. The following paragraphs describe the assumptions and calculations used to generate the values in Table 1.

Influent wastewater characteristics

Wastewater streams from municipal activities (bathing, toilet flushing, kitchens, etc.) vary in strength, as described in the Metcalf & Eddy text on Wastewater Engineering: Treatment, Disposal, and Reuse (1991, 2003). For this project, wastewater at FOBs was assumed to be slightly greater than moderate in strength. This assumption was based on the fact that water supply at FOBs is limited, resulting in a more concentrated waste stream. Key water quality parameters were BOD, assumed to be 300 mg/L; COD, assumed to be 700 mg/L; and total concentration of ammonia and organic nitrogen, assumed to be 60 mg/L (Table B1). Variations in these values would affect the outcome of the estimates. Higher COD and ammonia loadings would result in more methane and hydrogen production, but would also likely require larger tank sizes for the AnMBR system to achieve the target level of BOD reduction. In addition to quality parameters, flow rates (Q) were also calculated based on the number of personnel at a base. These values were adapted from SERDP guidance documentation (Noblis 2010).

Table B1. Influent water quality parameter values used for estimates.

Parameter	Symbol	Value and Units
Biochemical Oxygen Demand	BOD	300 mg/L
Chemical Oxygen Demand	[COD]	700 mg/L
Ammonia concentration	[NH ₃ -N]	60 mg/L

Renewable fuel yields

Renewable fuel yields were calculated based on contaminant loading rates and expected system performance. Multiplying quality parameter values by the daily flow rate yielded daily loading rates for COD and ammonia. Methane and hydrogen yields were then calculated assuming 95% recovery, 90% conversion efficiency, per the following equations:

Methane production estimation

$$CH_4 \left(\frac{kg}{day} \right) = Q \left(\frac{m^3}{day} \right) \times \left(\frac{1000 L}{1 m^3} \right) \times [COD] \left(\frac{mg}{L} \right) \times \left(\frac{1 kg}{10^6 mg} \right) \times \left(\frac{0.25 m^3 CH_4}{1 kg COD} \right) \times \left(\frac{0.61 kg CH_4}{1 m^3 CH_4} \right) \times (0.9)$$

Hydrogen production estimation

$$H_2 \left(\frac{kg}{day} \right) = Q \left(\frac{m^3}{day} \right) \times \left(\frac{1000 L}{1 m^3} \right) \times [NH_3 \cdot N] \left(\frac{mg}{L} \right) \times \left(\frac{1 kg}{10^6 mg} \right) \times (0.95) \times (0.9) \times \left(\frac{3}{2} \times \frac{2 kg H_2}{14 kg NH_3 \cdot N} \right)$$

Table B2. Renewable fuel yield estimates.

Base size	Flow rate Q	COD loading rate	NH ₃ loading rate	CH ₄ yield	H ₂ yield
Personnel	m ³ /day	kg/day	kg/day	kg/day	kg/day
50	6.7	4.7	0.4	0.64	0.07
500	67	47	4	6.4	0.73
1500	200	140	12	19.2	2.19
10000	1333	933	80	128.1	14.7

The values in Table B2 were then applied to calculate the amount of energy available for use at the FOB after fuel conversion. In the proposed system, electricity generation from methane would be achieved using a micro-turbine co-generator that combusts methane to produce electricity. Recovered waste heat would be used to heat the AnMBR reactor and for other onsite heating applications, such as water heating. Microturbines can recover 35% of the fuel energy in the form of electricity, and 85% of the total energy when heating is considered. Methane has a specific energy content of 12 kwh/kg. With fuel cell technology, a kilogram of hydrogen can produce 16.2 kwh of electrical energy, after conversion efficiency is considered.

CH₄ Energy Generation

$$E_{CH_4} \left(\frac{kwh}{day} \right) = (CH_4 \text{ yield}) \left(\frac{kg CH_4}{day} \right) \times \left(\frac{12 kwh}{1 kg CH_4} \right) \times (0.85)$$

H₂ Electricity Generation

$$E_{H_2} \left(\frac{kwh}{day} \right) = (H_2 \text{ yield}) \left(\frac{kg \ H_2}{day} \right) \times \left(\frac{16.2 \ kwh}{1 \ kg \ H_2} \right)$$

Energy usage

Full-scale membrane bioreactor plants that rely on aerobic processes were analyzed for energy efficiency (Wallis-Lage and Levesque 2009). 66% of the energy requirements for the MBR were due to aeration. Average total energy requirements were 1 kwh/m³ of water treated. At smaller, FOB-relevant scales, it is estimated that 2 kwh/m³ would be realistic for aerobic MBRs. Based on the data presented in this study and calculations below, the following estimates for energy requirements for an AnMBR were generated (Table B3).

Table B3. Energy requirement estimates for an AnMBR.

Task	Energy Requirement (kwh/m ³)
AnMBR mixing	0.10
Membrane scouring (Gas recirculation)	0.20
Permeate pumping	0.10
Other pumping	0.10
Heating	0.58

AnMBR Heating Energy

$$E_{heating} = Q \left(\frac{m^3}{day} \right) \times \left(\frac{1000 \ L}{1 \ m^3} \right) \times \left(\frac{1 \ kg \ H_2O}{1 \ L} \right) \times \left(\frac{4.187 \ kJ}{1 \ kg \ C} \right) \times \left(\frac{0.000278 \ kwh}{1 \ kJ} \right) \times (35 - 25)(C) \times (0.05)$$

Calculation Assumes: Reactor Temperature 35 °C; Ambient Temperature 25 °C; Heat Recovery Efficiency of 95%.

Energy cost savings

Energy cost savings, relative to competing aerobic membrane bioreactor technology, were estimated based on fuel costs for generating electricity onsite, using the burdened fuel cost described in a recent SERDP FOB study (Noblis 2010) and the data from Table B4.

Table B4. Renewable energy recovery estimates.

Base size	Flow rate Q	CH ₄ Energy Produced	H ₂ Energy Produced	Energy Used	Net Energy	Energy Savings (vs. aerobic MBR)	Energy Cost Savings
Personnel	m ³ /day	kwh/day	kwh/day	kwh/day	kwh/day	kwh/day	\$/yr
50	6.7	6.5	1.2	7.5	0.2	13.5	14.5K
500	67	65	12	75	1.7	135	145K
1500	200	196	36	231	5.2	405	435K
10000	1333	1306	237	1544	35	2701	2.7M

Water demand reduction

Water demand reductions were estimated by assuming that 25% of the effluent from the wastewater treatment system would be directed to reuse applications. These estimates are not relative to competing aerobic membrane bioreactors, which also produce water of suitable quality for reuse.

Sludge reduction

Sludge volume reduction estimates were based on text book data (Metcalf & Eddy) for aerobic vs. anaerobic systems (0.27 vs. 0.116 kg dry solids per kg COD, assumed 10% solids).

System size

System size is dominated by the AnMBR reactor component. Thus, system size is calculated as a product of hydraulic retention time design goal and hourly flow rate, with an additional 20% of space factored for sludge accumulation and other components. Variations in flow rate and organic loading are expected to be absorbed by facilitating rapid mass transfer to sequester organics for retention and anaerobic processing.

Acronyms

ACE	Anaerobic-Clinoptilolite-Electrolysis
ADS	Anaerobic Digestion Sludge
AnMBR	Anaerobic Membrane Reactor
AP	Acid Phase
BAC	Biologically Activated Carbon
BOD	Biochemical Oxygen Demand
CERL	Construction Engineering Research Laboratory
COD	Chemical Oxygen Demand
DoD	Department of Defense
EC	E. Coli
ERDC	Engineer Research and Development Center
FOB	Forward Operating Base
GAC	Granular Activated Carbon
HER	Hydrogen Evolution Reactions
HRT	Hydraulic Retention Time
ISO	International Standardization Organization
IX	Ion Exchange
MP	Methane Phase
OLR	Organic Loading Rate
OU	Ohio University
PES	Polyethersulfone
PS	Primary Sludge
ROI	Return on Investment
ROWPU	Reverse Osmosis Water Purification Unit
SCOD	Soluble Chemical Oxygen Demand

SERDP	Strategic Environmental Research and Development Program
SS	Suspended Solids
TCOD	Total Chemical Oxygen Demand
TS	Total Solid
TSS	Total Suspended Solids
UIUC	University of Illinois at Urbana-Champaign
UF	Ultrafiltration
VS	Volatile Solid
VFA	Volatile Fatty Acid